Jimma University

Jimma Institute of Technology

School of Postgraduate Studies

Faculty of Electrical and Computer Engineering

Control and Instrumentation Engineering

Particle Swarm Optimization Based Optimal Design of Six-phase Induction Motor for Electric Propulsion of Submarines

By: Lelisa Diriba

RM 2717/12

A Research Paper Submitted to Faculty of Eectrical and Computer Engineering, Jimma Institute of Technology, Jimma University in Partial Fulfillment of the Requirements for the Degree of Masters of Science in Control and Instrumentation Engineering.

Advisor:- Dr.Amruth.R.T.

Co-Advisor:-Tesfabirhan Shoga

December 2021

Jimma, Ethiopia

Jimma University

Jimma Institute of Technology

School of Postgraduate Studies

Faculty of Electrical and Computer Engineering

Control and Instrumentation Engineering

Particle Swarm Optimization Based Optimal Design of Six-phase Induction Motor for Electric Propulsion of Submarines

By: Lelisa Diriba

APPROVED BY BOARD OF EXAMINERS

Dean, School of Post Graduate	Signature
Dr. Amruth. T	Signature
Advisor	
Mr.Tesfabirhan. S	Signature
Co-Advisor	
Internal Examiner	Signature
Dr.Perashant Alluvada	
External Examiner	Signature

Dr. Dereje Shiferaw

Abstract

Research reveals that multiphase motors in electric submarine propulsion systems are highly recommended because of their improved reliability and effciency than the traditional three phase motors. This thesis presents comparison of optimal model and design of six phase squirrel cage induction motor for electric propulsion of submarines by using Particle Swam Optimization (PSO). In this thesis also the design of six phase squirrel cage induction motor is simulated by ANSYS Motor-CAD and the simulation results are compared in order to find the fittest method and also the performance to electric propulsion of submarines, considering the influence of design upon the motor performance. The six- phase squirrel cage induction motor is cost effective, reliable and more efficient for the electric propulsion of submarines compared to the conventional three phase motor. In the study, first initial parameters of six phase squirrel cage induction motor have been determined and then these parameters have been compared with optimized values by GA and PSO optimization. The motor design is optimized using efficiency, power losses and material cost as the fitness function. The research paper also highlights the use of ANSYS Motor-CAD for the design of six phase squirrel cage induction motor and it also presents the simulation results along with Two Dimensional and Three-Dimensional geometry. The result shows that the weight and power loss is reduced to 161kg and 0.9359Kw respectively, while efficiency and power factor is increased to 0.95 and 0.87 respectively when PSO is used. This shows that the result is promising.

Key Words:

Declaration

I, the researcher, declare that this thesis work is my original work, has not been presented for any other degree or professional qualification in this or any other universities, and all sources of materials used for the thesis work have been fully acknowledged.

Lelisa Diriba Wogi   —————-

Name   Signature

Place: Jimma Institute of Technology, JIT

Jimma University, JU

Jimma,

Ethiopia.

This thesis has been submitted for examination with my approval as a university advisor and Co-Advisor.

Dr. Amruth.T   —————

Name   Signature

Mr. Tesfabirhan.S   ——————

Name   Signature

Acknowledgments

Contents

List of Figures

List of Tables

List of Abbreviations

PSO...................Particle Swam Optimization

DSIM...................Dual Stator Induction Motor

AC .... Alternating Current

Mw ....Megawatt

2D ....Two Dimensional

3D ....Three Dimensional

SPIM.................. Six Phase Induction Motor

V/f.................. Voltage to Frequency

Flux2D.................. Flux in to Dimensional

PID .... Proportional Integral Derivative

FEA..................Finite Element Analysis

GA ....Genetic Algorithm

ACO..................Ant Colony Optimization

PhD.................. Doctoral of Philosophy

TSP.................. travelling salesman problem

Bav.................. Air gap flux density or Specific Magnetic loading

ac..................Specific Electric loading

D..................stator core diameter

L..................core length of stator

WDT.................. Winding Distribution Table

Q.................. input apparent power

KVA.................. Kilo Volt Ampere

C0.................. Output coefficient

v.................. Peripheral Velocity

KVA.................. Kilo Volt Ampere

C0.................. Output coefficient

CHAPTER ONE

1   INTRODUCTION

Modern submarines are complex types of machines that exists today, revolutionizing the marines and witnessing a burst in its daily operation with the presence of multiphase motors intended for underwater research, maintenance, or military purposes. The intentions of military submarine are attacking enemy surface Ships or Submarines and also serve as portable missile launchers and their subtle nature, makes them Suitable for surveillance, deployment of special forces in enemy territory, etc. All these makes submarines very popular for the military power of developed countries. Six phase induction machine is a dual stator induction machine with two sets of three phase currents and this is visualized because of that Dual Stator Induction Motor(DSIM) is like paralleling two three phase induction motors. So, instead of using two three phase induction motor for propulsion of submarines a single DSIM can replace the two and the cost is reduced while reliability is also increased [**?**].

Different types of AC motors are used for the electric propulsion of submarines. These motor types are Synchronous Machines, Squirrel Cage Induction Machines, Permanent Magnet Synchronous Machines and High Temperature Superconducting AC Synchronous Machines. Since the six-phase squirrel cage induction motor has a very simple design and is inherently robust, it is less expensive than a similarly rated Permanent Magnet Synchronous Motor. The six-phase squirrel cage induction motor is approximately 15% less expensive than the Permanent Magnet Synchronous Motor. Induction motors are the most applicable electric machines in the industries not limited only to the industries but to the transportation system and other modern life application because of simple reasons ranging from low cost effectiveness, high reliability, robustness, mechanical simplicity, higher torque and low maintenance when compared to other rotating machines. The simple and rugged construction of the induction motor contributes to its reliability and makes it attractive for electric propulsion applications. So, that conventional three phase induction motors have been used as a standard for electrical AC drives for the industries even though they have inherent setback with respect to performance as regards the loss of phase conditions [**?**]. A major problem referring to machine models is the limitation to three-phase loss of phases. Under this loss of phase condition, the three-phase induction motor does not offer the adequate operation such as output power and torque as required n electric propulsion applications. Also, they can be utilized in hazardous environments such as mining, pumping and blowing operations [**?**]. To rid of this problem among the groups of multiphase motors, the six-phase has received more attention due its simplicity in converting a conventional three phase machine to six-phase. This poly-phase system having a three phase induction motor have two stator windings sets spatially shifted by 30 degrees electrical with separated neutrals as for a star configuration. Therefore, this is one of the means to over-come the inherent setbacks as highlighted as regards the loss of phase conditions in induction motors. Six-phase induction motors are utilized for industrial uses when a high-power drive is required. A six-phase induction motor is created by increasing the number of phases in a three-phase induction motor. The system's reliability improves as a result of the use of Six-phase induction motors. In the rotor circuit, the harmonic current is likewise minimized. The rotor copper loss and ripple

torque are lowered as a result of this reduction. When compared to its equivalent, the three phase induction motor, the efficiency of the SPIM is higher. Six-phase induction motors is used for traction purposes. It's also employed in the case of electric propulsion systems in ships and aircraft [?]. Multiphase induction machine finds its applicability in the area of high degree reliability demand as in more electric aircrafts, electric submarine propulsion, electric vehicles and hybrid electric vehicles. In recent years, squirrel cage Induction motors used most widely in industry due to the ease of operation, high reliability, cost saving, easy to work and maintenance, sturdy structure and low noise more than other motors [?].

Optimum design of six phase squirrel cage induction motor has gained great attention now a days and presented a novel method for multi-objective design and optimization of six phase induction machines. In this case, the proposed method had more efficient than traditional design methods because it found an optimal design with no heuristic approaches or design iterations. Particle Swarm Optimization (PSO) algorithm has compared to manual deign in this research paper with the aim of finding which is more suitable for design of motor optimization for submarines. PSO had the ability to find the correct optimal solution, but finding which one has better performance in finding the global optimum. The research paper presents an optimal design of six phase squirrel cage induction motor for having optimal size and efficiency. For this purpose, Particle Swarm Optimization (PSO) algorithm is applied which are new optimization algorithm and it has not been used for Optimum design of such motors yet. Optimization is performed with an objective function which is a combination of maximum efficiency and minimum size.

1.1   Statement of the problem

Most of the time convectional three phase motors are used in the propulsion of submarines. The semiconductors power device got stress from the high phase current and also if one of the phase line is failed, motor is stopped. Dual three phase induction motor is used in the electric propulsion of submarines in order to produce more power, still costly, needs third harmonic current injection for torque improvement and there is problem of weight.This makes the propulsion difficult. The proposed system improves the above stated problems by employing optimal design of six phase induction motor and optimizing the variables. These variables are then used to calculate the performance of the designed motor. The life cycle of a control system demands several optimization in several steps that are in the phases of process modeling and design. Recent observations carried out suggest increasing interest in the six-phase induction motor. After much literature review it is observed that more research efforts have not been applied in this new area in terms of the optimal model and design of six phase induction motor for submarine application. For the six-phase induction motors, the generation of high order (fifth and seventh) current harmonics is one of the setbacks in this poly-phase induction motor. This makes the motor size to be increased and the cost also, as to take care of additional losses but still have advantages which may worth it in some areas of application like submarines. But, more advanced intelligent optimization techniques contain usually much more parameters, which must be appropriately optimized.

Research Questions

The questions that arises and I hope to answer are:

- Is the application of particle swarm optimization technique is better for six phase squirrel cage induction motor design for electric propulsion of submarines? Why?

- How can the proposed system be used in the best way to obtain the best performance?

- Under which optimization techniques optimized parameters of six phase squirrel cage induction motor is obtained?

- How can the proposed system be applied to a submarine propulsion?

1.2 Objectives of Study

1.2.1 General Objective

The main objective of this thesis is to design six-phase induction motor for electric propulsion of submarines based on particle swarm optimization techniques.

1.2.2 Specific Objectives

The specific objectives are:-

- To design optimal six phase squirrel cage induction motor for electric propulsion of submarines.

- To reduce weight of six phase squirrel cage induction motor by using intelligent optimization techniques.

- To test the designed six phase squirrel cage induction motor using ANSYS Motor-CAD.

- To examine the effect of PSO design on the performance of six phase squirrel Cage induction motor.

1.3 Significance of the study

Intelligent optimization techniques are essential in our daily lives, in engineering and in industry. These techniques are applied in almost all fields of applications. It optimizes to minimize cost and energy consumption, or to maximize profit, output, performance and efficiency. Optimization is imperative in the real world because of limitations in resources, time and money. From the optimization techniques one is swarm intelligence algorithms, derived from the social behavior of animals that consist of a group of non-intelligent simple agents with no central control structure and no self-organization to systematize their behavior, So, by this method optimized six phase squirrel cage induction motor is modeled and designed for electric propulsion of submarines results in the above stated advantage. Optimization is performed with an objective function which is a combination of maximum efficiency and minimum size.

1.4 Scope of the study

The study shall be limited to mathematical modeling and designing of six phase squirrel cage induction motor in MATLAB/SIMULINK, testing and simulating of the designed Six phase squirrel cage induction motor by using ANSYS Motor-CAD, applying PSO for optimum model and design of six phase squirrel cage induction motor and compare and contrast the performance of manual design with PSO.

1.5 Limitations

A six-phase squirrel cage induction motor will be designed in ANSYS Motor-CAD. The 3D or physical design of six-phase squirrel cage induction motor will take too much time. The six phase squirrel cage induction motor prototype is also not developed.

1.6 Thesis Organization

This research paper is organized into five chapters. These are as follows.
Chapter 1 particle swarm optimization will be proposed for optimal design of six phase induction motor for submarine applications. **Chapter 2** a comprehensive review of literature is presented. **Chapter 3** describes the theory and operation principle of induction motor. Dynamical modeling of Six Phase Induction Motor and Optimization based on particle swarm optimization and its principle is presented. The details model and stability analysis of six phase induction motor particle swarm optimization based optimal design is presented. **Chapter 4** this chapter discussed on simulation of the optimally designed system on Matlab/Simulink and ANSYS MotorCAD including simulation result. Compares and contrasts the theoretical results with the simulation results to verify the nature and stable operation of proposed system. **Chapter 5** draws the conclusion from the work done in this thesis and recommend for further research area.

CHAPTER TWO

2 LITERATURE REVIEW

Multiphase electric machines can be categorized as synchronous and asynchronous machines. From these multiphase electric machines six-phase induction machine has more advantages and has improved performance compared to the three-phase induction motor [**?**].

Dual stator induction motors provide substantially higher efficiency and torque than identical three phase induction motors. Even though the initial cost of a dual stator induction motor is more than that of a comparable three phase motor, the efficiency and torque are substantially higher [**?**].

The starting torque transients of the six-phase induction motor and three phase induction motor are almost qualitatively the same, but speed transients of six-phase induction motor indicate greater robustness at operation with load than three phase induction motor and developed six phase induction motor Simulink model for simulation different control modes [**?**].

In the other paper about the Transient Analysis and Modeling of Six Phase Asynchronous Machine, it is presented that the redesigned motor can work as a both three phase machine and as six phase. This idea is extended to the submarines, to use a six phase motor to replace two three phase motors, and money is saved redesigning the machine with higher reliability. The loss of a phase does not stop the motor from running. In submarines mostly Naval War ships, reliability is a criterion in designing a submarines. Also rather than using two three phase induction motors for propulsion of submarines, a single SPIM can replace the two and the cost is reduced and reliability increased which is the actual aim of this work [**?**].

Also the other paper was focused on thermal analysis of a three-phase induction motor based on motor-CAD, flux2D, and MATLAB shows that squirrel cage three phase induction motor has been examined successfully by Motor-CAD and MATLAB together with finite element method (based on Flux2D) under full load and Motor-CAD results illustrate in a good manner all heat exchanges between different parts of the motor [**?**]-[**?**].

The other paper focused on design of optimal PID controller for three phase induction motor based on ant colony optimization, shows that by using Ant Colony Algorithm optimal parameters of PID and an optimum induction motor performance will be obtained. With the optimization parameters of PID, optimum response performance for induction motor speed is indicated by the settling time response and minimum overshoot compared to the normal PID method which is uncontrolled system [**?**].

The other paper of a post fault controller for scalar controlled asymmetrical six-phase induction machines proves that the machine could optimally be controlled during open phase fault condition under either open-loop or closed-loop speed control modes, while scalar V/f-based controller does not require accurate information about the machine parameters while provides a robust and straightforward control in applications that do not require a high dynamic response [**?**].

The other paper compared optimally designed three phase squirrel-cage induction motors with an existing motor of the same rating and uses Genetic Algorithm optimization techniques for optimizing three phase squirrel cage induction motor. The program that analyzes

and optimizes induction motors and evaluates the performance of the design has been developed and comparison of the final optimum designs with the existing design indicates that performance of the designed three phase induction motor is greater than that of existing motor, which in turn results in loss reduction and improve the efficiency and power factor in electric motor driven systems. And also operating cost is reduced while performance improvement [**?**].

In the other paper about the optimization design of the squirrel cage induction motor, it is presented a novel method for multi objective design and optimization of three phase induction machines. In this case, the proposed method had more efficient than traditional design methods because it found an optimal design with no heuristic approaches or design iterations. The optimal design results are verified by FEA. The results provided useful insight for the drive system designers. PSO and GA algorithms has compared in this paper with the aim of finding which algorithm is more suitable for motor design optimization. The results indicated the PSO and GA both had the ability to find the correct optimal solution, but PSO had a better performance in finding the global optima. Also, in terms of the computational efficiency, PSO had a lower performance degrading with a smaller population size and higher robustness to its running coefficients. The comparison results provided that PSO should be preferred over GA particularly when computational time is a limiting factor [**?**].

Now a day's optimum design of squirrel cage induction motor has gained great attention in the area of propulsion of electric vehicles, submarines etc. due to its performance improvements [**?**].

In the other work done in 2018, investigates the performance of a rotor-caged induction motor equipped with distributed and concentrated stator windings considering the same lamination design for both the winding. By using winding function and FEA method six phase induction motor with 2-pole distributed winding performance is evaluated. Both of the winding have their own advantages and disadvantages on over the other [**?**].

In the work of Altered Grey Wolf Optimization and Taguchi Method with FEA for Six-Phase Copper Squirrel Cage Rotor Induction Motor Design, Taguchi method and FEA methods are used as multi objective function to achieve faster optimized value selection and convergent speed. The multi-objective optimization design with high-performance property aims to achieve lower starting current, lower losses, lower input power, higher efficiency, higher output torque, and higher power factor [**?**].

Convectional three phase induction motor uses more current per phase which leads to more copper losses, and this decreases the range of the electric vehicle than that of six phase induction motor. The simulation result shows that SPIM requires lesser current per phase, such that, the range of the car increases along with the capability to meet the higher starting torque required. Here both three phase and six phase induction machines are compared and the later one gives improved efficiency and starting transient torque. Replacements of convectional three phase induction motor by six phase induction motor for a vehicle is not that much tedious or not costly which makes easy replacements. And also a vehicle supplied by six phase induction motor decreases power consumption which is improvements to the conventional ones using three phase motor drives or depends on fossil fuel [**?**].
The Ant Colony Optimization (ACO) algorithm is introduced by Marco Dorigo in his Doctoral Philosophy(PhD) Thesis in 1992. This algorithm initially applied to the travelling salesman problem (TSP). The ant colony optimization field has experienced fastest growth

and is the most recent nature inspired stochastic meta-heuristic based optimization technique that has been successfully used in complex routing problems or hard optimization problem and can be extended to solve many discrete optimization problems. Ant colony optimization is derived from the process by which the ant colonies find the shortest route from their nest to a food source and back to their nest. It is the algorithm that searches for an optimal path based on the behavior of ants seeking a path between their colony and source of food. Colonies of real ants communicate with each other through the use of chemicals called pheromones. Pheromone is a chemical substance that is deposited by the ants to show the path travelled by them to the other ants. This chemical is deposited along the path an ant travels when they are in search of food. Naturally ants choose a shorter path and the ants on the shorter path deposits these chemicals at a faster rate. The more the deposited pheromone on the path, the next ants will choose that path still creating a more pheromone deposition. Ants navigate from the source to the food and deposits pheromone. Since pheromone is evaporated with time shortest path is identified by the concentration of pheromone deposited. The more the concentration of pheromone increases the probability of the path is being followed. The ACO algorithm was used to help of some problem and the challenges faced for solving the problems. The ACO discusses about the biological inspiration and behavior of ant colony and then relates with the real-life problems [**?**].

The other paper of A New Multiphase Rotor Model for the Squirrel Cage Rotor of a Six-phase Induction Machine states the impacts of multiphase rotor on six phase induction motor performances [**?**].

In the work of Optimisation of a High Speed Copper Rotor Induction Motor for a Traction Application,states that the effects of high speed copper rotor for traction purposes such as submarines, vehicles, etc [**?**]. In case of selecting specific magnetic loading and specific electric loading proper attention should be given. There is merits and demerits of selecting the values based on the design requirements [**?**].

Particle Swarm Optimization (PSO)

In 1995's Particle swarm optimization (PSO) concept was first introduced by Dr. Eberhart and Dr. Kennedy. Particle swarm optimization is an evolutionary computation technique inspired through sociological behavior associated with swarms such as bird flocking or fish harmonies. It is a global optimization technique that relies on collective intelligence (swarm intelligence) for solving global optimization problems and to find an optimal solution. Several scientists proposed particle swarm optimization and later developed some computational simulations of organisms movement such as birds flocks and harmonies of fishes. These simulations were heavily relying on the computation of the distances between the particles. In developing particle swarm optimization, the fundamental point is a hypothesis in which the exchange of information among each particles offers some sort of evolutionary advantage and particle swarm optimization shows similar characteristics to the evolutionary computation techniques, which are based on a population of solutions. The particle swarm optimization algorithm exhibits common evolutionary computation attributes including initialization with a population of random solutions and searching for optima by updating generations. Potential solutions, called birds or particles. Each particle in the particle swarm optimization algorithm is a potential solution for the optimization problem.

Introduction to Submarine

A submarine is a submersible craft that can operate independently underwater. It is not the same as a submersible, which has restricted underwater capabilities. The term is most usually used to describe a large, crewed ship. It is also occasionally used to refer to remotely driven vehicles and robotics, as well as medium-sized or smaller vessels, such as the midget submarine and the wet sub, in historical or colloquial contexts. Submarines are traditionally referred to as boats rather than ships by naval tradition, regardless of their size, and the term submarine developed as a shorter form of submarine boat. Submarines were originally widely utilized during World War I, and they are today found in a wide range of navies. Attacking enemy surface ships, attacking other submarines, aircraft carrier protection and ballistic missile submarines as part of a nuclear strike force are just a few of the military applications. Submarines have a variety of civilian applications, including marine science, salvage, exploration, and facility inspection and maintenance. Submarines can also be customized to undertake more specialized tasks, such as search-and-rescue missions or underwater cable repair. Submarines are also utilized for undersea archaeology and tourism. Most big submarines have a cylindrical body with hemispherical ends and a vertical structure, usually amidships, that houses communications, sensing, and periscope systems. At the back, there's a propeller (pump jet) and different hydrodynamic control fins. Smaller, deep-diving, and specialist submarines may depart dramatically from the standard configuration. Submarines use diving planes and adjust the amount of water and air in their ballast tanks to modify their buoyancy when submerging and surfacing. To control its buoyancy, the submarine has ballast tanks and auxiliary or trim tanks that can be alternately filled with water or air. When the submarine is on the surface, the ballast tanks are filled with air and the submarine's overall density is less than that of the surrounding water. As the submarine dives, the ballast tanks are flooded with water and the air in the ballast tanks is vented from the submarine until its overall density is greater than the surrounding water and the submarine begins to sink (negative buoyancy). A supply of compressed air is maintained aboard the submarine in air asks for life support and for use with the ballast tanks. In addition, the submarine has movable sets of short wings called hydroplanes on the stern (back) that help to control the angle of the dive. The hydroplanes are angled so that water moves over the stern, which forces the stern upward; therefore, the submarine is angled downward. To keep the submarine level at any set depth, the submarine maintains a balance of air and water in the trim tanks so that its overall density is equal to the surrounding water (neutral buoyancy). When the submarine reaches its cruising depth, the hydroplanes are leveled so that the submarine travels level through the water. Water is also forced between the bow and stern trim tanks to keep the sub level. The submarine can steer in the water by using the tail rudder to turn starboard (right) or port (left) and the hydroplanes to control the fore-aft angle of the submarine. In addition, some submarines are equipped with a retractable secondary propulsion motor that can swivel 360 degrees. When the submarine surfaces, compressed air ows from the air asks into the ballast tanks and the water is forced out of the submarine until its overall density is less than the surrounding water (positive buoyancy) and the submarine rises. The hydroplanes are angled so that water moves up over the stern, which forces the stern downward; therefore, the submarine is angled upward. In an emergency, the ballast tanks can be filled quickly with high-pressure

air to take the submarine to the surface very rapidly [30].

Submarine Navigation

Submarine navigation requires unique abilities and technologies not available to surface ships. Submarines spend longer time underwater, travel greater distances, and cruise at higher speeds, increasing the difficulty of underwater navigation. Submarines in the military go underwater in complete darkness, with no windows or lighting. They can't utilize their active sonar systems to ping ahead for underwater threats like undersea mountains, drilling rigs, or other submarines because they're in stealth mode. Anti-submarine warfare detection devices such as radar and satellite monitoring prevent surface operations to gain navigational fixes. Antenna masts and antenna-equipped periscopes can be raised to acquire navigational signals, but only for a few seconds or minutes in areas of extensive observation; contemporary radar equipment can detect even a slim periscope, and submarine shadows can be seen clearly from the air. Navigational Technologies Surfaced submarines arriving and leaving port navigate similarly to typical ships, with a few additional issues due to the fact that the boat spends the most of its time below the waterline, making it difficult for other vessels to detect and identify them. Submarines have an inertial navigation system that constantly updates position by measuring the boat's motion. It allows the boat to navigate while remaining submerged beneath the surface because it does not rely on radio transmissions or celestial observations. The submarine must update its position using outside navigational radio signals on a regular basis to ensure accuracy. Inertial Navigation System An inertial navigation system (INS) is a navigation device that uses a computer, motion sensors (accelerometers), and rotation sensors (gyroscopes) to calculate the position, orientation, and velocity (direction and speed of movement) of a moving object continuously by dead reckoning without the use of external references. Mobile robotics and vehicles such as ships, aircraft, submarines, guided missiles, and spaceships all use INSs. Inertial navigation systems or closely comparable technologies are also known as inertial guidance systems, inertial instruments, inertial measurement units (IMU), and a variety of others. Inertial navigation is a self-contained navigation system that uses accelerometer and gyroscope readings to track an object's position and orientation in relation to a predefined beginning point, orientation, and velocity. Three orthogonal rate-gyroscopes and three orthogonal accelerometers are frequently found in inertial measurement units, which measure angular velocity and linear acceleration, respectively. It is feasible to track a device's position and orientation by processing data from these devices. The INS is utilized for a variety of purposes, including aircraft navigation, tactical and strategic missiles, satellites, submarines, and ships. It is also installed in some mobile phones for the purpose of tracking and locating them. Small and light inertial navigation systems are now available thanks to recent breakthroughs in the design of microelectromechanical systems (MEMS). These advancements have broadened the scope of potential applications to encompass human and animal motion capture. A computer and a platform or module housing accelerometers, gyroscopes, or other motion-sensing sensors are included in an INS. The INS receives its starting position and velocity from another source along with the initial orientation, and then computes its own updated position and velocity by combining data from the motion sensors. Once initialized, an INS has the advantage of not need any external references to establish its position, orientation, or

velocity. An INS may detect changes in its geographic position (e.g. moving east or north), velocity (moving at a different speed and direction), and orientation. It accomplishes this by monitoring the system's linear acceleration and angular velocity. It is resilient to jamming and deceit because it does not require an external reference. Gyroscopes measure the sensor frame's angular velocity in relation to the inertial reference frame. The system's present orientation is known at all times by using the system's original orientation in the inertial reference frame as the initial condition and integrating the angular velocity. This is similar to a blindfolded passenger in a car being able to feel the automobile turn left and right or tilt up and down as it climbs or descends hills. The passenger can tell which way the automobile is going based on this information. Accelerometers measure the moving vehicle's linear acceleration in the sensor or body frame, but only in directions that can be measured relative to the moving system.

Sonar

Sonar (sound navigation and ranging) is a technology for navigating, measuring distances, communicating with and detecting things on or beneath the surface of the water, such as other vessels, using sound propagation (typically underwater, as in submarine navigation). Active sonar emits sound pulses and listens for echoes, whereas passive sonar simply listens for the sound created by vessels. Sonar can be used to locate targets in the water and to measure the echo characteristics of those targets. Prior to the development of radar, acoustic locating in the air was used. The apparatus that generates and receives sound is also referred to as sonar. Sonar systems use acoustic frequencies that range from very low (infrasonic) to very high (ultrasonic). Underwater acoustics, often known as hydro acoustics, is the study of underwater sound.

Active sonar

Active sonar uses a sound transmitter and a receiver. Active sonar creates a pulse of sound, often called a ping, and then listens for reflections (echo) of the pulse. This pulse of sound is generally created electronically using a sonar projector consisting of a signal generator, power amplifier and electro acoustic transducer. A transducer is a device that can transmit and receive acoustic signals. A beam former is usually employed to concentrate the acoustic power into a beam, which may be swept to cover the required search angles. Generally, the electro-acoustic transducers are of the Tonpilz type and their design may be optimized to achieve maximum efficiency over the widest bandwidth, in order to optimize performance of the overall system. In general, electro-acoustic transducers of Tonpilz type, and their design can be optimized to achieve optimal efficiency throughout the widest bandwidth possible, hence improving total system performance. The duration from transmission of a pulse to reception is measured and converted into a range using the known speed of sound to determine the distance to an object. Several hydrophones are used to measure the bearing, and the set measures the relative arrival time to each, or an array of hydrophones is used to measure the relative amplitude in beams generated by a process known as beam forming. Because the use of an array limits the spatial response, multi beam systems are employed to give extensive coverage. The target signal and noise are subsequently processed using

various signal-processing techniques, which for small sonars may be as simple as energy measurement. It is then presented to a judgment device, which determines if the output is the desired signal or noise. This decision device could be a human operator with headphones or a display, or it could be software in more advanced sonars. Additional methods may be used to classify and pinpoint the target, as well as measure its velocity. The pulse could be a steady chirp or a chirp with a shifting frequency (to allow pulse compression on reception). Simple sonars typically employ the former, with a filter wide enough to account for probable Doppler shifts caused by target movement, while more advanced sonars employ the latter. Since the advent of digital processing, digital correlation techniques have been used to create pulse compression. Multiple beams are common in military sonars to offer all-around coverage, whereas simple ones only cover a restricted arc, however the beam can be rotated slowly by mechanical scanning. The Doppler effect can be utilized to detect a target's radial speed, especially when single frequency transmissions are used. The velocity is calculated by measuring the frequency difference between the transmitted and received signals.

Passive sonar

Passive sonar listens but does not convey information. It is frequently utilized in military settings, but it is also used in science applications, such as identifying fish in diverse aquatic environments for presence/absence investigations This phrase can be applied to nearly any analytical approach employing remotely generated sound in the broadest sense, albeit it is usually limited to procedures used in an aquatic environment. For determining the source of a detected sound, passive sonar uses a variety of techniques. The majority of vessels in the United States, for example, use 60 Hz alternating current power systems. The 60 Hz sound from the windings can be emitted from the submarine or ship if transformers or generators are positioned without sufficient vibration insulation from the hull or become flooded. Because all European submarines and practically every other nation's submarine have 50 Hz power systems, this can assist identify its nationality. Passive sonar may be able to detect "transients," or sound sources that come and go (such as a wrench being dropped). Until recently, signals were detected by an experienced, trained operator, but computers are increasingly capable of doing so. Although passive sonar systems contain huge acoustic databases, the sounds are normally classi ed manually by the sonar operator. Noise limitations Because of the noise generated by the vehicle, passive sonar aboard automobiles is usually severely limited. As a result, many submarines use nuclear reactors that can be cooled without the use of pumps via silent convection, or fuel cells or batteries that can also work silently. The propellers on vehicles are likewise designed and manufactured to produce as little noise as possible. Cavitation is the sound made by high-speed propellers creating small bubbles in the water. To lessen the effect of noise generated by the watercraft, the sonar hydrophones can be trailed behind the ship or submarine. Propeller A propeller is a type of fan that converts rotational motion into thrust to convey power. The forward and back surfaces of the airfoil-shaped blade create a pressure differential, which accelerates a

uid behind the blade. A marine propeller is sometimes referred to as a screw propeller or screw, but there is a different class of propellers known as cycloidal propellers, which are distinguished by a higher propulsive efficiency compared to the screw propeller's as well

as the ability to throw thrust in any direction at any time. The propeller of a ship is the most important component since it provides the necessary propulsion. Marine propellers are manufactured from corrosion-resistant materials as they are made operational in seawater which is a corrosion accelerator. The materials utilized for making marine propellers are an alloy of stainless steel and aluminum. Other popular materials employed are alloys of nickel, bronze, and aluminum lighter than other materials and have higher durability.

Types Of Marine Propellers

Propellers are divided based on several factors. The classification of various types of propeller is described below:

By Number of Blades Attached

Propeller blades may alter from 3 blade to 4 blade propeller and sometimes even a five-blade propeller. Nevertheless, the most regularly used are three-blade and four-blade propellers. However, the most commonly used are four blades and five-blade propellers. The propeller efficiency is the highest for a propeller with a minimum number of blades, i.e. two-blade propeller. But to obtain strength factor and to consider the heavy loads subjected by the ship, sea, and weather, two-blade propellers are not applied for merchant ships.

Three-blade propeller

A three-blade propeller has the features of cheaper manufacturing cost than other types of propeller, made up of aluminum alloy, acceleration is better than the other types of propeller, low-speed handling is not much effective and gives a reliable high-speed performance.

Four-blade propeller

A four-blade propeller has the features of higher manufacturing cost than three-blade propellers, have better durability and strength, are customarily made of stainless-steel alloys, gives excellent low-speed handling and performance, presents a better fuel economy than all the other types of propeller and has a greater holding power in rough seas.

Five-blade propeller

A five-blade propeller has the features of has minimum vibration compared to all the other types of propeller, manufacturing cost is more leading of all and have greater holding power in rough seas.

Six-Blade Propeller

Six-blade propellers have the characteristics of relatively high manufacturing cost, has most minimum vibration compared to all the other types of propeller, have greater holding power in rough seas and produced pressure field over the propeller reduced.

By Pitch of The Blade

The pitch of a propeller can be described as the displacement that a propeller performs for every full revolution of 360 degree. The organization of the propellers based on the pitch is as follows:

Fixed Pitch Propeller

The blades in the fixed pitch propeller are permanently connected to the hub. The fixed pitch type propellers are cast, and the position of the blades and the pitch position is always fixed and cannot be adjusted during the operation. They are typically made from copper alloy. Fixed pitch propellers are reliable and robust as the system doesn't include any hydraulic and mechanical connection as in Controlled Pitch Propeller (CPP). The manufacturing, operational, and installation costs are lower than the CPP type. The maneuverability of the fixed-pitch propeller is also not as great as CPP. This design maintains thrust efficiency while lowering cavitation, resulting in a quiet, stealthy design.

Controllable Pitch Propeller

In a Controlled Pitch type propeller, it is possible to adjust the pitch by rotating the blade about its vertical axis utilizing mechanical and hydraulic arrangement. This helps drive machinery at constant load with no reversing mechanism needed as the pitch can be modified to match the expected operating condition. Thus, the maneuverability enhances, and the engine efficiency also rises. This disadvantage includes the probability of oil pollution as the hydraulic oil in the boss, which is utilized for regulating the pitch, may leak out. It is a complicated and costly system from both the establishment and operational point. Moreover, the pitch can get held in one position, making it difficult to maneuver the engine.

coordinates in the problem space and tries to search the best position through flying in a multidimensional space, which are associated with the best solution (called best fitness), it has achieved so far called pbest. Another best value called gbest that is tracked by the global version of the particle swarm optimizer is the overall best value and its location is obtained so far by each particle in the population. The PSO consists of changing the velocity of each particle toward its local best and global best locations and each candidate solution has an associated velocity. The velocity is adjusted through an updating equation that considers the experience of the corresponding particle and the experience of the other present particles in the population.

Hypothesis

The modeling of six phase squirrel cage induction machine generally retained, relies on several hypotheses which are now recalled. The first hypothesis consists in assuming that the magneto-motive forces created by different stator and rotor phases are spread in a sinusoidal way along the air gap, when those windings are crossed by a constant current. An appropriate dispersion of the winding in space allows reaching this aim. The machine air gap

is also supposed to be constantly thick, the notching effects, generating space harmonics are ignored. These hypotheses will allow restricting the modeling of fundamental components (low frequency) of alternative quantities. For this modeling, hypothesis about the physical behavior of the materials are expressed:

- The magnetic fields are not saturated, are not submitted to the hysteresis phenomenon and are not the center of Foucault's current (for all practical purposes, the magnetic circuit is leafed through to limit the effects). This allows defining linear inductions.

- The skin effect is not taken into account.

- The temperature in the motor stays constant whatever the operating point is, which leads to constant parameters in mathematical models (stationary).

These hypotheses will allow adding the associated fluxes to the different currents, using proper constant inductions, characterizing coupling by sinusoidal variations of the mutual inductions and representing induction flows by a spatial vector. They allow the development of modeling with a limited complexity and thus the development of control strategies which can be implemented in practice. In fact the parameters of these models vary in saturation, skin effect and temperature. These variations influence on the different control strategies performances.

The identified gaps are: -

- Supplying a six phase induction motor from a single six phase inverter for more torque improvement that is supplying two or more multiphase induction motors from single six-phase inverter (multi motor operation) didn't considered.

- Which motor winding types whether distributed winding or concentrated winding configuration best fits of the six phase induction motor for electric propulsion of submarines didn't stated. So finding the novel suitable solution for this motor winding type selection for torque improvement still left.

- Effects of the material selection from which stator and rotor is made up off on the magneto motive force produced and on the weight of six phase induction motor for submarine application.

- The effects of optimized values of six phase induction motor parameters on the size and weight of the motor didn't considered.

- ANSYS Motor Cad of the optimized values of the six phase induction motor is not designed and comparison with the un-optimized six phase induction motor is not done.

So this thesis improves the above stated gaps through presenting an application of Particle Swam Optimization (PSO) algorithm to optimize the parameters in the design of a six-phase squirrel cage induction motor for electric propulsion of submarines. The proposed method is used to estimate optimum stator and rotor resistances, the stator and rotor leakage reactance' s, and the magnetizing reactance in the steady-state equivalent circuit of the six-phase induction motor in turn used to minimize weight, maximize efficiency and minimize cost.

CHAPTER THREE

3 DESIGN METHODOLOGY OF SIX PHASE INDUCTION MOTOR

3.1 Data collection

The approaches or procedure applied for the design of six-phase squirrel cage induction motor in this thesis is as follows. First of all, information of six-phase squirrel cage induction motor parameters will be collected. These parameters are: number of slots and their size, stator bore, D, active length L, air gap length, no of phases etc. Also additional data will be collected from secondary sources to obtain frequency, electric density magnetic loading, electric load, winding factor etc.

The thesis consists of several stages, including the creation of an intelligent algorithm on the MATLAB m-file software, modeling and designing of six phase squirrel cage induction motor on a MATLAB Simulink, and implementing and applying an intelligent algorithm to six phase squirrel cage induction motor. They are described in the following sections. The mathematical model and d-q-0 model tor the six-phase squirrel cage induction motor shall developed and the simulation of the developed mathematical model shall carry out by MATLAB/ Simulink and ANSYS Motor-CAD The designed package for six phase squirrel cage induction motor shall undergo optimization process using ACO and PSO and this procedure shall be based on the weight factor equations and sizing equations.

- Gathering and survey related works from various literature and publications ,

- Study and design the appropriate modelling of six-phase squirrel cage induction motor,

- The six-phase squirrel cage induction motor MATLAB/Simulink simulation shall be developed and designed for electric propulsion of submarines,

- Examine the effects of various optimization techniques on the operating conditions of the six-phase squirrel cage induction motor and

- Evaluate the performance of the system based on simulation results.

Traditionally designers start to design electrical motors by heuristically selecting values of design parameters, and then follow an iterative tuning process trying to achieve design specifications.

A) The sizing equation

The sizing equation of traditional electric machine design is given as follows [?]:-

$$S = 11 * K_w * B_{av} * ac * (\frac{D}{1000})^2 * \frac{L}{1000} * n \tag{3.1}$$

where: S is the motor rating in Watt

Bav is the specific magnetic loading in Tesla

ac is the specific electrical loading in A/m

D is the stator inner diameter in mm

L is the motor active length in mm

Kw is the winding factor, and

n is the rated speed in revolutions per second.

Values for Bav and ac are selected by the designer at the start of the design process.

B) Selection of the aspect ratio

After Bav and ac are selected by the designer, the $D^2 * L$ value of the machine is then calculated by sizing equation. For a machine with its pole number denoted by p, an aspect ratio is defined as follows [?].

$$\alpha = \frac{L}{\frac{\pi * D}{P}} = \frac{L}{Y} \tag{3.2}$$

where Y is the pole pitch in meters

C) Selection of current density

For a certain rated current I, the current density J_s determines the cross sectional area of the used copper wire A_{wire}, as given below [?].

$$A_{wire} = \frac{I}{J_s} \tag{3.3}$$

D) Electrical machine design process

First a prior assumption of machine efficiency and power factor p/ have to be made and the machine rating S in VA is calculated by the following formula [?].

$$S = \frac{P_{out}}{eff * Pf} \tag{3.4}$$

where P_{out} is the specified machine rated output power

After the value for S is calculated, values for Bav, ac and α are selected to calculate D and L according to the sizing equation.

Design Approaches

The design optimization of motor requires choice of the objective function. Usually concerns performance features that represented by the multi objective function like optimizing the stator copper loss, optimizing the stator rotor loss, optimizing the stator iron loss and optimizing full load efficiency.

Overall System Flowchart

The overall flowchart given below shows that each step from title selection to the final optimized design of six pase squirrel cage induction motor.
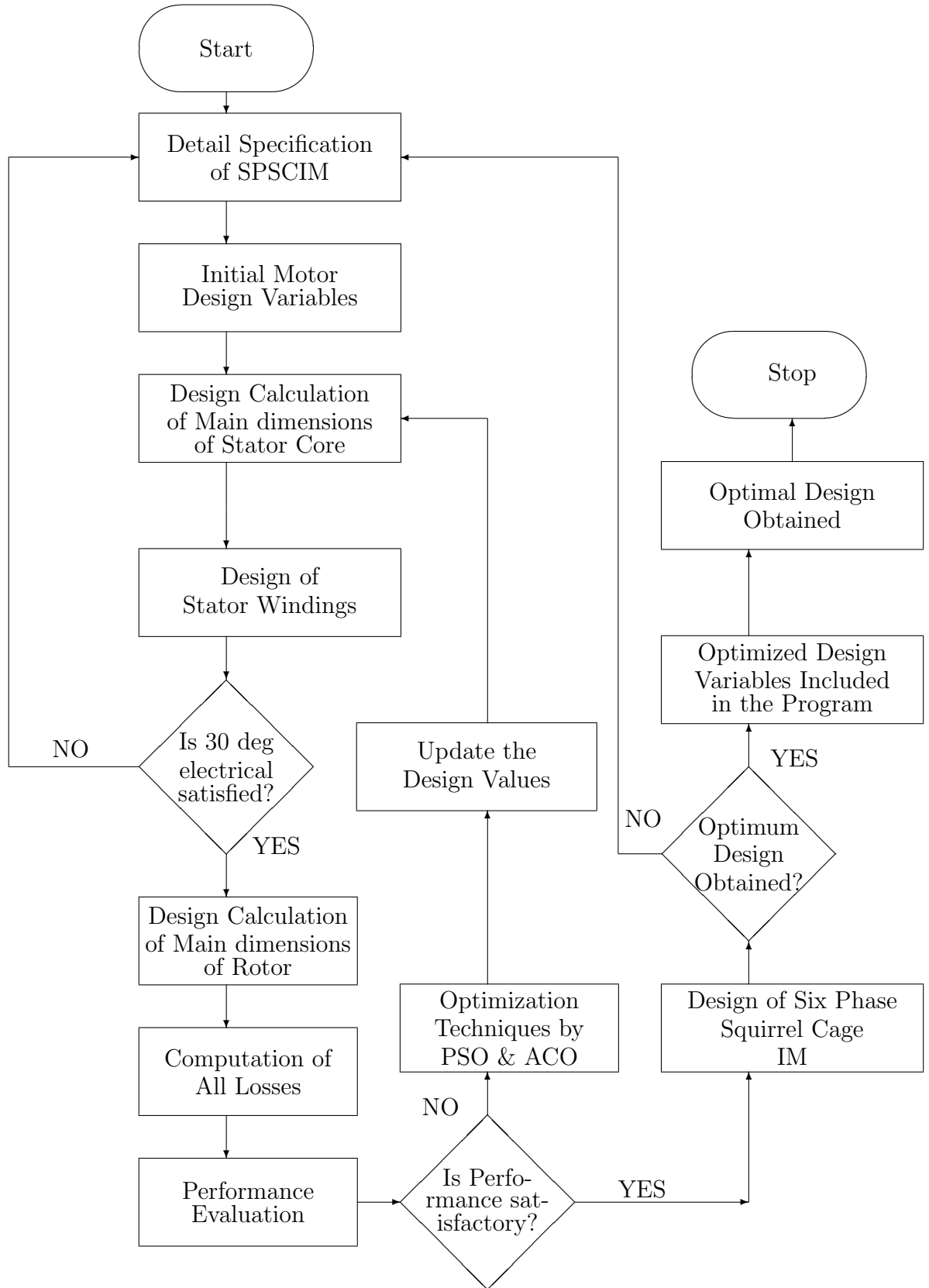
Figure 3.1: Overall System Flowchart

3.2   Theoretical Background

Six phase induction motor is an alternate current motor wherein currents withinside the stator winding is hooked up to the deliver units make up a flux which motives currents to be introduced withinside the rotor winding; those currents interact with the flux to supply rotation. The rotor gets electric power in exactly the equal manner as the secondary of a winding transformer receiving its power from primary. That is why an induction motor can be known as rotating transformer wherein primary winding is stationary however the secondary is unfastened to rotate. Based on their rotor types six phase induction motors are classified into :-

- Squirrel cage induction motor: The rotor of this motor could be very available and is composed of bars of aluminium (copper) with shorting rings on the end.

- Wound rotor induction motor: The rotor of this motor consist a 3 section windings that's star linked with terminals introduced out to slip rings for external connections.

From this types, squirrel cage induction motor is extra usually utilized in enterprise because of:

- Robust: No brushes and no contacts on rotor shaft

- Easy to manufacture

- Maintenance free besides for bearing and stator winding

- The copper loss is low and the performance of the motor is high because of the rotor has very low resistance.

Therefore, the motor manufacturing enterprise such as ABB (Asea Brown Boveri) and SIEMENS enterprise attention on imposing of the squirrel cage induction motor in wide variety due to the customer favored this form of motor because of its benefits indicated above.

3.3   Six Phase Squirrel Cage Induction Motor

An Alternating Current induction motor includes electromagnetic components of Stationary segment called the stator and of Rotating element called the rotor. These components are made up of an electric powered circuit (made of insulated copper conductor for stator winding and aluminum conductor for rotor bar winding), to carry current and a magnetic circuit (made of laminated silicon metal), to carry magnetic flux. Let as provide an explanation for stator and rotor of six phase squirrel cage induction motor one by one as follows to recognize all of the inner and outside a part of the motor.

3.3.1   Stator of Six Phase Squirrel Cage Induction Motor

The stator is the outer stationary segment of an induction motor, which includes the outer cylindrical frame of the motor referred to as yoke, that is made from welded sheet metal, the

magnetic path, which contains a set of slotted metal laminations called stator core pressed into the cylindrical area interior the outer frame, set of insulated electric windings, that are located into the slots of the laminated stator.

3.3.2 Rotor of Six Phase Squirrel Cage Induction Motor

Rotor is the rotating segment of an induction motor, which includes a set of slotted silicon metal laminated, pressed collectively to shape a cylindrical magnetic and electric circuit. Squirrel cage rotor includes a set of aluminum or copper bars set up into the slots, which are related to an end-ring at every end of the rotor. The other components, that are required to finish the layout of vital factors of an induction motors are: two end-flanges to assist the two bearings, one on the driving-end and the other at the non driving-end, in which the driving offers up will have the shaft extension, two units of bearings to assist the rotating shaft, steel shaft for transmitting the mechanical strength to the load, Cooling fan located on the non driving end to furnish pressured cooling for the stator and rotor, Terminal box on top of the yoke or on side to receive the outside electric connections. The crucial purpose of designing an induction motor is to benefit the entire physical dimensions of all of the components of the motor to fulfill the consumer specifications. The following are the design vital factors that are required.

- The most important dimensions of the motor

- Stator windings

- Design of rotor and its windings

- Performance characteristics

In order to get the above design information the designer desires the consumer specs consisting of Rated output power, efficiency, power factor, rated voltage, number of phases, number of poles, magnetic loading, electric loading, rotor speed, supply frequency, connection of stator winding, type of rotor winding, running conditions, shaft extension information etc. In addition to this specification the designer ought to have the critical factors associated with design equations primarily based totally mostly on which the layout technique is initiated, information concerning the a number of choice of diverse parameters, statistics concerning the availability of particular materials and the restricting values of a number of overall performance parameters consisting of iron and copper losses, no load current, power factor, temperature upward jostle and performance. Let as outline the parameters that display the physical dimensions of the motor which is considered throughout the design. Those dimensions are the primary size of the motor, stator size and the rotor size. Before beginning to decide the value of the size of the motor, the specification of the motor is selected. The requirements to choose out the specification of the motor are as follows.

3.3.3 Criteria for Choice of power factor and efficiency

The standards for the selection of power factor and efficiency under complete load situation depends on the rating of the motor. As the machine rating increases there is a power problem

and successfully of the machine size additionally increases. This is take area due to the fact if the rating of the machine will maximize percentage magnetizing current and losses come to be lower. To decide the volume of the motor, the particular magnetic and electric loading values are required.

3.3.4   Choice of Specific Magnetic loading or Air gap flux density(Bav)

The air gap flux density is one of the primary factors for figuring out core loss. There is moreover every different limitation for choosing of specific magnetic loading among them the flux density in teeth is tons much less, than 1.8 Tesla and flux density with inside the core is between 1.3-1.7 Tesla, for 50 Hz motor, 0.35 – 0.6 Tesla is selected. Within this hassle, choice of specific magnetic loading of better value has a few advantages such as motor length is reduced, cost of the motor decreases and overload ability increases.

3.3.5   Choice of Specific Electric loading (ac)

The specific electric loading shows the whole stator ampere conductor over the periphery. The choice of excessive charge of unique electric loading has the subsequent merits and demerits The merits are reduced size of motor and reduction of the cost. The demerits are lower overload capacity, higher quantity of conductor required, copper losses is excessive and increased temperature rise. The normal electric loading varies from to 10 000 ac/m – 450 000 ac/m. After proper defining of unique magnetic and electric loading, then with the aid of using the output equation the volume or the product of motor is decided. Then the main dimension of the motor is decided primarily based at the standards of the separation of stator bore diameter and gross core length.

3.3.6   The Main Dimension of Six Phase Squirrel Cage Induction Motor

The predominant dimensions of induction motor consist of the stator core diameter (D) and core length of stator (L) as proven within the figure below.
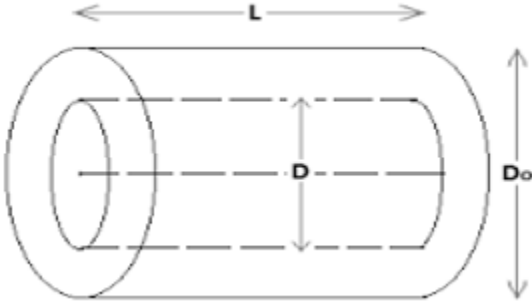

Figure 3.2: Main Dimension of Induction Motor [?]

Separation of D and L

To separate D and L there are a number of design issues based totally on which a appropriate ratio among stator core length and pole pitch may be assumed. The separation requirements of outer diameter and length of stator core are summarized as follows.

- To obtain good overall efficiency: between 1.4 upto 1.6

- To obtain minimum overall cost: between 1.5 upto 2

- To obtain good power factor: between 1 upto 1.3

- To obtain good overall Design: between 1 upto 1.1

Design sheet

The design data for 30hp can be seen in the table **??**. At the completion of the design process, this design sheet lists the data needed for design and material conceptualization. It is separated into three categories: general data, stator data, and rotor data. The general data for the design of six-phase induction motor is given in the table below. As power factor is improved through power factor correction method an excellent efficiency design performs a completely crucial function at the overall performance of induction motors specifically to minimize losses and temperature rise withinside the motor. Therefore it's far really useful to design an induction motor for high-quality performance except specified. Using the requirements in Table above D and L may be separated from D^2L product. However the acquired values of D and L ought to fulfill the circumstance imposed on the value of peripheral velocity. For the everyday plan of an induction motors, the calculated diameter of the motor need to be such that the peripheral velocity must be beneath 30 m/s. However, in case of specifically designed rotor the peripheral velocity may be advanced till 60 m/s. After keeping apart and locating out the values of the crucial dimensions of the motor, the inner parameters of the stator are determined.

3.3.7 Stator Parameters

The stator of an induction motor comprises of stator core and stator slots. There are unique types of stator slots which might be employed in induction motor. Because of the operating overall performance of the induction motors; efficiency, power factor and starting torque highly relies upon the shape of the slots. Therefore, it is crucial to pick out suitable slot for the stator. The three kinds of stator slots are semi closed slots, tapered slots and Circular slots. In the semi-closed slots, slot opening is a great deal smaller than the width of the slot. Hence in this kind of slots assembly of windings is more tough and takes extra time in comparison to open slots and for that reason it's miles costlier. However the air gap traits are higher in comparison to open type slots. In the tapered slots, the opening could be an entire lot smaller than the slot width. However the slot width could be diverse from top of the slot to bottom of the slot with minimum width at the bottom. The circular slot isn't always used most of the time because of issue for construction.

Table 3.1: General design specification of six phase induction motor

Output Power	30hp/22.4KW
Input voltage	415V
Number of poles	4
Speed	1470rpm
Friction and windage losses	3% of output power
Stray losses	1% of output power
Operating temperature	75℃
Type of load	Constant power
Operation motor	Motor
Specific magnetic loading	0.45 Tesla
Specific electric loading	30000 amp.cod/m
Stator current density	1.5 A/mm^2
Stacking factor	0.9
Rotor current density	2 A/mm^2
End current density	8 A/mm^2
End ring mean diameter	4 cm
Space factor	0.4
Lip	1.5 mm
Wedge	3.5 mm
Allowance skewing factor	40 mm
Flux density in stator core	1.4 Tesla
Flux density in rotor core	1.3 Tesla

Selection of number of stator slots

During the design stage, number of stator slots should be precise decided as such this number impacts the cost, weight and working characteristics of the motor. But there are no any regulations for deciding the number of stator slots considering the advantages and disadvantages of deciding on better extensive range slots. We have the subsequent advantages and drawbacks of deciding on better quantity of stator slots. The advantages are reduction in teeth pulsation losses, reduction in leakage reactance and higher over load capacity. The disadvantages are Increasing weight, increasing cost, Increasing magnetizing current, increasing iron losses, poor cooling, increased temperature rise and reduction in efficiency. Based on the above factors, the number of slots per pole per phase is chosen as foremost value. Within attention of the above factors, the chosen number of slot must fulfill the consideration of stator slot pitch at the air gap surface, which must be between 1.5 to 2.5cm.

Slot size

As indicated above, in Figure above there are three types of slots which might be employed for carrying stator windings or conductors of induction motors. These conductors are suitably
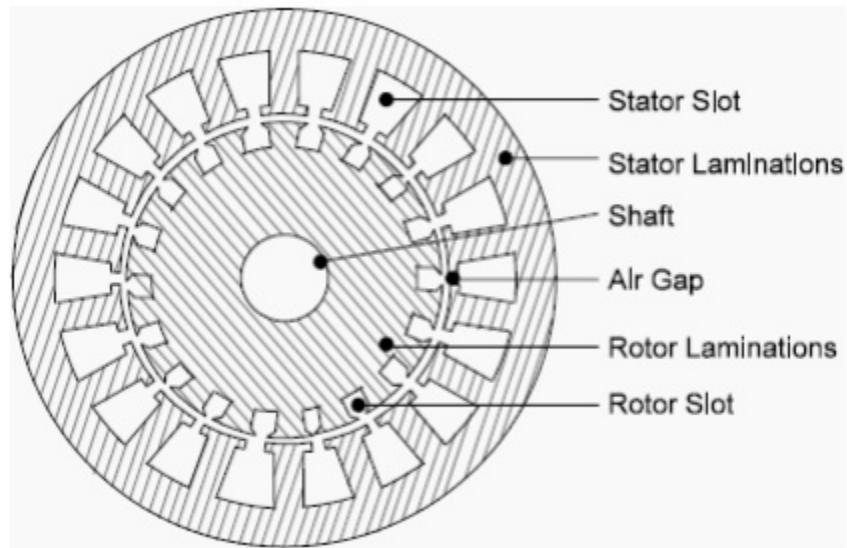
Figure 3.3: Stator and Rotor Slot [?]

prepared along the depth and width of the winding. Stator slots should not be too extensive, major to thin enamel width, which makes the teeth susceptible and maximum flux density can also additionally exceed the permissible limit. Therefore slot width must be decided such that the flux density in teeth must be under permissible limit. In addition, the slots should now no longer be too deep otherwise, the leakage reactance increases. Proper slot insulation as according to the voltage rating of the machine must be supplied before placing the insulated coil with inside the slots, which is known as the slot liner inside a thickness of 0.5mm to 0.7mm. Suitable thickness of insulation referred to as coil separator separates the two layers of coils that have a thickness comparable to slot liner. Wedge is placed on the top of the slot to keep the coils in position within a thickness of 3.5mm to 5mm. Lip of the slot are taken 1mm to 2mm. Slot within conductor and insulation information are shown in Figure below.
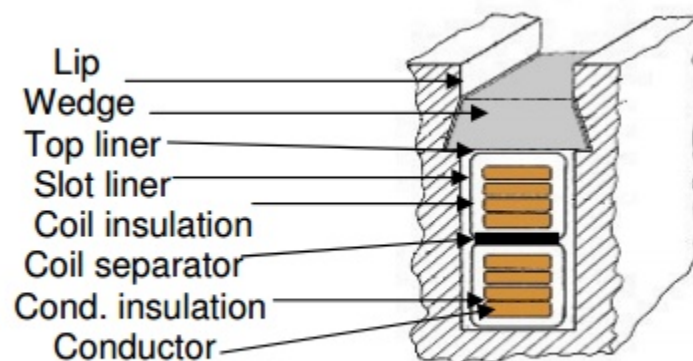
Figure 3.4: Section of slot with conductor and insulation [?]
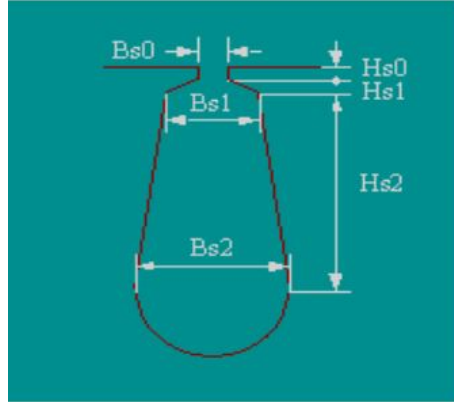
Figure 3.5: Stator shape and Slot dimension [**?**]

Stator winding

Windings were broadly studied for three-phase machines in the past; the critical goal turned into to obtain sinusoidal magneto motive forces. This property implies accurate traits for machines supplied without delay by means of manner of three-phase voltages. With the advent of superior contemporary controls, the need of this winding constraint for the dressmaker Can be re-examined. When each aspect of a coil occupies a slot definitely barring any special coil lying on top of it and the range of coils equals half of the range of slots, the winding is acknowledged as single layer winding. In concentric(chain) windings short-pitched coils cannot be used. The laying of concentrated winding is predicated upon at the coil span and the number of slots per pole per phase. Chain winding may be in shape of half-coiled or whole-coiled. The coils consisting of a pair of pole phase groups underneath of adjacent poles are concentric in case of half coiled concentric winding. The overhangs of those windings are generally organized in or three separate levels or planes. This arrangement is provided a good way to keep away from the crossing of coils below one section group. In whole-coiled concentric windings, each pole phase group is cut up up in to units of concentric coils and every set sharing its return coil aspects with those of some other pole segment crew in the identical phase. Single layer winding is common in small ac machines of power rating underneath 15hp, though this by means of and huge relies upon on the manufacturer. And such machines have huge amount of conductors per slot. In brushless dc machines and permanent magnet synchronous machines single layer fractional slot winding is commonly used. Single layer windings have more efficiency and quieter operations because of the openings of their slim slots. Single layer windings are mainly insulated due to the end connections, which might be separated via huge air areas, which lead them to appropriate for high voltages. The absence of inter layer separator is because of more area issue. Mesh winding is applicable in alternating present day stator winding and the coil span is strange. It is composed of prolonged and short conductors and the variety is predicated upon at the sort of slots per pole per phase. The longer conductors occupy odd slots whilst the short conductors occupy even slots. The lengthy and short conductors are connected. Winding diagram techniques were a challenge of research for decades of the preceding century. Many strategies were developed, every one characterized with the resource

26

of a few benefits and drawbacks. Nowadays, the star of slots is the maximum vast plan device for electrical machine windings. The star slots technique turned into as soon as primarily based on winding distribution table, lets in the layout of all m-phase single or double-layer windings (consisting of overlapping and non-overlapping ones), offering rapid and automatic winding designs. The winding distribution technique is based on the development of a winding distribution table, which permits the task of a completely unique stator slot to a winding phase section. Winding distribution table is a winding diagram example in table shape that may be utilized in a design tool. In this table each row corresponds to a phase (m) and number of columns equals to slots per phase (S_s/m). The definition of the winding distribution table starts with the aid of assigning the slot number one to the primary cell of table (row 1, column 1) .Then, the slot number 2 is assigned to the cell whose distance is same to pole pair cells from the primary one, the slot number 3 to the cell whose distance is same to pole pair cells from the second one, following the orientation of the innovative numbering of the cells of table. If the bear in mind ends in a filled cell, the adjoining empty cell could be crammed with the counted slot. The manner maintains till the table is definitely filled by means of using the slot numbers. The stator data is the information that the software uses to create the stator model.

Table 3.2: Stator Parameters

Stator parameters	value
Slot number	48
Stator lamination Diameter	296mm
Stator bore	195mm
Tooth width	11mm
Slot depth	22mm
Tooth tip depth	1.5mm
Slot opening	1mm
Tooth tip angle	30°

Rotor Parameters

Rotor is the rotating segment of induction motor. There are varieties of rotor construction. One is the squirrel cage rotor and the alternative is the slip ring rotor. Based at the form of its rotor induction motors are named as squirrel cage or slip (wound) ring motor. Most of the induction motor are squirrel cage kind. These are because of the truth of squirrel cage rotor type is having the advantage of rugged, easy in construction, and relatively cheaper. This paper center of interest at the constructing of squirrel cage rotor kind, which is, composed bars of aluminum accommodated in rotor slots that are shorted at give up ring. Before starting describing, the parameters of the rotor allow as outline the air gap between stator and rotor. There is a few hole between stator and rotor that is referred to as an air gap size and a very critical part. The size of the air gap affects the overall performance parameters of the induction motor like power factor, magnetizing current, over load capacity, cooling

and noise. Therefore, size of the air hole is selected considering the benefits and dangers of large air hole length having the advantages of reduction in unbalanced magnetic pull, minimization in tooth pulsation, reduction in noise, increasing cooling, increased overload capability and drawbacks of decreasing power factor and increasing magnetizing current. Because of magnetizing current and power factor being very essential parameters in deciding the overall performance of induction motors, the induction motors are designed for maximum value of air gap or minimal air gap possible.

Number of Rotor Slots

   Numbers of rotor slots are decided on proper on the subject of number of stator slots in any other case unwanted effects might be decided on the beginning of the motor. Crawling and Cogging are the phenomena that are determined because of wrong aggregate of variety of rotor and stator slots and Also, induction motor develops unpredictable hooks and cusps in motor characteristics or the motor run with lot of noise.
The rotor data is the information that the software uses to create the rotor model.

Table 3.3: Rotor Parameters

Rotor parameters	value
Slot number	38
Pole numbers	4
Bar opening	1mm
Bar opening depth	1mm
Bar tip angle	30°
Rotor tooth width	18mm
Air gap	11mm
Shaft diameter	27mm

Shape and Size of the Rotor slots

   In general semi closed with very slim openings is employed for the rotor slots. In case of completely closed slots, the rotor bars are force in shape into the slots from the sides of the rotor. The rotors with closed slots are giving higher overall performance to the motor with inside the following manner.

- As the rotor is closed, the rotor surface is easy on the air gap and eventually the motor draws lower magnetizing current.

- Reduced noise because the air gap characteristics are higher reduced starting current. From this points, it is able to be concluded that semi closed slots are extra suitable and as a end result it is employed in rotors.
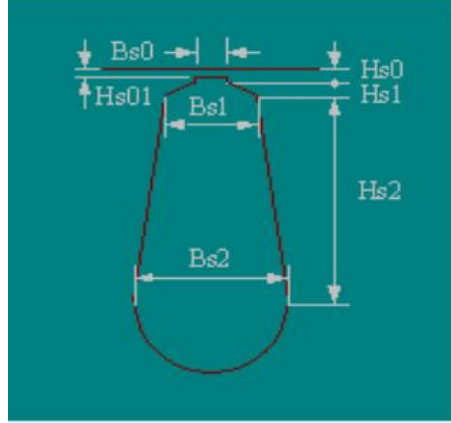
Figure 3.6: Rotor shape and its slot dimension [**?**]

3.4 DESIGN OF SIX PHASE SQUIRREL CAGE INDUCTION MOTOR

Design is a work, which has a user perspective and drives development primarily based totally on your particular customer's needs. Designing frequently necessitates considering the aesthetic, functional, economic and dimensions of every the sketch item and sketch technique. It might also additionally comprise great research, thought, modelling, interactive adjustment, and redesign. The most important cause of designing of an induction motor is to obtain the entire physical dimensions of all of the components of the motor to meet the customer specifications. Those physical dimensions are first modelled by the use of the standard mathematical formula. The formulas required to model an induction motor are starting with the output equation.

3.4.1 Output Equation

It is the mathematical expression, which gives the relation among the variety of physical and electric parameters of the electric machine. In a six-phase induction motor the output equation decide the input apparent power (Q) in KVA that is given by [**?**].

$$Q = \frac{(output in KW)}{(Efficiency * PowerFactor)} \tag{3.5}$$

The input apparent power (KVA rating) of the six phase motor is given by [**?**].

$$Q = 6 * V_{ph} * I_{ph} * 10^{-3} KVA \tag{3.6}$$

where
V_{ph} = Induced EMF per phase (Applied Voltage per phase)
I_{ph} = Current per phase
The voltage induced in the stator winding due to flux induced in the stator is given by [**?**].

$$V_{ph} = 4.44 * T_{ph} * \phi_m * fs * Kw \tag{3.7}$$

where

T_{ph}= No. of turns per phase

ϕ_m= Flux per pole in the air gap

Kw = Winding factor

fs=Supply frequency

The relationship between supply frequency, pole of the motor and synchronous speed is given as follows.

$$fs = \frac{(P * N_s)}{120} = \frac{(P * ns)}{2} \tag{3.8}$$

where

P=Number of poles

N_s= Synchronous speed in RPM

ns = Synchronous speed in RPS

3.4.2 Specific Magnetic Loading (Bav)

The specific magnetic loading in the motor is the product of the flux induced per pole and the total number of pole. In other ways, it is defined as the average value of flux density over the whole surface of air gap in the motor, which is determined as follows.

$$B_{av} = \frac{(Total flux in the air gap)}{(Area of flux path in the gap)} = \frac{(P * \phi_{m)}}{(\pi * D * L)} \tag{3.9}$$

where

D= Stator bore diameter

L= Stator core length

By rewriting equation (**??**), the flux produced per pole is given as follows [**?**].

$$\phi_m = \frac{(B_{av} * \pi * D * L)}{P} \tag{3.10}$$

Total number of conductors on stator of six-phase induction motor is obtained as= $6 * 2T_{ph} = 12 * T_{ph}$

Total Ampere Conductors on Stator= $12 * T_{ph} * I_{ph}$

3.4.3 Specific Electric Loading(ac)

Specific electric loading is defined as the root mean square ampere conductors per meter of armature periphery at the air gap surface or simply defined as electric loading per meter of periphery.

$$ac = \frac{(Total armature ampere conductor)}{(Armature periphery at the air gap)} = \frac{(12T_{ph} * I_{ph})}{(\pi * D)} \tag{3.11}$$

Rewriting equation (**??**), we have the following.

$$T_{ph} * I_{ph} = \frac{(ac * \pi * D)}{12} \tag{3.12}$$

Substituting equation (**??**) into equation (**??**), we have

$$Q = 6 * 4.44 * T_{ph} * I_{ph} * \phi_m * fs * Kw * 10^{-3} KVA \tag{3.13}$$

Substituting equation (**??**), (**??** and (**??**) into equation (**??**), we have

$$Q = 6 * 4.44 * (\frac{ac * \pi * D}{12}) * (\frac{Bav * \pi * D * L}{P}) * (\frac{P * ns}{2}) * Kw * 10^{-3} KVA \tag{3.14}$$

and simplifying, we have

$$Q = 10.955 * B_{av} * ac * \pi^2 * D^2 * L * Kw * ns * 10^{-3} KVA \tag{3.15}$$

Now rewriting equation (**??**), we have

$$Q = (10.955 * Bav * ac * \pi^2 * Kw) * D^2 * L * ns * 10^{-3} KVA \tag{3.16}$$

The output coefficient of motor is given by

$$C0 = 10.955 * B_{av} * ac * \pi^2 * Kw * 10^{-3} \tag{3.17}$$

where $C0$ is called output coefficient Substituting equation (**??**) into equation (**??**), we have

$$Q = C0 * D^2 * L * ns \ KVA \tag{3.18}$$

Equation (**??**) is called output equation of an induction motor.

3.4.4   Factors Affecting Size of Machine

Now the volume of the motor is determined from output equation by finding the value of D^2L and we have

$$D^2 L = \frac{Q}{(C0 * ns)} \tag{3.19}$$

To calculate the main dimensions of the motor; stator core diameter (D) and stator core length (L) must be separated from product first. Equation (**??**) shows that for an induction motor of given rating in KVA, the size or volume of the active parts as given by D^2L depends upon two factors which is output coefficient C0 and the synchronous speed ns. The higher the values of C0 and ns, the volume D^2 L and therefore the size of the machine decreases. Thus to obtain smallest dimensions of the machine the output coefficient C0 must be selected highest possible. Since C0 is proportional to Bav and ac, we conclude that the size and hence the cost of the machine decreases if higher values of Bav and ac are used. Now how much high values of Bav and ac could be used will obviously be decided by the designer by analyzing their effect on important aspects like losses, efficiency, temperature rise, power factor etc. Therefore, only such values of Bav and ac could be used which give the required specifications, performance characteristics coupled with maximum reliability, good efficiency and minimum cost.

Choice of Specific Magnetic Loading (Bav)

The selection of Bav directly affects the core loss and magnetizing current and as a result has an important impact on the power factor, further the flux and consequently the flux density determines the pull out torque.

Power Factor: higher value of Bav means higher value of flux to pass via requiring large magnetizing current. Power factor will become very poor because of magnetizing current is in quadrature with the applied voltage. Therefore, small value of Bav is selected from the power factor point of view. The selected value of Bav appropriate when there is no saturation is occurred in any part of the magnetic circuit. Saturation needs huge magnetizing current and consequently poor energy element.

Core Loss: both the components of the middle loss i.e. hysteresis and eddy current relies upon flux density. An excessive value of Bav way multiplied quantity of core loss affecting the efficiency.

Over Load Capacity: higher value of Bav means large value of flux per pole. For the given voltage per phase, lesser quantity of turns per phase are needed, lowering the leakage reactance, reduced leakage reactance means large dia. of circle diagram and large over load capacity. Summarizing, a small Bav offers good power factor and decreased core loss but a small over load potential. On the other hand, a high Bav offers poor power factor and large quantity of core loss however an amazing over load capacity. Consequently, a moderate value of Bav is to be decided on. For preferred reason, its value can be between 0.3 to 0.6 Tesla.

Choice of Specific Electric Loading (ac)

The following are the factors that are directly influenced by ac selection:

Temperature rise: A high ac value results in increased armature copper losses and, as a result, a higher temperature rise.

Overload capacity: A high ac value results in larger turns per phase and, as a result, higher leakage reactance. This reduces the circle diagram's diameter, resulting in a lower overload capacity value.

Voltage: High-voltage motors require more insulation area than low-voltage motors. As a result, the slot space factor is less. If higher ac is chosen for such motors, a greater armature diameter is required, resulting in a larger motor size. As a result, a high ac value is limited due to temperature rise, overload capacity, and winding voltage. Depending on the machine's capacity and the above conditions, the value of ac ranges from 5000 to 45000 amp.cond/m.

Separation of D And L

To separate D and L there are numerous layout concerns based totally on which a suitable ratio among stator core length and pole pitch may be assumed. Those numbers of layout issues are acquiring of proper power factor, acquiring of desirable performance and minimizing of the typical cost. Among those concerns acquiring of unique performance has a prime component at the life of the motor and the ratio of the core length to the pole pitch. The pole pitch is given by [?].

$$\tau = \frac{(\pi * D)}{P} \tag{3.20}$$

By the use of above equation and ratio of the core length to pole pitch, the main dimensions of the motor is decided. After keeping apart and decide the main dimensions of the motor the next step is modeling of the stator.

Choice of Peripheral Velocity (v)

The peripheral velocity of an induction motor is a significant consideration in its design. The predicted diameter of an induction motor should be such that the peripheral speed does not exceed 30 m/s in a standard design. The diameter D's peripheral velocity is calculated to see if it is within the acceptable limit. If the peripheral velocity exceeds the limit, the diameter D must be recalculated or special care must be given. This important consideration is the design of a unique rotor construction, which will be costly. The peripheral speed of this particular rotor design can range from 60 to 75 meters per second. The perimeter or circumferential velocity of the rotor is referred to as the peripheral velocity. The peripheral velocity is calculated by multiplying the circumference by the velocity.

$$v = \pi * D * ns \frac{m}{sec} \tag{3.21}$$

3.5 Modeling Of Six Phase Squirrel Cage Induction Motor Stator

Stator is the stationary component of an induction motor which is composed of core and stator slots which is equipped for placing stator winding. The model of stator part of the motor determines all parameters of the stator such as number of slot, number of turns per phase, stator phase current, number of conductor used per phase, conductor cross sectional area, area of stator slot, mean turn length, width of stator teeth, flux density in stator teeth, stator core depth and outer diameter of stator. Number of stator slots during the layout stage number of stator slots should be nicely decided on as such these number impacts the cost, weight and operating characteristics of the motor. The stator slot pitch is given by

$$\tau_{ss} = \frac{(\pi * D)}{Ss} \tag{3.22}$$

where
Ss= number of stator slot
τ_{ss}= stator slot pitch

Turns per phase

To determine number of turns per phase of stator winding first determine the induced voltage which is equal to the applied phase voltage is determined as follows.

$$V_{ph} = 4.44 * T_{ph} * fs * \phi_m * Kw \tag{3.23}$$

From equation (**??**) number of turns per phase is determined as follows.

$$T_{ph} = V_{ph}/(4.44 * fs * \phi_m * Kw) \tag{3.24}$$

Number of conductor per phase

After determining number turns per phase the number of conductor per phase in stator winding is determined as follows.

$$Z_{ph} = 2 * T_{ph} \tag{3.25}$$

where
$Zph=$ Number of conductors per phase
The total number of conductor in six-phase induction motor is determined as follows.

$$Z = 6 * 2 * Tph = 12 * Tph \tag{3.26}$$

where
$Z=$ Total number of conductors per phase
Number of conductor per slot is determined as follows.

$$Z_s = \frac{12 * T_{ph}}{S_s} = \frac{Z}{S_s} \tag{3.27}$$

where
$Z=$total number of conductor in stator winding
$Z_s=$number of conductor per slot

Conductor cross sectional area

The cross sectional area of stator conductors is decided from the stator current per phase and suitably decided on value of current density for the stator windings. The area of the stator conductor is given as

$$as = \frac{I_s}{\delta_s} \tag{3.28}$$

where
$\delta_s=$current density in stator winding
$I_S=$ stator current per phase
$as =$cross sectional area of stator conductor

A appropriate value of current density must be decided on considering its benefits and drawbacks. Advantages of better value of current densities are reduction in cross section, reduction in weight, reduction in cost and drawbacks are increase in resistance, increase in copper loss, increase in temperature rise, reduction in efficiency etc. Shape and size of the conductor may be determined primarily based on the conductor cross sectional area. The current density of stator conductor, δ_s is usually assumed between 3 to 5 A/mm^2.

Area of stator slot

Slot is occupied with the aid of using the conductors and the insulation (space factor). Space factor is a constant number which indicate the space of slot occupied by insulation. Almost 25% of the stator area is employed with the aid of using insulation. Once the number

of conductors per slot and cross sectional area of the conductor is determined slot size is decided as

$$s = Z_s * a_s \qquad (3.29)$$

where
$s=$ Slot size
Then the stator slot area is found as copper section per slot/space factor.

$$A_s = \frac{(Z_s * a_s)}{s_f} \qquad (3.30)$$

where
$A_s=$Stator slot area
$s_f=$ space factor
Space factor varies from 0.25 to 0.4.

Length of mean turn of stator winding

Mean turn Length of stator winding is determined by the following formula [?].

$$l_{mt} = 2L + 2.3\tau_p * 0.24 \qquad (3.31)$$

Width of stator teeth

The width of stator teeth is the difference between slot pitch and slot width which is given as

$$W_{st} = \tau_s - w_s = \frac{\phi_m}{\frac{(S_{ss})}{P} * L_i B_{st})} \qquad (3.32)$$

Stator teeth design

The flux density in the stator teeth can be determined as follows.

$$B_{st} = \frac{\phi_m}{(toothareaperpole)} \qquad (3.33)$$

$$B_{st} = \frac{\phi_m}{(numberofteethperpole * netironlength * widthoftooth)} \qquad (3.34)$$

$$B_{st} = \frac{\phi_m}{(\frac{S_{ss}}{P} * L_i W_{st})} \qquad (3.35)$$

where
$L_i=$net iron length=L+ stacking factor
Stacking factor is assumed as 0.95, which is standard for induction motor design.

Stator core depth

There is a certain solid component above the slots with inside the stator that is known as the depth of the stator core. This depth of the stator core may be calculated with the aid of using deciding on appropriate value for the flux density with inside the stator core. Generally the flux density with inside the stator core varying between 1.2 to 1.4 Tesla. Depth of the stator core may be calculated as follows. Flux inside the stator core is half of the flux per pole inside the motor.

$$Area of cross section of stator core = \frac{\phi_m}{(2B_{cs})} \tag{3.36}$$

$$Area of cross section of stator core = L_i d_{cs} \tag{3.37}$$

Since both equation (**??**) and equation (**??**) are both equal, we can equate to find the depth of stator core as follows.

$$d_{cs} = \frac{\phi_m}{(2 * L_i B_{cs})} \tag{3.38}$$

Moreover, the outer diameter of the stator core is determined as follows.

$$D_o = D + 2d_{ss} + 2d_{cs} \tag{3.39}$$

Air Gap Length Determination

The magnetizing current, mechanical factors, pulsation losses, and cooling from the gap surfaces all influence the length of the air gap. The length of the air gap is determined by the following elements. These are the following: Power-factor: The air gap generally consumes the most amount of magneto motive force to pass the flux across it from various areas of the magnetic circuit of a rotating electric machine. As a result, the larger the air gap, the more ampere turns are necessary to pass the flux through it. This will necessitate a significant amount of magnetizing current. The magnetizing current, which accounts for a major portion of the no-load current, tends to diminish the machine's power factor. To get a high power factor, the air gap length Lg must be kept short. Overload capacity: With a long air gap length, the total leakage reactance is minimized. As a result, a low leakage reactance indicates a high overload capacity. To have a large overall over load capacity, the air gap length Lg should be large. Leakage flux varies inversely with the air gap length, resulting in pulsation losses and noise. As a result, a big air gap reduces pulsation loss and noise. The length of the air gap is calculated as follows.

$$L_g = 0.2 + 2\sqrt{DL} \tag{3.40}$$

where

L_g= air gap length between stator and rotor

3.6   Modeling of Six Phase Squirrel Cage Induction Motor Rotor

In order to avoid undesirable effects at the starting of the motor, numbers of rotor slots must be carefully selected in relation to number of stator slots. Those undesirable effects

that comes into being are cogging, crawling, synchronous hooks and noisy. Therefore when selecting the number of rotor slot we must take care to avoid those problems by selecting in the proper combination. Rules for selecting rotor slots To avoid crawling and cogging (and magnetic locking), follow these steps: For a six-phase motor, the difference between the number of stator and rotor slots should not be equal to ±6p. To avoid synchronous hooks and cusps, make sure that the difference between stator and rotor slots is not equal to ±p, ±2p or ±5p. The difference between the number of stator slots and the number of rotor slots shall not equal ±1, ±2, ± (p ± 1) or ± (p ± 2).

Design of rotor bars

Rotor bar current

The rotor bar current of a squirrel cage induction motor is determined by the following formula.

$$I_b = \frac{12 * I_s T_{ph} * kw * p_f}{S_r} \tag{3.41}$$

where
   I_b=rotor bar current
   p_f=power factor

Cross sectional area of rotor bar

The cross sectional area of the rotor bar can be determined by dividing rotor bar current to current density for rotor bars that is assumed as standards. Because the rotor's cooling conditions are better than the stator's, a higher current density can be expected, resulting in a smaller sectional area, higher resistance, rotor conductor losses, and lower efficiency. In other words, when rotor resistance increases, starting torque increases. The rotor bar current density can be estimated to be between 2 and 7 mm^2 based on these merits and demerits. The cross sectional area of the rotor bars can be calculated as follows after assuming current density.

$$A_b = \frac{I_b}{\delta_b} \tag{3.42}$$

where
   A_b=area of rotor bar
   δ_b=current density of rotor bar
   The size of the conductor can be chosen from a standard once the cross sectional area of the rotor bar has been determined.

Size and shape of rotor slots

Rotor slots are commonly used as semi-closed or closed slots with very small or narrow holes. In the case of closed slots, the rotor bars are forced into the slots from the sides of the rotor. As a result, rotors with closed slots provide the motor with better overall performance. Because the air gap characteristics are greater lowered starting current and the rotor surface is smooth at the air gap when the rotor is closed, the motor draws lower magnetizing current

and produces less noise. As a result of these two factors, semi-closed slots are more suited and, as a result, are used in rotors.

Length of rotor bar

The length of the rotor bar is calculated by adding the stator core length and the skewing allowance length. The skewing factor is around 20% of the total length of the core.

$$l_b = L + Skewing Allowance \tag{3.43}$$

where
l_b= rotor bar length

Resistance of rotor bar

The resistivity of the conductor is chosen from sort of conductor used and after knowing the length of the rotor bars the resistance of the rotor bars are often determined as follows.

$$r_b = \frac{\rho_b l_b S_r}{A_b} \tag{3.44}$$

where
r_b= rotor bar resistance
ρ_b= resistivity of the bar conductor

End ring current

All the rotor bars are short circuited by connecting them to the top rings at both the top of rotor. The rotating magnetic flux produced induce an electromotive force within the rotor bars, which can be sinusoidal over one pole pitch. Because the rotor may be a short-circuited body, there's a current flow because of this electromotive force induced. The end ring current is determined as follows.

$$I_e = \frac{I_b S_r}{\pi * P} \tag{3.45}$$

End Ring Area

A cross section area of end rings are determined after determination of end ring current and assuming suitable value for current density within the end rings as follows.

$$A_e = \frac{I_e}{\delta_s} \tag{3.46}$$

where
I_e=end ring current
δ_s=current density in end ring
A_e=area of end ring

Two end ring resistance

The two end ring resistances are calculated from the mean length of the current path in end ring. The mean length of the current path in end ring can be determined as follows.

$$l_{me} = \pi * D_{me} \tag{3.47}$$

where
l_{me}=mean length of current path
D_{me}= mean diameter of end ring
The mean diameter of end ring is assumed as 4 to 6cm less than that of rotor inner diameter. The the end ring resistance is calculated as follows.

$$r_e = \frac{\rho * l_{me}}{A_e} \tag{3.48}$$

where
r_e=resistance of one end ring
But we have two end rings, therefore we multiply it by 2.

$$R_e = 2\frac{\rho * l_{me}}{A_e} \tag{3.49}$$

where
R_e=resistance of two end ring

Area of rotor tooth

The area of rotor tooth can be determined by the following formula.

$$A_{tr} = \frac{W_{tr} L_i S_r}{P} \tag{3.50}$$

where
A_{tr}= area of the rotor tooth
W_{tr}= width of rotor teeth
L_i= net iron length

Flux density in rotor tooth

The flux density in rotor tooth can be calculated as follows.

$$B_t r = \frac{\phi}{A_{tr}} = \frac{\phi}{\frac{(S_r)}{P} * W_t r L_i} \tag{3.51}$$

Where B_{tr}= flux density in rotor tooth

Rotor core depth

The length of the rotor core excluding the depth of the rotor slot is called rotor core depth. It is determined as follows.

$$d_{rc} = \frac{\phi_c}{B_{tr}L_i} = \frac{\phi}{2B_{rc}L_i} \tag{3.52}$$

where
d_{rc}=rotor core depth Then the inner diameter of rotor is obtained as follows.

$$D_{ir} = D_r - 2d_{rs} - 2d_{rc} \tag{3.53}$$

where
D_{ir}=inner rotor diameter
d_{rs}=rotor slot depth

Performance of motor

The performance of an induction motor can be calculated using stator and rotor design data. No load current, no load losses, load losses, no load power factor, full load power factor, full load efficiency, full load slip, and shaft torque are the characteristics in question. The performance value of the determined induction motor can be used to justify stator and rotor parameter values. No-load current Induction motors have no load current as a result of core loss current and magnetizing current. The following formula can be used to calculate the magnetizing current.

$$I_m = \frac{\pi * P * AT}{6T_{ph}Kw} \tag{3.54}$$

where
AT= total magnetizing magneto motive force

Air gap magnetomotive force

After calculating the effective air gap length, which is affected by stator and rotor slot opening and ducts on the air gap, the air gap magnetomotive force may be estimated. The stator slot opening's gap construction factor is calculated as

$$k_{gss} = \frac{y_{ss}}{y_{ss} - k_{css}B_{s0}} \tag{3.55}$$

where
k_{gss}=gap construction factor due to stator slots
k_{css}=carter's coefficient for stator slot opening
The rotor slot opening gap construction factor is calculated as

$$k_{gsr} = \frac{y_{sr}}{y_{sr} - k_{csr}B_{r0}} \tag{3.56}$$

where
k_{gsr}=gap construction factor due to rotor slots

k_{csr}=carter's coefficient for rotor slot opening

The gap construction factor is calculated as a result of both stator and rotor slot opening.

$$k_{gs} = k_{gss}k_{gsr} \qquad (3.57)$$

where

k_{gs}=gap construction factor due to slot

The slot opening and ducts' overall gap construction factor is calculated as

$$k_g = k_{gs}k_{ds} \qquad (3.58)$$

where

k_g=over all gap construction factor

k_{ds}=gap construction factor due to ducts

By multiplying the air gap length by the overall gap construction factor, the effective air gap between the stator and the rotor may be calculated.

$$l_{ge} = l_g k_g \qquad (3.59)$$

50 where

l_{ge}= effective air gap length

l_g=air gap length

Now the required magnetomotive force in the air gap is determined as

$$mmf_g = \frac{B_g l_{ge} * 10^{-3}}{2\mu_o} \qquad (3.60)$$

where

mmf_g= air gap magnetomotive force

B_g=air gap flux density

μ_o=permeability in free space= $4\pi * 10^{-7}$

Magnetomotive force in the teeth of the stator

After determining the flux density in the stator teeth, the ampere-turns per meter required is calculated using the BH curve of the material that the stator core is comprised of. The magnetomotive force in stator teeth is then calculated as follows:

$$mmf_{st} = AT_{st}d_{ss} * 10^{-3} \qquad (3.61)$$

where

mmf_{st}= Magnetomotive force in stator teeth

AT_{st}=ampere turns per meter in stator teeth corresponding to flux density in stator teeth

d_{ss}=depth of stator slot

Magnetomotive force in the core of the stator

The flux density in the stator core is assumed, and the ampere-turn per meter corresponding to this value is calculated using the BH curve of the steel utilized for the stator core. Then, in the stator core, mmf is written as

$$mmf_{sc} = AT_{sc}l_{sc} \tag{3.62}$$

where
mmf_{sc}= Magnetomotive force in stator core
AT_{sc}=ampere turns per meter in stator core corresponding to flux density in stator core
l_{sc}= length of magnetic path through stator core
The length of magnetic path through stator core is determine as The length of magnetic path through stator core is determined as follows.

$$l_{sc} = \frac{(\pi * (D + 2d_{ss} * 10^{-3} + d_{cs} * 10^{-3})}{3P} \tag{3.63}$$

Rotor teeth magnetomotive force

Flux density in rotor teeth is assigned, and the ampere-turn per meter corresponding to this flux density is read from the BH curve of the steel used in rotor manufacturing. The mmf in rotor teeth is then calculated as

$$mmf_{rt} = AT_{rt}d_{sr} * 10^{-3} \tag{3.64}$$

where
mmf_{rt}= magnetomotive force in rotor teeth
AT_{rt}=ampere turns per meter in rotor teeth corresponding to flux density in rotor teeth
d_{sr}= rotor slot depth

Rotor core magnetomotive force

After determining the flux density in the rotor core, the BH curve is used to calculate the ampere turns per meter required in the rotor core. The mmf in the rotor core is then calculated as

$$mmf_{rc} = AT_{rc}l_{rc} \tag{3.65}$$

where
mmf_{rc}= magnetomotive force in rotor core
AT_{rc}=ampere turns per meter in rotor core corresponding to flux density in rotor core
l_{rc}= length of magnetic path through rotor core
The sum of the ampere-turn in the air gap, stator core, rotor core, stator teeth, and rotor teeth equals the total ampere-turn in the motor. The following is how it is determined.

$$AT = AT_g + mmf_{st} + mmf_{sc} + mmf_{rt} + mmf_{rc} \tag{3.66}$$

where AT = total magnetomotive force required

No load losses

The constant losses in induction motors are iron loss in the stator core, iron loss in the stator teeth, stray loss, friction, and windage losses.

Iron loss in stator teeth

Iron loss in stator teeth is determined according to the following steps. First volume of the teeth is determined as follows.

$$V_{st} = A_{st}pd_{ss} * 10^{-3}m^3 \tag{3.67}$$

where
V_{st}=volume of stator teeth
A_{st}=area of stator teeth per pole
Secondly, weight of the teeth is determined by multiplying the volume of teeth by density of the core material.

$$W_{st} = V_{st} * Corematerialdensity \tag{3.68}$$

where
W_{st}=weight of stator teeth
Lastly, iron loss in stator teeth is the product of the specific iron loss for the material from which the core is made and weight of the teeth.

$$P_{fest} = W_{st} * Specificironloss \tag{3.69}$$

where
P_{fest}=iron loss in stator teeth

Iron loss in stator core

Iron loss in stator core is determined according to the following steps. First volume of the stator core is determined as follows.

$$V_{sc} = (D + 2d_{ss} * 10^{-3})(\pi * L * d_{cs} * 10^{-3})m^3 \tag{3.70}$$

where
V_{st}=volume of stator core
Secondly, weight of the stator core is determined by

$$W_{sc} = V_{sc} * Densityofironcore \tag{3.71}$$

where
W_{sc}=weight of stator core
Lastly, iron loss in stator teeth core can be given as

$$P_{fesc} = W_{sc} * Specificironloss \tag{3.72}$$

P_{fesc}=iron loss in stator teeth

Loss component current per phase

The loss component current per phase at no load is the ratio of the total no load loss to the supply phase voltage determined as follows.

$$I_{nlc} = \frac{Total\, no\, load\, losses}{6V_{ph}} \tag{3.73}$$

where

I_{nlc}= no load loss component current

Then no load current is depend on magnetizing and core loss component current and calculated as follows.

$$I_0 = \sqrt{I_m^2 + I_{nlc}^2} \tag{3.74}$$

where

I_0= no load current

I_m= magnetizing current

Then no load power factor is given as

$$pf_{nl} = \frac{I_nlc}{I_0} \tag{3.75}$$

pf_{nl}=no load power factor

Slip

The rotation speed of an induction motor is slower than the rotation speed of the magnetic field, which is known as synchronous speed. Slip is the difference between the rotation of an induction motor's rotor and the rotation of the magnetic field in the motor. The full load slip is calculated as

$$S = \frac{n_s - n_m}{n_s} \tag{3.76}$$

where

S=Slip

n_s= synchronous speed in revolution per second

n_m=mechanical speed of the rotor in revolution per second

Output torque

The output torque is given as

$$\tau_{sh} = \frac{Output\, power}{Shaft\, angular\, speed} = \frac{P_{output}}{\omega_m} \tag{3.77}$$

where

τ_{sh}=shaft torque

Efficiency

Efficiency indicates how much percent of the electrical power converted to mechanical power and how much power is lost. It is determined as

$$\eta = \frac{Outputpower}{Inputpower} * 100 \tag{3.78}$$

3.7 Mathematical Modelling of Six-Phase Squirrel Cage Induction Motor

In order to model the six-phase induction machine,the dq transformation is applied and the synchronous reference frame is adopted. Six-phase induction motor can be modelled in two ways. These are:

- Mathematical model of the six phase induction motor is assumed as same as the model of dual stator (DSIM) three-phase induction motor or

- By representing, six phase induction motor by dynamic equivalent per phase circuit.

The sinusoidal voltage equation of a six-phase induction machine is written as follows,

$$V_{as} = V cos\omega_e t \tag{3.79}$$

$$V_{bs} = V cos\omega_e t - \frac{\pi}{3} \tag{3.80}$$

$$V_{cs} = V cos\omega_e t - \frac{2\pi}{3} \tag{3.81}$$

$$V_{ds} = V cos\omega_e t - \frac{3\pi}{3} \tag{3.82}$$

$$V_{es} = V cos\omega_e t - \frac{4\pi}{3} \tag{3.83}$$

$$V_{fs} = V cos\omega_e t - \frac{5\pi}{3} \tag{3.84}$$

The dq axis reference frame is fixed in the rotor, which rotates at speed of ω_r. The dq voltage equations of six-phase induction motor are expressed as follows in a r reference frame.

$$V_{q1} = R_{s1}i_{q1} + \omega_k * \psi_{d1} + p\psi_{q1} \tag{3.85}$$

$$V_{d1} = R_{s1}i_{d1} - \omega_k * \psi_{q1} + p\psi_{d1} \tag{3.86}$$

$$V_{q2} = R_{s2}i_{q2} + \omega_k\psi_{d2} + p\psi_{q2} \tag{3.87}$$

$$V_{d2} = R_{s2}i_{d2} - \omega_k\psi_{q2} + p\psi_{d2} \tag{3.88}$$

$$V_{qr} = R_r i_{qr} + (\omega_k - \omega_r)\psi_{dr} + p\psi_{qr} \tag{3.89}$$

$$V_{dr} = R_r i_{dr} - (\omega_k - \omega_r)\psi_{qr} + p\psi_{dr} \tag{3.90}$$

where V_{q1}, V_{q2}, are stator q -axis voltage components,

V_{d1}, V_{d2}, are stator d -axis voltage components,

V_{qr}, V_{dr}, are rotor q -axis and d-axis voltage components,

R_{s1}, R_{s2} are stator q-axis resistances,

R_r is rotor resistance,

p is $\frac{d}{d_t}$ operator,

ω_k is synchronous speed and

ω_r is rotor speed

The flux linkage equations are given below.

$$\psi_{q1} = L_{l1} i_{q1} + L_{lm}(i_{q1} + i_{q2}) + L_{mq}(i_{q1} + i_{q2} + i_{qr}) \tag{3.91}$$

$$\psi_{d1} = L_{l1} i_{d1} + L_{lm}(i_{d1} + i_{d2}) + L_{md}(i_{d1} + i_{d2} + i_{dr}) \tag{3.92}$$

$$\psi_{q2} = L_{l2} i_{q2} + L_{lm}(i_{q1} + i_{q2}) + L_{mq}(i_{q1} + i_{q2} + i_{qr}) \tag{3.93}$$

$$\psi_{d2} = L_{l2} i_{d2} + L_{lm}(i_{d1} + i_{d2}) + L_{md}(i_{d1} + i_{d2} + i_{dr}) \tag{3.94}$$

$$\psi_{qr} = L_{lr} i_{qr} + L_{mq}(i_{q1} + i_{q2} + i_{qr}) \tag{3.95}$$

$$\psi_{dr} = L_{lr} i_{dr} + L_{md}(i_{d1} + i_{d2} + i_{dr}) \tag{3.96}$$

where

ψ_{q1}, ψ_{q2} are stator q -axis flux linkage components,

ψ_{d1}, ψ_{d2} are stator d -axis flux linkage components,

ψ_{qr}, ψ_{dr} are rotor q -axis and d -axis flux-linkage components,

i_{q1}, i_{q2} are stator q -axis current components,

i_{d1}, i_{d2} are stator d -axis current components,

i_{qr}, i_{dr} are rotor q -axis and d -axis current components,

L_{l1}, L_{l2} are stator leakage inductances,

L_{mq} is air gap inductance of q -axis,

L_{md} is air gap inductance of d -axis,

L_m is air gap inductance,

L_{lm} is stator mutual leakage inductance and

L_{lr} is rotor leakage inductance,

The above equation suggests the overall equivalent circuit of six phase squirrel cage induction motor. The dynamic equivalent representation is modeled and developed with assumption of presence of similar three phase windings in the stator with their leakage inductance L_{l1} and mutual leakage inductance L_{lm}.

To find the interdependence of each variables, substituting flux linkage expressions equation (**??**)-(**??**) into voltage equations equation (**??**)-(**??**), to drive the dependence of voltages on current in rotating reference frame is obtained as follows: First assume the following for simplicity.

$$L_m = L_{mq} = L_{md} \tag{3.97}$$

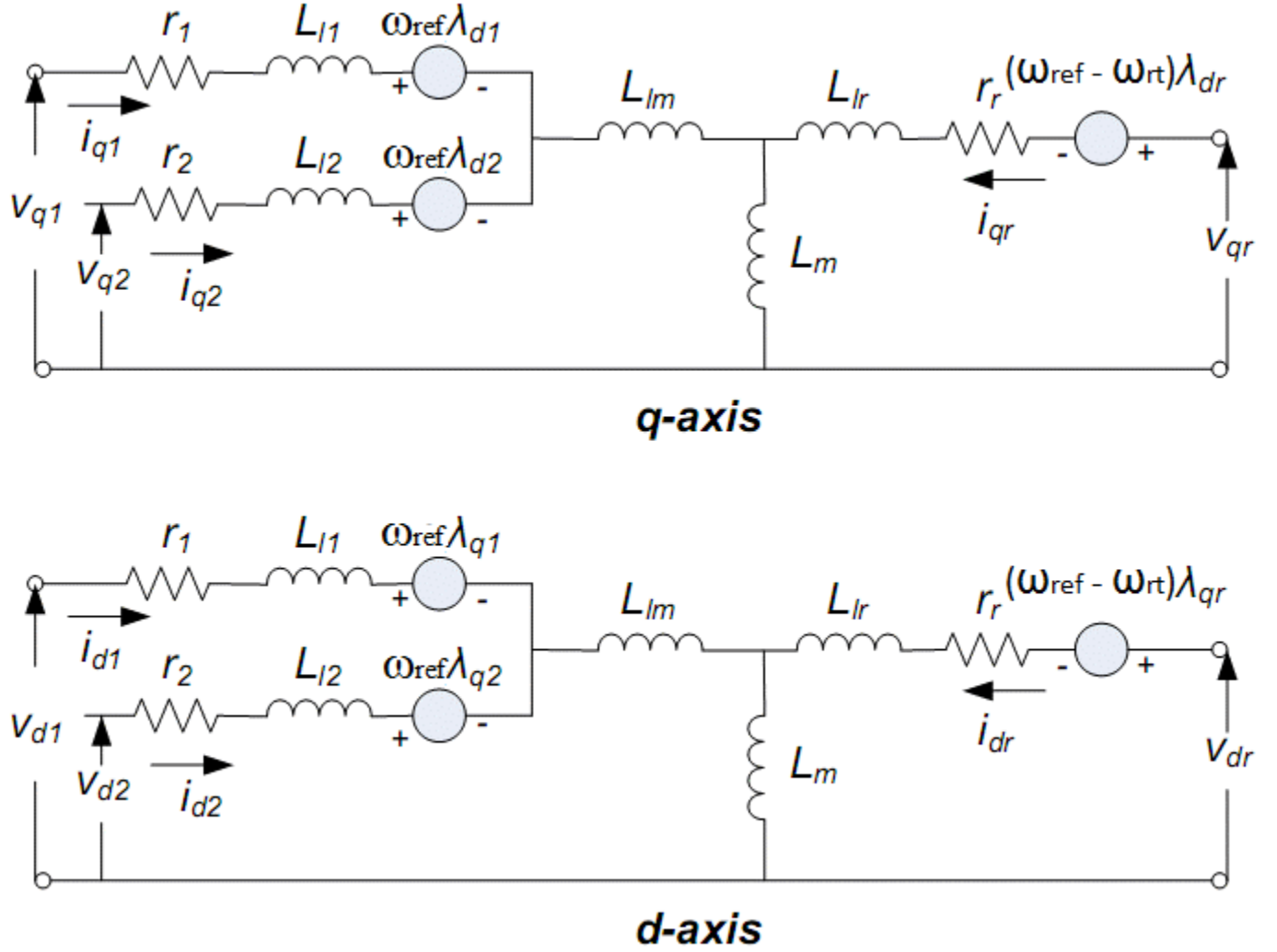$$L_1 = L_{l1} + L_{lm} + L_m \tag{3.98}$$

q-axis

d-axis

Figure 3.7: Dynamic Equivalent Circuit of Six-phase Induction Motor [?].
a) q-axis equivalent circuit of a six-phase induction motor in arbitrary reference frame
b) d-axis equivalent circuit of a six-phase induction motor in arbitrary reference frame

$$L_2 = L_{lm} + L_m \tag{3.99}$$

$$L_3 = L_{l2} + L_{lm} + L_m \tag{3.100}$$

$$L_r = L_{lr} + L_m \tag{3.101}$$

Substituting equation (??) and equation (??) into the equation (??), we have the following.

$$V_{q1} = R_{s1}i_{q1} + \omega_k(L_{l1}i_{d1} + L_{lm}(i_{d1} + i_{d2}) + L_{md}(i_{d1} + i_{d2} + i_{dr})) + p(L_{l1}i_{q1}$$
$$+ L_{lm}(i_{q1} + i_{q2}) + L_{mq}(i_{q1} + i_{q2} + i_{qr})) \tag{3.102}$$

By rearranging the above equation we have

$$V_{q1} = R_{s1}i_{q1} + \omega_k i_{d1}(L_{l1} + L_{lm} + L_{md}) + \omega_k i_{d2}(L_{lm} + L_{md}) + \omega_k i_{dr}(L_{md})$$
$$+ pi_{q1}(L_{l1} + L_{lm} + L_{mq}) + pi_{q2}(L_{lm} + L_{mq}) + pi_{qr}L_{mq} \tag{3.103}$$

47

Then substituting equation (**??**), (**??**) and (**??**) into equation (**??**), we have the following simplified equation.

$$V_{q1} = R_{s1}i_{q1} + \omega_k L_1 i_{d1} + \omega_k L_2 i_{d2} + \omega_k L_m i_{dr} + L_1 p i_{q1} + L_2 p i_{q2} + L_m p i_{qr} \qquad (3.104)$$

Substituting equation (**??**) and equation (**??**) into the equation (**??**), we have the following.

$$V_{d1} = R_{s1}i_{d1} - \omega_k(L_{l1}i_{q1} + L_{lm}(i_{q1} + i_{q2}) + L_{md}(i_{q1} + i_{q2} + i_{qr})) + p(L_{l1}i_{d1}$$
$$+ L_{lm}(i_{d1} + i_{d2}) + L_{mq}(i_{d1} + i_{d2} + i_{dr})) \qquad (3.105)$$

By rearranging the above equation, we have

$$V_{d1} = R_{s1}i_{d1} - \omega_k i_{q1}(L_{l1} + L_{lm} + L_{md}) - \omega_k i_{q2}(L_{lm} + L_{md}) - \omega_k i_{qr}(L_{md})$$
$$+ p i_{d1}(L_{l1} + L_{lm} + L_{mq}) + p i_{d2}(L_{lm} + L_{mq}) + p i_{dr)}L_{mq} \qquad (3.106)$$

Then substituting equation (**??**), (**??**) and (**??**) into equation (**??**), we have the following simplified equation.

$$V_{d1} = R_{s1}i_{d1} - \omega_k L_1 i_{q1} - \omega_k L_2 i_{q2} - \omega_k L_m i_{qr} + L_1 p i_{d1} + L_2 p i_{d2} + L_m p i_{dr} \qquad (3.107)$$

Substituting equation (**??**) and equation (**??**) into the equation (**??**), we have the following.

$$V_{q2} = R_{s2}i_{q2} + \omega_k(L_{l2}i_{d2} + L_{lm}(i_{d1} + i_{d2}) + L_{md}(i_{d1} + i_{d2} + i_{dr})) + p(L_{l2}i_{q2})$$
$$+ L_{lm}(i_{q1} + i_{q2}) + L_{mq}(i_{q1} + i_{q2} + i_{qr})) \qquad (3.108)$$

By rearranging the above equation we have

$$V_{q2} = R_{s2}i_{q2} + \omega_k(L_{lm} + L_{md})i_{d1} + \omega_k(L_{l2} + L_{lm} + L_{md})i_{d2} + \omega_k(L_{md})i_{dr}$$
$$+ p i_{q2}(L_{l2} + L_{lm} + L_{mq}) + p i_{q1}(L_{lm} + L_{mq}) + p i_{dr}(L_{mq}) \qquad (3.109)$$

Then substituting equation (**??**), (**??**) and (**??**) into equation (**??**) we have the following simplified equation.

$$V_{q2} = R_{s2}i_{q2} + \omega_k L_2 i_{d1} + \omega_k L_3 i_{d2} + \omega_k L_m i_{dr} + L_3 p i_{q2} + L_2 p i_{q1}$$
$$+ L_m p i_{dr} \qquad (3.110)$$

Substituting equation (**??**) and equation (**??**) into the equation (**??**), we have the following.

$$V_{d2} = R_{s2}i_{d2} - \omega_k(L_{l2}i_{q2} + L_{lm}(i_{q1} + i_{d2}) + L_{md}(i_{q1} + i_{q2} + i_{qr})) + p(L_{l2}i_{d2})$$
$$+ L_{lm}(i_{d1} + i_{d2}) + L_{mq}(i_{d1} + i_{d2} + i_{dr})) \qquad (3.111)$$

By rearranging the above equation we have

$$V_{d2} = R_{s2}i_{d2} - \omega_k(L_{lm} + L_{md})i_{q1} - \omega_k(L_{l2} + L_{lm} + L_{md})i_{q2} - \omega_k(L_{md})i_{qr}$$
$$+ p i_{d2}(L_{l2} + L_{lm} + L_{mq}) + p i_{d1}(L_{lm} + L_{mq}) + p i_{dr}(L_{mq}) \qquad (3.112)$$

Then substituting equation (**??**), (**??**) and (**??**) into equation (**??**), we have the following simplified equation.

$$V_{d2} = R_{s2}i_{d2} - \omega_k L_2 i_{q1} - \omega_k L_3 i_{q2} - \omega_k L_m i_{qr} + L_3 p i_{d2} + L_2 p i_{d1} + L_m p i_{dr} \qquad (3.113)$$

Substituting equation (**??**) and equation (**??**) into the equation (**??**), we have the following.

$$V_{qr} = R_r i_{qr} + (\omega_k - \omega_r)(L_{lr} i_{dr} + L_{md}(i_{d1} + i_{d2} + i_{dr})) + p(L_{lr} i_{qr} + L_{mq}(i_{q1} + i_{q2} + i_{qr})) \quad (3.114)$$

By rearranging the above equation we have

$$V_{qr} = R_r i_{qr} + (\omega_k - \omega_r))(L_{md})i_{d1} + (\omega_k - \omega_r)(L_{md})i_{d2} + (\omega_k - \omega_r)(L_{lr} + L_{md})i_{dr}$$
$$+(L_{mq})p i_{q1} + (L_{mq})p i_{q2} + (L_{lr} + L_{mq})p i_{dr} \quad (3.115)$$

Then substituting equation (**??**) and (**??**) into equation (**??**), we have the following simplified equation.

$$V_{qr} = R_r i_{qr} + (\omega_k - \omega_r)L_m i_{d1} + (\omega_k - \omega_r)L_m i_{d2} + (\omega_k - \omega_r)L_r i_{dr}$$
$$+L_m p i_{q1} + L_m p i_{q2} + L_r p i_{qr} \qquad (3.116)$$

Substituting equation (**??**) and equation (**??**) into the equation (**??**), we have the following.

$$V_{dr} = R_r i_{dr} - (\omega_k - \omega_r)(L_{lr} i_{qr} + L_{md}(i_{q1} + i_{q2} + i_{qr})) + p(L_{lr} i_{dr} + L_{mq}(i_{d1} + i_{d2} + i_{dr})) \quad (3.117)$$

By rearranging the above equation we have

$$V_{dr} = R_r i_{dr} - (\omega_k - \omega_r))(L_{mq})i_{q1} - (\omega_k - \omega_r)(L_{mq})i_{q2} - (\omega_k - \omega_r)(L_{lr} + L_{mq})i_{qr}$$
$$+(L_{md})p i_{d1} + (L_{md})p i_{d2} + (L_{lr} + L_{md})p i_{dr} \quad (3.118)$$

Then substituting equation (**??**) and (**??**) into equation (**??**), we have the following simplified equation.

$$V_{dr} = R_r i_{qr} - (\omega_k - \omega_r)L_m i_{q1} - (\omega_k - \omega_r)L_m i_{q2} - (\omega_k - \omega_r)L_r i_{qr}$$
$$+L_m p i_{d1} + L_m p i_{d2} + L_r p i_{dr} \qquad (3.119)$$

Now rewriting equation (**??**), (**??**), (**??**), (**??**), (**??**) and (**??**) in the following manner

$$V_{q1} = R_{s1}i_{q1} + \omega_k L_1 i_{d1} + 0 i_{q2} + \omega_k L_2 i_{d2} + 0 i_{qr} + \omega_k L_m i_{dr} + L_1 p i_{q1} + 0 p i_{d1}$$
$$+L_2 p i_{q2} + 0 p i_{d2} + L_m p i_{qr} + 0 p i_{dr} \qquad (3.120)$$

$$V_{d1} = R_{s1}i_{d1} - \omega_k L_1 i_{q1} - \omega_k L_2 i_{q2} + 0 i_{d2} - \omega_k L_m i_{qr} + 0 i_{dr} + 0 p i_{q1} + L_1 p i_{d1}$$
$$+0 p i_{q2} + L_2 p i_{d2} + 0 p i_{qr} + L_m p i_{dr} \qquad (3.121)$$

$$V_{q2} = 0 i_{q1} + \omega_k L_2 i_{d1} + R_{s2}i_{q2} + \omega_k L_3 i_{d2} + 0 i_{qr} + \omega_k L_m i_{dr} + L_2 p i_{q1} + 0 p i_{d2}$$
$$+L_3 p i_{q2} + 0 p i_{d2} + L_m p i_{qr} + 0 p i_{dr} \qquad (3.122)$$

$$V_{d2} = R_{s2}i_{d2} - \omega_k L_2 i_{q1} - \omega_k L_3 i_{q2} - \omega_k L_m i_{qr} + 0pi_{q1} + L_2 pi_{d1} + 0pi_{q2}$$
$$+ L_3 pi_{d2} + 0pi_{qr} + L_m pi_{dr} \qquad (3.123)$$

$$V_{qr} = 0i_{q1} + (\omega_k - \omega_r)L_m i_{d1} + 0i_{q2} + (\omega_k - \omega_r)L_m i_{d2} + R_r i_{dr} + (\omega_k - \omega_r)L_r i_{dr}$$
$$+ L_m pi_{q1} + 0i_{d1} + L_m pi_{q2} + 0i_{d2} + L_r pi_{qr} + 0i_{dr} \qquad (3.124)$$

$$V_{dr} = -(\omega_k - \omega_r)L_m i_{q1} + 0i_{d1} - (\omega_k - \omega_r)L_m i_{q2} + 0i_{d2} - (\omega_k - \omega_r)L_r i_{qr} + R_r i_{dr}$$
$$+ 0pi_{q1} + L_m pi_{d1} + 0pi_{q2} + L_m pi_{d2} + 0pi_{qr} + L_r pi_{dr} \qquad (3.125)$$

Now using state variable method, equation (**??**) -(**??**) can be represented in a state variable form as follows.

$$
\begin{bmatrix} V_{q1} \\ V_{d1} \\ V_{q2} \\ V_{d2} \\ V_{qr} \\ V_{dr} \end{bmatrix} =
\begin{bmatrix}
R_{s1} & \omega_k L_1 & 0 & \omega_k L_2 & 0 & \omega_k L_m \\
-\omega_k L_1 & R_{s1} & -\omega_k L_2 & 0 & -\omega_k L_m & 0 \\
0 & \omega_k L_2 & R_{s2} & \omega_k L_3 & 0 & -\omega_k L_m \\
-\omega_k L_2 & 0 & -\omega_k L_3 & R_{s2} & -\omega_k L_m & 0 \\
0 & (\omega_k - \omega_r)L_m & 0 & (\omega_k - \omega_r)L_m & R_r & (\omega_k - \omega_r)L_r \\
-(\omega_k - \omega_r)L_m & 0 & -(\omega_k - \omega_r)L_m & 0 & -(\omega_k - \omega_r)L_r & R_r
\end{bmatrix}
$$

$$
* \begin{bmatrix} i_{q1} \\ i_{d1} \\ i_{q2} \\ i_{d2} \\ i_{qr} \\ i_{dr} \end{bmatrix} +
\begin{bmatrix}
L_1 & 0 & L_2 & 0 & L_m & 0 \\
0 & L_1 & 0 & L_2 & 0 & L_m \\
L_2 & 0 & L_3 & 0 & L_m & 0 \\
0 & L_2 & 0 & L_3 & 0 & L_m \\
L_m & 0 & L_m & 0 & L_r & 0 \\
0 & L_m & 0 & L_m & 0 & L_r
\end{bmatrix}
\begin{bmatrix} pi_{q1} \\ pi_{d1} \\ pi_{q2} \\ pi_{d2} \\ pi_{qr} \\ pi_{dr} \end{bmatrix}
$$

Or in simple form X'=AI+BpI

where

$$
A = \begin{bmatrix}
R_{s1} & \omega_k L_1 & 0 & \omega_k L_2 & 0 & \omega_k L_m \\
-\omega_k L_1 & R_{s1} & -\omega_k L_2 & 0 & -\omega_k L_m & 0 \\
0 & \omega_k L_2 & R_{s2} & \omega_k L_3 & 0 & -\omega_k L_m \\
-\omega_k L_2 & 0 & -\omega_k L_3 & R_{s2} & -\omega_k L_m & 0 \\
0 & (\omega_k - \omega_r)L_m & 0 & (\omega_k - \omega_r)L_m & R_r & (\omega_k - \omega_r)L_r \\
-(\omega_k - \omega_r)L_m & 0 & -(\omega_k - \omega_r)L_m & 0 & -(\omega_k - \omega_r)L_r & R_r
\end{bmatrix}
$$

$$
B = \begin{bmatrix}
L_1 & 0 & L_2 & 0 & L_m & 0 \\
0 & L_1 & 0 & L_2 & 0 & L_m \\
L_2 & 0 & L_3 & 0 & L_m & 0 \\
0 & L_2 & 0 & L_3 & 0 & L_m \\
L_m & 0 & L_m & 0 & L_r & 0 \\
0 & L_m & 0 & L_m & 0 & L_r
\end{bmatrix}
$$

3.7.1   Mechanical Model

The mechanical model of a six-phase induction machine is the equation of motion of the machine and the driven load, as shown below. The figure **??** suggests the following equation.
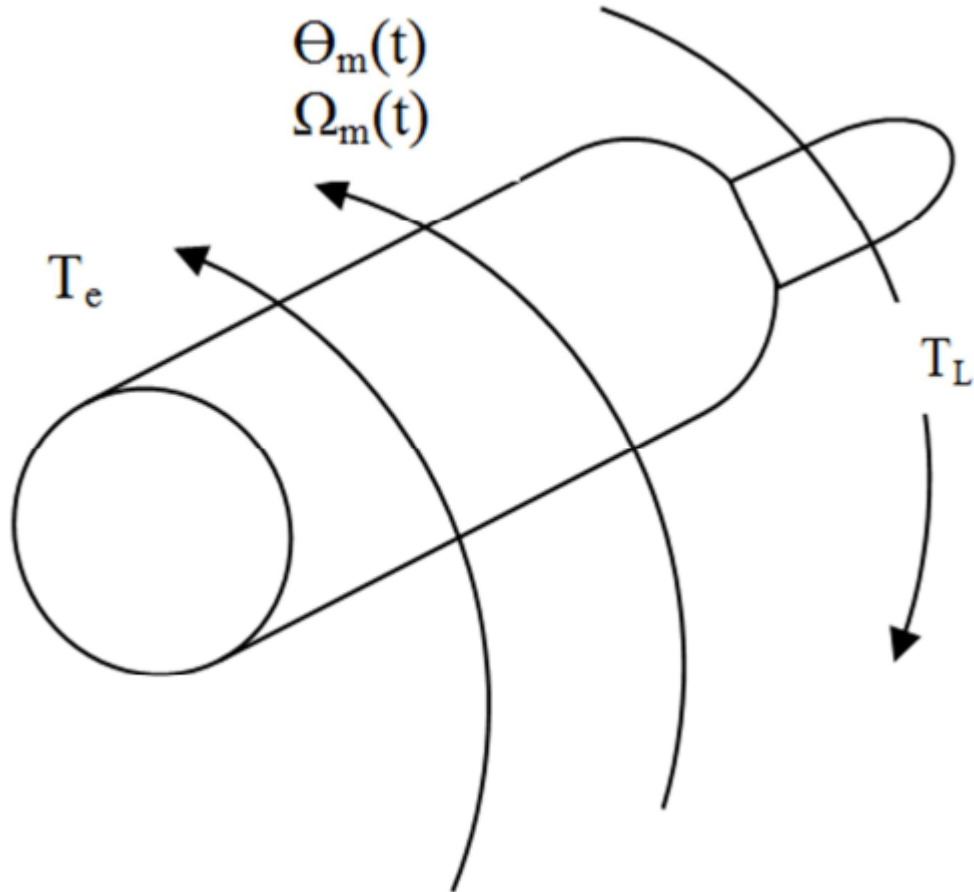

Figure 3.8: Induction Motor Mechanical Model [?].

$$J_m * p^2 * \theta_m = Te - B - TL \qquad (3.126)$$

The combined rotor and load viscous friction (B) is appropriately zero, so that, we have the following equation from equation (**??**).

$$J_m * \frac{d}{dt^2}^2 * \theta_m = Te\text{-}TL \qquad (3.127)$$

Now decomposing equation (**??**) into two first-order differential equation gives the following result. Since

$$\frac{d}{dt}(\theta_m) = \omega_m \qquad (3.128)$$

Therefore, we have

$$J_m * \frac{d}{dt}\left(\frac{d}{dt}(\theta_m)\right) = (Te\text{--}TL) \tag{3.129}$$

Substituting equation (**??**) into equation (**??**), we obtain the following.

$$J_m * \frac{d}{dt}(\omega_m) = (Te\text{--}TL) \tag{3.130}$$

We know that

$$\omega_r = \omega_m * \frac{d}{dt} \tag{3.131}$$

And

$$\theta_r = \theta_m * \frac{d}{dt} \tag{3.132}$$

where
  ω_m= angular velocity of the rotor,
  θ_m= rotor angular position,
  θ_r= electrical rotor angular position,
  ω_r= electrical angular velocity,
  J_m= combined rotor and load inertia coefficient and
  TL= load torque

3.7.2 Linearization of Equations for Stability Analysis of Six Phase Induction Motor

While developing the linearized model of the motor, some important simplifying assumptions are made:

- Both sets of stator winding's are symmetrical so as to have a perfect sinusoidal distribution along the air-gap,

- Existence of space harmonics is neglected, ensuring the flux and magneto motive forces are sinusoidal in space,

- Saturation and hysteresis effects are neglected,

- Skin effect is neglected, winding's resistance are not dependent on frequency.

The voltage equations of stationary reference axes are given by the matrix equations as follows.

$$V = Ri + Lpi + G\theta \cdot i \tag{3.133}$$

where p is d/dt
  V is voltage vectors,
  i is current vectors,
  R is the resistance matrix,
  L is the inductance matrix and
  G is the rotational inductance matrix

$\theta\cdot$ is speed

The Torque equations of stationary reference axes are given by the matrix equations as follows.

$$T_1 = F\theta\cdot + Jp\theta\cdot - i_t Gi \tag{3.134}$$

where

Tl is the shaft torque,

F is the friction coefficient,

$F\theta\cdot$ is the frictional torque,

$Jp\theta\cdot$ is the inertia torque,

J is the moment of inertia and

$i_t Gi$ is the electromechanical torque

Assumptions

$F\theta\cdot$ is assumed to be proportional to the speed $\theta\cdot$

$i_t Gi$ is assumed that the currents are not complex or currents must be real.

Suppose that the system is running under steady state constant speed conditions represented by the equations above. When there is a small displacement from these steady state conditions, the equations may be written as follows.

$$(V + \Delta V) = R(i + \Delta i) + Lp(i + \Delta i) + G(\theta\cdot + \Delta\theta\cdot)(i + \Delta i) \tag{3.135}$$

$$(T_1 + \Delta T_1) = F(\theta\cdot + \Delta\theta\cdot) + Jp(\theta\cdot + \Delta\theta\cdot) - (i + \Delta i)_t G(i + \Delta i) \tag{3.136}$$

Neglecting the second-order small quantities and then subtracting the steady state equation (**??**) and (**??**) from Equation (**??**) and (**??**), respectively, the equations describing the small displacements after simplifications will be given by

$$\Delta V = R\Delta i + Lp\Delta i + G\Delta\theta\cdot i + G\theta\cdot\Delta i \tag{3.137}$$

$$\Delta T_1 = F\Delta\theta\cdot + Jp\Delta\theta\cdot - \Delta i_t Gi - i_t G\Delta i \tag{3.138}$$

Now $\Delta\theta\cdot$ is a scalar so that $G\Delta\theta\cdot i$ is equal to $Gi\Delta\theta\cdot$ and $\Delta i_t Gi$ is a scalar and is, therefore, equal to its own transpose $i_t G_t\Delta i$. $\theta\cdot$, i, and i_t are the steady state values.

The relationship between small changes in applied voltage and torque and the associated variations in current and speed from steady state values is given by the two equations above. From equation (**??**) to (**??**), the voltage equations for the six-phase induction machine with currents as state variables may be expressed in the synchronously rotating reference frame by setting $\omega_k = \omega_e$ as

$$V = ZI \tag{3.139}$$

where

$$V = \begin{bmatrix} v_{q1} \\ v_{d1} \\ v_{q2} \\ v_{d2} \\ v'_{qr} \\ v'_{dr} \end{bmatrix}, I = \begin{bmatrix} i_{q1} \\ i_{d1} \\ i_{q2} \\ i_{d2} \\ i'_{qr} \\ i'_{dr} \end{bmatrix}$$

Now using equation (**??**),(**??**),(**??**),(**??**),(**??**) and (**??**) we are going to derive for electrical transient impedance matrix [Z]. These equations are rearranged and written as follows.

$$V_{q1} = \frac{R_{s1} + p(x_1 + x_{lm})}{\omega_b} i_{q1} + \frac{\omega_e(x_1 + x_{lm})}{\omega_b} i_{d1} + \frac{p(x_{lm} + x_m)}{\omega_b} i_{q2} + \frac{\omega_e(x_{lm} + x_m)}{\omega_b} i_{d2}$$
$$+ \frac{px_m}{\omega_b} i'_{qr} + \frac{\omega_e x_m}{\omega_b} i'_{dr} \quad (3.140)$$

$$V_{d1} = -\frac{\omega_e(x_1 + x_{lm})}{\omega_b} i_{q1} + \frac{R_{s1} + p(x_1 + x_{lm})}{\omega_b} i_{d1} - \frac{\omega_e(x_{lm} + x_m)}{\omega_b} i_{q2}$$
$$+ \frac{p(x_{lm} + x_m)}{\omega_b} i_{d2} - \frac{\omega_e x_m}{\omega_b} i'_{qr} + \frac{px_m}{\omega_b} i'_{dr} \quad (3.141)$$

$$V_{q2} = \frac{p(x_m + x_{lm})}{\omega_b} i_{q1} + \frac{\omega_e(x_m + x_{lm})}{\omega_b} i_{d1} + \frac{R_{s2} + p(x_2 + x_{lm})}{\omega_b} i_{q2} + \frac{\omega_e(x_2 + x_{lm})}{\omega_b} i_{d2}$$
$$+ \frac{px_m}{\omega_b} i'_{qr} + \frac{\omega_e x_m}{\omega_b} i'_{dr} \quad (3.142)$$

$$V_{d2} = -\frac{\omega_e(x_m + x_{lm})}{\omega_b} i_{q1} + \frac{p(x_m + x_{lm})}{\omega_b} i_{d1} - \frac{\omega_e(x_2 + x_{lm})}{\omega_b} i_{q2}$$
$$+ \frac{R_{s2} + p(x_2 + x_{lm})}{\omega_b} i_{d2} - \frac{\omega_e x_m}{\omega_b} i'_{qr} + \frac{px_m}{\omega_b} i'_{dr} \quad (3.143)$$

$$V'_{qr} = \frac{px_m}{\omega_b} i_{q1} + \frac{(\omega_e - \omega_r)\omega_e x_m}{\omega_b^2} i_{d1} + \frac{px_m}{\omega_b} i_{q2} + \frac{(\omega_e - \omega_r)\omega_e x_m}{\omega_b^2} i_{d2}$$
$$+ \frac{R'_r + px'_r}{\omega_b} i'_{qr} + \frac{(\omega_e - \omega_r)\omega_e x'_r}{\omega_b^2} i'_{dr} \quad (3.144)$$

$$V'_{dr} = -\frac{(\omega_e - \omega_r)\omega_e x_m}{\omega_b^2} i_{q1} + \frac{px_m}{\omega_b} i_{d1} - \frac{(\omega_e - \omega_r)\omega_e x_m}{\omega_b^2} i_{q2} + \frac{px_m}{\omega_b} i_{d2}$$
$$+ \frac{(\omega_e - \omega_r)\omega_e x'_r}{\omega_b^2} i'_{qr} + \frac{R'_r + px'_r}{\omega_b} i'_{dr} \quad (3.145)$$

Rewriting the above equations (??) to (??) in the matrix form we have the following.

$$
\begin{bmatrix} V_{q1} \\ V_{d1} \\ V_{q2} \\ V_{d2} \\ V'_{qr} \\ V'_{dr} \end{bmatrix} =
\begin{bmatrix}
\frac{R_{s1}+p(x_1+x_{lm})}{\omega_b} & \frac{\omega_e(x_1+x_{lm})}{\omega_b} & \frac{\omega_e(x_{lm}+x_m)}{\omega_b} & \frac{\omega_e(x_{lm}+x_m)}{\omega_b} & \frac{px_m}{\omega_b} & \frac{\omega_e x_m}{\omega_b} \\
-\frac{\omega_e(x_1+x_{lm})}{\omega_b} & \frac{R_{s1}+p(x_1+x_{lm})}{\omega_b} & -\frac{\omega_e(x_{lm}+x_m)}{\omega_b} & \frac{p(x_{lm}+x_m)}{\omega_b} & -\frac{\omega_e x_m}{\omega_b} & \frac{px_m}{\omega_b} \\
\frac{p(x_m+x_{lm})}{\omega_b} & \frac{\omega_e(x_m+x_{lm})}{\omega_b} & \frac{R_{s2}+p(x_2+x_{lm})}{\omega_b} & \frac{\omega_e(x_2+x_{lm})}{\omega_b} & \frac{px_m}{\omega_b} & \frac{\omega_e x_m}{\omega_b} \\
-\frac{\omega_e(x_m+x_{lm})}{\omega_b} & \frac{p(x_m+x_{lm})}{\omega_b} & \frac{\omega_e(x_2+x_{lm})}{\omega_b} & \frac{R_{s2}+p(x_2+x_{lm})}{\omega_b} & \frac{(\omega_e-\omega_r)\omega_e x_m}{\omega_b^2} & \frac{px_m}{\omega_b} \\
\frac{px_m}{\omega_b} & \frac{(\omega_e-\omega_r)\omega_e x_m}{\omega_b^2} & \frac{px_m}{\omega_b} & \frac{(\omega_e-\omega_r)\omega_e x_m}{\omega_b^2} & \frac{R'_r+px'_r}{\omega_b} & \frac{(\omega_e-\omega_r)\omega_e x'_r}{\omega_b^2} \\
-\frac{(\omega_e-\omega_r)\omega_e x_m}{\omega_b^2} & \frac{px_m}{\omega_b} & -\frac{(\omega_e-\omega_r)\omega_e x_m}{\omega_b^2} & \frac{px_m}{\omega_b} & -\frac{(\omega_e-\omega_r)\omega_e x'_r}{\omega_b^2} & \frac{R'_r+px'_r}{\omega_b}
\end{bmatrix}
\begin{bmatrix} i_{q1} \\ i_{d1} \\ i_{q2} \\ i_{d2} \\ i_{qr} \\ i_{dr} \end{bmatrix}
$$

So from the above matrix representations we have got impedance matrix [Z].

$$
Z =
\begin{bmatrix}
\frac{R_{s1}+p(x_1+x_{lm})}{\omega_b} & \frac{\omega_e(x_1+x_{lm})}{\omega_b} & \frac{p\omega_e(x_{lm}+x_m)}{\omega_b} & \frac{\omega_e(x_{lm}+x_m)}{\omega_b} & \frac{px_m}{\omega_b} & \frac{\omega_e x_m}{\omega_b} \\
-\frac{\omega_e(x_1+x_{lm})}{\omega_b} & \frac{R_{s1}+p(x_1+x_{lm})}{\omega_b} & -\frac{\omega_e(x_{lm}+x_m)}{\omega_b} & \frac{p(x_{lm}+x_m)}{\omega_b} & -\frac{\omega_e x_m}{\omega_b} & \frac{px_m}{\omega_b} \\
\frac{p(x_m+x_{lm})}{\omega_b} & \frac{\omega_e(x_m+x_{lm})}{\omega_b} & \frac{R_{s2}+p(x_2+x_{lm})}{\omega_b} & \frac{\omega_e(x_2+x_{lm})}{\omega_b} & \frac{px_m}{\omega_b} & \frac{\omega_e x_m}{\omega_b} \\
-\frac{\omega_e(x_m+x_{lm})}{\omega_b} & \frac{p(x_m+x_{lm})}{\omega_b} & \frac{\omega_e(x_2+x_{lm})}{\omega_b} & \frac{R_{s2}+p(x_2+x_{lm})}{\omega_b} & \frac{(\omega_e-\omega_r)\omega_e x_m}{\omega_b^2} & \frac{px_m}{\omega_b} \\
\frac{px_m}{\omega_b} & \frac{(\omega_e-\omega_r)\omega_e x_m}{\omega_b^2} & \frac{px_m}{\omega_b} & \frac{(\omega_e-\omega_r)\omega_e x_m}{\omega_b^2} & \frac{R'_r+px'_r}{\omega_b} & \frac{(\omega_e-\omega_r)\omega_e x'_r}{\omega_b^2} \\
-\frac{(\omega_e-\omega_r)\omega_e x_m}{\omega_b^2} & \frac{px_m}{\omega_b} & -\frac{(\omega_e-\omega_r)\omega_e x_m}{\omega_b^2} & \frac{px_m}{\omega_b} & -\frac{(\omega_e-\omega_r)\omega_e x'_r}{\omega_b^2} & \frac{R'_r+px'_r}{\omega_b}
\end{bmatrix}
$$

From the above machine equations (141) and Z another matrix G is derived which is given by

$$
G =
\begin{bmatrix}
0 & 0 & 0 & 0 & 0 & 0 \\
0 & 0 & 0 & 0 & 0 & 0 \\
0 & 0 & 0 & 0 & 0 & 0 \\
0 & x_m & 0 & x_m & 0 & x'_r \\
-x_m & 0 & -x_m & 0 & -x'_r & 0
\end{bmatrix}
$$

When the method of linearization is applied to equation (??), the resulting sub-matrices are as follows:

$$
\Delta V = \begin{bmatrix} \Delta v_{q1} \\ \Delta v_{d1} \\ \Delta v_{q2} \\ \Delta v_{d2} \\ \Delta v'_{qr} \\ \Delta v'_{dr} \end{bmatrix},
\Delta i = \begin{bmatrix} \Delta i_{q1} \\ \Delta i_{d1} \\ \Delta i_{q2} \\ \Delta i_{d2} \\ \Delta i'_{qr} \\ \Delta i'_{dr} \end{bmatrix},
Gi = \begin{bmatrix} 0 \\ 0 \\ 0 \\ 0 \\ x_m(i_{d1} + i_{d2}) + x'_r i'_{dr} \\ -x_m(i_{q1} + i_{q2}) - x'_r i'_{qr} \end{bmatrix},
$$

$$
Z = R + Lp + G\theta' \tag{3.146}
$$

$$
[i_t(G + G_t)] = \begin{bmatrix} x_m i'_{dr} & -x_m i'_{qr} & x_m i'_{dr} & -x_m i'_{qr} & -x_m(i_{d1} + i_{d2}) & x_m(i_{q1} + i_{q2}) \end{bmatrix}
$$

$$
[\Delta T_1] = \Delta T_1 \tag{3.147}
$$

$$
[(F + Jp)] = 2Hp \tag{3.148}
$$

$$
[\Delta \theta'] = \frac{\Delta \omega_r}{\omega_b} \tag{3.149}
$$

It is clear that with the applied voltages of rated frequency, the ratio of ω_e to ω_b is unity. However, in variable-speed drive systems, the linearized equations are stated with ω_e explicitly added to permit applied voltage of a constant frequency different than the rated. In variable-speed drive systems, varying the firing angle of the inverter changes the frequency of the applied stator voltages. As a result, the frequency of the stator voltages is employed as a controllable variable in various applications.

As a result, if frequency is a system variable, a minor change in frequency may be accounted for by allowing the reference frame speed to vary by substituting ω_e with $(\omega_e + \Delta\omega_e)$. This characteristic may be included in the six-phase induction motor's linearized equation; however, it is only relevant in variable-speed drive systems. It's easier to express the equation in the form supplied by separating the derivative components as follows.

$$Epx = Fx + u \tag{3.150}$$

where

$$
u = \begin{bmatrix} \Delta v_{q1} \\ \Delta v_{d1} \\ \Delta v_{q2} \\ \Delta v_{d2} \\ \Delta v'_{qr} \\ \Delta v'_{dr} \\ \Delta T_1 \end{bmatrix}, x = \begin{bmatrix} \Delta i_{q1} \\ \Delta i_{d1} \\ \Delta i_{q2} \\ \Delta i_{d2} \\ \Delta i'_{qr} \\ \Delta i'_{dr} \\ \frac{\Delta \omega_r}{\omega_b} \end{bmatrix}
$$

And decomposing matrix Z into differential and non differential we have the following.

$$
E = \frac{1}{\omega_b} \begin{bmatrix}
(x_1 + x_{lm}) & 0 & (x_{lm} + x_m) & 0 & x_m & 0 & 0 \\
0 & (x_1 + x_{lm}) & 0 & (x_{lm} + x_m) & 0 & x_m & 0 \\
(x_m + x_{lm}) & 0 & (x_2 + x_{lm}) & 0 & x_m & 0 & 0 \\
0 & (x_m + x_{lm}) & 0 & (x_2 + x_{lm}) & 0 & x_m & 0 \\
x_m & 0 & x_m & 0 & x'_r & 0 & 0 \\
0 & x_m & 0 & x_m & 0 & x'_r & 0 \\
0 & 0 & 0 & 0 & 0 & 0 & 2Hp
\end{bmatrix}
$$

$$
F = \begin{bmatrix}
R_{s1} & \frac{\omega_e(x_1+x_{lm})}{\omega_b} & 0 & \frac{\omega_e(x_{lm}+x_m)}{\omega_b} & 0 & \frac{\omega_e x_m}{\omega_b} & 0 \\
-\frac{\omega_e(x_1+x_{lm})}{\omega_b} & R_{s1} & -\frac{\omega_e(x_{lm}+x_m)}{\omega_b} & 0 & -\frac{\omega_e x_m}{\omega_b} & 0 & 0 \\
0 & \frac{\omega_e(x_m+x_{lm})}{\omega_b} & R_{s2} & \frac{\omega_e(x_2+x_{lm})}{\omega_b} & 0 & \frac{\omega_e x_m}{\omega_b} & 0 \\
-\frac{\omega_e(x_m+x_{lm})}{\omega_b} & 0 & \frac{\omega_e(x_2+x_{lm})}{\omega_b} & R_{s2} & \frac{(\omega_e-\omega_r)\omega_e x_m}{\omega_b^2} & 0 & 0 \\
0 & \frac{(\omega_e-\omega_r)\omega_e x_m}{\omega_b^2} & 0 & \frac{(\omega_e-\omega_r)\omega_e x_m}{\omega_b^2} & R'_r & \frac{(\omega_e-\omega_r)\omega_e x'_r}{\omega_b^2} & m \\
-\frac{(\omega_e-\omega_r)\omega_e x_m}{\omega_b^2} & 0 & -\frac{(\omega_e-\omega_r)\omega_e x_m}{\omega_b^2} & 0 & -\frac{(\omega_e-\omega_r)\omega_e x'_r}{\omega_b^2} & R'_r & -n \\
x_m i'_{dr} & -x_m i'_{qr} & x_m i'_{dr} & -x_m i'_{qr} & -x_m(i_{d1}+i_{d2}) & -x_m(i_{q1}+i_{q2}) & 0
\end{bmatrix}
$$

where
m=$(x_m(i_{d1} + i_{d2}) - x'_r i'_{dr})$

n=$x_m(i_{q1} + i_{q2}) - x'_r i'_{qr}$

In the analysis of linear system, it is convenient to express the linear differential equations in the form:

$$px = Ax + Bu \tag{3.151}$$

Equation(**??**) is the fundamental form of the linear differential equations commonly referred as state equation. Equation (**??**) may be written as

$$px = E^{-1}Fx + E^{-1}u \tag{3.152}$$

which is in the form of Equation (**??**) with A=$E^{-1}F$ and $B = E^{-1}$

Non Linear Stability Check of Six Phase Induction Motor

The operation of induction motor drives is complicated by variations in stator and rotor resistance caused by saturation, skin effect, or temperature changes. The controller's performance is influenced by these resistance variations and the system is non linear. Now rearranging and combining the state equation of six phase induction motor given by equation (**??**) -(**??**) and expressing the equation in terms of derivative of current, we have the following.

$$\frac{d}{dt}\begin{bmatrix} i_{ds} \\ i_{qs} \\ \psi_{dr} \\ \psi_{qr} \end{bmatrix} = \begin{bmatrix} -A & \omega_e & B & C\omega_r \\ -\omega_e & -A & C\omega_r & B \\ D & 0 & -E & \omega_{sl} \\ 0 & D & -\omega_{sl} & E \end{bmatrix}\begin{bmatrix} i_{ds} \\ i_{qs} \\ \psi_{dr} \\ \psi_{qr} \end{bmatrix} + \begin{bmatrix} F & 0 \\ 0 & F \end{bmatrix}\begin{bmatrix} V_{ds} \\ V_{qs} \end{bmatrix}$$

where

$A = (1 - (\frac{L_m^2}{L_s*Lr}) * L_s) * (R_s * R_r * \frac{L_m^2}{Lr^2})$

$B = (1 - \frac{L_m^2}{L_s*Lr} * L_s) * (R_s * R_r * \frac{L_m}{Lr^2})$

$C = (1 - \frac{L_m^2}{L_s*Lr} * L_s) * \frac{L_m}{Lr})$

$D = R_r * \frac{L_m}{Lr}$

$E = \frac{L_m}{Lr}$

$F = (1 - (\frac{L_m^2}{L_s*Lr}) * L_s)$

As it can see from matrix equation above, the mathematical equation of the induction motor is nonlinear and is in the fifth order of equation, in which many variables are known. To make a system simpler the singular perturbation theory is used to reduce the order of the induction motor. According to that theory, the part of the system which operated at slower speed assumes as constant. In induction motor drive system the mechanical dynamics operated at much slower speed as compared to the current dynamics and electromagnetic dynamics. So, the flux and rotor speed assumed to be constant and drive the state space equation of induction motor as given in equation below. So by this simplification order of the equation reduced to second order in which the states of the equations are only the d-axis stator and q-axis stator currents.

$$\frac{d}{dt}\begin{bmatrix} i_{ds} \\ i_{qs} \end{bmatrix} = \begin{bmatrix} -A & \omega_e & B & C\omega_r \\ -\omega_e & -A & C\omega_r & B \end{bmatrix}\begin{bmatrix} i_{ds} \\ i_{qs} \end{bmatrix} + \begin{bmatrix} F & 0 \\ 0 & F \end{bmatrix}\begin{bmatrix} V_{ds} \\ V_{qs} \end{bmatrix}$$

In the case of field orientated control of six phase induction motor, to achieve field orientation, the q-axis torque component perpendicular to the rotor flux, and the d-axis flux component aligned in the direction of it. At this condition:

$\psi_{qr} = 0$ and $\psi_{dr} = \psi_r = L_m i_{ds}$

Let the two-control parameters c1 and c2 define as given below that can simplify the equation

$c1 = \frac{R_s}{(1 - (\frac{L_m^2}{L_s * L_r}) * L_s)}$ and $c2 = R_r * \frac{L_m}{L_r}$

Therefore by simplifying the equation, we have the following.

$$\frac{d}{dt} i_{ds} = c1 i_{ds} + c2 \frac{i_{qs}^2}{\psi_{dr}} + \omega_r i_{qs} + \frac{V_{ds}}{(1 - (\frac{L_m^2}{L_s * L_r}) * L_s)} \tag{3.153}$$

$$\frac{d}{dt} i_{qs} = c1 i_{qs} - c2 \frac{i_{qs}}{(1 - (\frac{L_m^2}{L_s * L_r}) * L_s) * L_m} - \frac{\omega_r}{(1 - (\frac{L_m^2}{L_s * L_r}))} i_{qs} + \frac{V_{qs}}{(1 - (\frac{L_m^2}{L_s * L_r}) * L_s)} \tag{3.154}$$

As it can be seen from c1 and c2 equation that the rotor and stator resistances estimated by the control parameters c1 and c2. After estimation, the controller compensates the resistances. The controller is designed to find control parameters c1 and c2 in such a way that the error arises between the actual and the evaluated values of d-axis and q-axis stator currents will be zero. The estimated currents are obtained from equations (??) and (??) as given below.

$$\hat{i_{ds}} = \hat{c1} \hat{i_{ds}} + \hat{c2} \frac{\hat{i_{qs}^2}}{\psi_{dr}} + \omega_r \hat{i_{qs}} + \frac{V_{ds}}{(1 - (\frac{L_m^2}{L_s * L_r}) * L_s)} \tag{3.155}$$

$$\hat{i_{qs}} = \hat{c1} \hat{i_{qs}} - \hat{c2} \frac{\hat{i_{qs}}}{(1 - (\frac{L_m^2}{L_s * L_r}) * L_s) * L_m} - \frac{\omega_r}{(1 - (\frac{L_m^2}{L_s * L_r}))} \hat{i_{qs}} + \frac{V_{qs}}{(1 - (\frac{L_m^2}{L_s * L_r}) * L_s)} \tag{3.156}$$

There is no specific method to find the Lyapunov function. However,the lyapunov stability theory is stated as follows. Generally,let us choose lyapunov function as

$$V = \frac{1}{2} \mathbf{e}^\top \mathbf{e}' \tag{3.157}$$

where

$$e = \begin{bmatrix} i_{ds} - \hat{i_{ds}} \\ i_{qs} - \hat{i_{qs}} \end{bmatrix}$$

Now substituting the vales of **e** int equation **??**, we have the following.

$$V = \tfrac{1}{2} \mathbf{e}^\top \mathbf{e}' = \mathbf{e}^\top * \begin{matrix} i_{ds} - \hat{i_{ds}} \\ i_{qs} - \hat{i_{qs}} \end{matrix}$$

Substituting the values of actual and estimated stator currents we have the following in expression of V.

$$V' = \mathbf{e}^\top \mathbf{e}' = \mathbf{e}^\top A \mathbf{e} + \mathbf{e}^\top B \mathbf{e_u} \tag{3.158}$$

where

$$\mathbf{e}' = \begin{bmatrix} c1 & \omega r \\ -\frac{\omega r}{(1-(\frac{L_m^2}{L_s * Lr})} & c1 \end{bmatrix} \begin{bmatrix} i_{ds} - \hat{i_{ds}} \\ i_{qs} - \hat{i_{qs}} \end{bmatrix} + \begin{bmatrix} \hat{i_{ds}} & \frac{i_{qs}^2}{\omega dr} \\ \hat{i_{qs}} & \frac{i_{qs}}{(1-(\frac{L_m^2}{L_s * Lr}) * L_m} \end{bmatrix} \begin{bmatrix} c1 - \hat{c1} \\ c2 - \hat{c2} \end{bmatrix}$$

where

$$A = \begin{bmatrix} c1 & \omega r \\ -\frac{\omega r}{(1-(\frac{L_m^2}{L_s * Lr})} & c1 \end{bmatrix}$$

$$B = \begin{bmatrix} \hat{i_{qs}} & \frac{i_{qs}}{(1-(\frac{L_m^2}{L_s * Lr}) * L_m} \end{bmatrix}$$

$$e_u = \begin{bmatrix} c1 - \hat{c1} \\ c2 - \hat{c2} \end{bmatrix}$$

Let us represents that

$$\begin{bmatrix} i_{ds} - \hat{i_{ds}} \\ i_{qs} - \hat{i_{qs}} \end{bmatrix} = \begin{bmatrix} ei_{ds} \\ ei_{qs} \end{bmatrix}$$

As per the Lyapunov stability theorem, V' is negative everywhere for the stability of the system. The first term in above matrix equation is negative as A matrix is negative definite and the second term prove to be negative, which is given by

$$\mathbf{e}\top B e_u = \begin{bmatrix} ei_{ds} & ei_{qs} \end{bmatrix} \begin{bmatrix} \hat{i_{ds}} & \frac{i_{qs}^2}{\omega dr} \\ \hat{i_{qs}} & \frac{i_{qs}}{(1-(\frac{L_m^2}{L_s * Lr}) * L_m} \end{bmatrix} \begin{bmatrix} c1 - \hat{c1} \\ c2 - \hat{c2} \end{bmatrix}$$

Eigenvalues of six phase induction machine

The eigenvalues give a straightforward method for describing an six phase induction motor's response under any balanced operating state. A non-oscillatory mode corresponds to a real eigenvalue. A decaying mode is represented by a negative real eigenvalue; the higher the magnitude, the faster the decay. A periodic instability is represented by a positive real eigenvalue. Each pair of conjugate eigenvalues corresponds to an oscillatory mode in complex eigenvalues. The damping is determined by the real component of the eigenvalue, whereas the frequency of oscillations is determined by the imaginary component. A damped oscillation has a negative real part, whereas rising amplitude oscillations have a positive real part. The machine's eigenvalues were calculated by utilizing a typical eigenvalue procedure to calculate the roots of linearized system matrix. Seven eigenvalues are produced because the model of the six-phase machine is defined by seven state variables. Six of the seven eigenvalues have three complex conjugate pairs, whereas one has just a real value.

Tools used for the study

Tools required for this studies are Ansys Motor-CAD and MATLAB/SIMULINK. Ansys Motor-CAD Evaluate motor topologies and concepts across the full operating range and produce designs that are optimized for size, performance and efficiency. Motor-CAD

software's have four integrated modules, Electro Magnetic, Thermal, Lab and Mechanical perform multi-physics calculations quickly and iteratively, so you can get from concept to final design in less time. MATLAB is required to execute the simulations for the analysis performed in the design of six phase induction motor. MATLAB software is used throughout the whole code development process like writing, compiling, debugging, and programming.

Variables and Constraints

In the design optimization of a six-phase induction motor, the independent variables taken into considerations are stator inner diameter, stator core length, stator slot width, rotor slot width, stator slot depth, rotor slot depth, stator yoke depth, rotor yoke depth, air gap length, end ring area, average air gap flux density and number of turns per stator phase. In the design optimization of a six-phase induction motor, the constraints considered in the optimization procedure represent maximum and minimum limits for motor performance. A minimum performance value (e.g., the performance variable has to be larger than this limit) was imposed on full load power factor, efficiency, nominal torque, break-down torque at base speed, depth of stator yoke, depth of rotor yoke, shaft diameter, stator teeth breadth, rotor teeth breadth and inertia constant. A maximum performance value (e.g., the performance variable has to be smaller than this limit) was imposed on temperature rise, no-load power factor, stator teeth flux density, rotor teeth flux density, current density in end ring and rotor speed.

Strategy

The algorithm's aim is for all of the particles to find the optimal location in a multidimensional hyper-volume. This is accomplished by giving all particles in the space beginning random locations and modest initial random velocities. The method works like a simulation, moving each particle's position depending on its velocity, the best known global position in the problem space, and the best known position of a particle. After each location update, the goal function is sampled. The particles cluster or converge on an optimum, or many optima, over time as a result of a mix of exploration and exploitation of known favorable positions in the search space.

Procedure

The Particle Swarm Optimization method is made up of a group of particles that move throughout the search space based on their own best previous position as well as the best past location of the entire swarm or a near neighbor. The velocity of a particle is adjusted in each iteration by:

$$V_{i(t+1)} = V_{i(t)} + C_1 * rand() * (p_i^{best} - p_{i(t)}) + C_2 * rand() * (p_g^{best} - p_{i(t)}) \qquad (3.159)$$

where

$V_{i(t+1)}$ is the new velocity for the ith particle,

C_1 and C_2 are the weighting coefficients for the personal best and global best positions respectively,

$p_{i(t)}$ is the ith particle's position at time t,

p_i^{best} is the ith particle's best known position, and

p_g^{best} is the best position known to the swarm.

The $rand()$ function generates a uniformly random variable which is an element of $[0, 1]$. Variants on this update equation consider best positions within a particles local neighborhood at time t. A particle's position is updated using:

$$p_{i(t+1)} = p_{i(t)} + v_{i(t)} \tag{3.160}$$

Optimization Problem formulation

The optimization of the six phase induction motor design is to select the independent variables otherwise the problem would have been very much complicated using too many variables. Therefore, variables selection is important in the motor design optimization.

A general nonlinear programming problem can be stated in mathematical terms as follows.

Find X $= f(x1, x2.....xn)$ such that $fi(x)$ is a minimum or maximum

$gi(x) \leq 0$, i= 1, 2, ... n

$fi's$ is known as objective function which is to be minimized or maximized;

$gi's$ are constants and

$xi's$ are the variables.

Finally, the design was take place by modeling internal and external part of the six phase induction motor. Then, simulation of the model was performed by using MATLAB and ANSYS Motor-CAD and the simulation result obtained from this software and the result of manual design is compared. Based on the results, the relevant conclusion and recommendation concerning the design of six phase induction motor was done.

3.8 Derivation of the objective function of six phase induction motor

The losses of six phase induction motor were used as the objective function. There are two main losses considered in six-phase induction motor. These are Copper Loss (Stator Copper Loss and Rotor Copper Loss) and Stator Iron Loss. The major losses that are found in the parts of induction motor that conduct variable flux-linkage with time are iron losses. The two mechanisms of iron loss are hysteresis and eddy current losses. Current flowing through the resistance of any windings causes Copper losses. Therefore, these losses can be minimized as follows:

- By reducing resistance,

- By increasing the cross-sectional area of conductors,

- By lowering the winding temperature,

- By using materials that have lower resistivity.

Most of the time copper conductor materials with increasing current densities can be used to reduce extra losses. The causes of hysteresis losses the electrical frequency while that of eddy current losses are related to the square of the electrical frequency. The performances of six phase induction motors are deeply affected by losses in the stator and rotor. To apply the particle swarm optimization, an objective function has to be defined to evaluate the six-phase squirrel cage induction motor design with overall good performance. The objective function includes all the geometric dimensions of the motor. The first objective function aims to minimize the total losses. Let us derive its mathematical equation with each losses for clarity.

Stator Copper Loss

A) Stator Copper Loss (Pst) is determined as follows

$$P_{st} = 6 * I_s^2 * R_s \tag{3.161}$$

However, the resistance is given by

$$R = (\rho * l)/a \tag{3.162}$$

In addition, rewriting the resistance formula for stator copper winding, we have

$$R_s = \frac{(\rho_{cu} * l_m t * N_{ph}}{a_{cu}} \tag{3.163}$$

Also current density is given as follows.

$$J_s = \frac{I_s}{a_{cu}} \tag{3.164}$$

Substituting equation (**??**) into equation (**??**), we have

$$R_s = \frac{\rho_{cu} * l_{mt} * N_{ph} * J_s}{I_s} \tag{3.165}$$

Now substituting equation (**??**) into equation (**??**), we have the following.

$$P_{st} = \frac{6 * \rho_{cu} * l_{mt} * N_{ph} * J_s * I_s^2}{I_s} \tag{3.166}$$

By simplifying equation (**??**) we have

$$P_s t = 6 * \rho_{cu} * l_{mt} * N_{ph} * J_s \tag{3.167}$$

B) Rotor Copper Loss (Prt) is the sum of the rotor bar loss and the rotor end ring loss.
Prt = Rotor bar loss (Pb) + End ring loss (Pe) Rotor bar loss (Pb) is found as follows

$$P_b = I_b^2 * R_b * S_r \tag{3.168}$$

But
$$R_b = \frac{\rho_{cu} * l_b}{a_b} \tag{3.169}$$

Also, we have
$$a_b = \frac{I_b}{J_b} \tag{3.170}$$

Substituting equation (??) into equation (??), we have
$$R_b = \frac{\rho_{cu} * l_b * J_b}{I_b} \tag{3.171}$$

Now substituting equation (??) into equation (??), we have the following.
$$P_b = \frac{I_b^2 * \rho_{cu} * l_b * J_b * S_r}{I_b} \tag{3.172}$$

By simplifying equation (??) we have
$$P_b = \rho_{cu} * l_b * J_b * S_r * I_b \tag{3.173}$$

End ring loss(Pe) can be determined as follows
$$P_e = 2 * I_e^2 * R_e \tag{3.174}$$

But
$$R_e = \frac{\rho_{cu} * l_e}{a_e} \tag{3.175}$$

Where le=mean length of current path in the end ring=circumference of end ring
$$l_e = \pi * D_e \tag{3.176}$$

Substituting equation (??) and (??) into equation (??) we have the following equation.
$$P_e = \frac{2 * I_e^2 * \rho_{cu} * \pi * D_e}{a_e} * R_e \tag{3.177}$$

In addition, we have
$$a_e = \frac{I_e}{J_e} \tag{3.178}$$

Substituting equation (??) into equation (??), we have
$$P_e = 2 * \pi * \rho_{cu} * J_e * I_e * D_e \tag{3.179}$$

Therefore, rotor copper loss becomes
$$P_{rt} = P_b + P_e \tag{3.180}$$
$$P_{rt} = P_b + P_e \tag{3.181}$$
$$P_{rt} = \rho_{cu} * l_b * J_b * S_r * I_b + 2 * \pi * \rho_{cu} * J_e * I_e * D_e \tag{3.182}$$

Now total copper loss is found by adding all copper losses.

$$P_{cu} = P_{st} + P_{rt} \tag{3.183}$$

$$P_{cu} = 6 * \rho_{cu} l_{mt} N_{ph} I_s J_s + \rho_{cu} l_b J_b S_r I_b + 2\pi * \rho_{cu} J_e I_e D_e \tag{3.184}$$

Equation (??) shows a six phase induction motor copper losses.
C) Stator Iron Loss (Pfe) Stator iron losses can be determined as follows.

$$P_{fe} = p_{fe}(V_t K_1 f^{K_2} B_{st}^{K_3} + V_c K_1 f^{K_2} B_{sc}^{K_3}) \tag{3.185}$$

Where V_t=Volume of teeth V_c=olume of core

$$V_t = w_{st} d_{ss} l_{ss} \tag{3.186}$$

$$V_c = \frac{(\pi * l)}{4}(D_o^2 - [D + 2d_{ss}]^2) \tag{3.187}$$

But, we have the following relationship.

$$D_o = D + 2d_s s + 2d_s c \tag{3.188}$$

By rearranging equation (??), we have the following.

$$D_o - 2d_{sc} = D + 2d_{ss} \tag{3.189}$$

Now substituting equation (??) into equation (??), we have

$$V_c = \frac{(\pi * l)}{4}(D_o^2 - [D_o - 2d_{sc}]^2) \tag{3.190}$$

By squaring the terms inside the brackets and simplifying equation (??), we obtain

$$V_c = \frac{(\pi * l)}{4}(D_o^2 - [D_o^2 - 4D_o d_{sc} + 4d_{sc}^2]) \tag{3.191}$$

$$V_c = \frac{(\pi * l)}{4}(D_o^2 - D_o^2 + 4D_o d_{sc} - 4d_{sc}^2]) \tag{3.192}$$

$$V_c = \pi * l(D_o d_{sc} - d_{sc}^2]) \tag{3.193}$$

$$V_c = \pi * l * d_{sc}(D_o - d_{sc}) \tag{3.194}$$

Substituting equation (??) into equation (??), we have

$$V_c = \pi * l * d_{sc}(D + 2d_{ss} + d_{sc}) \tag{3.195}$$

Finally substituting equation (??) and equation (??) into expression of stator iron loss in equation (??), we have

$$P_{fe} = p_f e(w_{st} d_{ss} l_{ss} K_1 f^{K_2} B_{st}^{K_3} + \pi * l * d_{sc}(D + 2d_{ss} + d_{sc}) K_1 f^{K_2} B_{sc}^{K_3})) \tag{3.196}$$

Therefore, Total Losses of six-phase induction motor is determined as follows. (P) = Total Copper Loss (Pcu) + Total Iron Loss (Pfe)

$$P_t = 6 * \rho_{cu} * l_{mt} * N_{ph} * J_s + \rho_{cu} * l_b * J_b * S_r * I_b + 2\pi * \rho_{cu} J_e I_e D_e +$$
$$p_f e(w_{st} d_{ss} l_{ss} K_1 f^{K_2} B_{st}^{K_3} + \pi * l * d_{sc}(D + 2d_{ss} + d_{sc}) K_1 f^{K_2} B_{sc}^{K_3}) \tag{3.197}$$

3.9   Weight Determination for Six Phase Induction Motor

Two important origins of losses to regulate modern (AC) motors are iron losses and copper losses. Iron losses are the fundamental losses with inside the elements that behavior variable flux-linkage with time. Two mechanisms of iron loss are hysteresis and eddy current losses. Copper losses are due to current flowing through the resistance of any windings. Copper losses may be reduced as follows: decreasing resistance, growing the cross-sectional location of conductors, reducing the winding temperature and the use of substances, which have decrease resistivity. Copper conductor substances with growing current densities may be carried out to lessen more losses. Both of those increase with growing flux density with inside the teeth and back iron. Hysteresis losses are associated with the electric frequency. Eddy current losses are associated with the rectangular of the electric frequency. The performances of induction motors are deeply laid low with a few losses of their stators and rotors. To apply particle swarm optimization technique, an objective function has to be described to assess six-phase squirrel cage induction motor layout with appropriate performance. This objective function may also consist of all of the geometric dimensions of the motor, and a huge subset of constraints need to be formulated to make certain the bodily attention of the Six Phase Squirrel Cage Induction Motor. These goal capabilities are given with inside the following. The first objective function pursuits to limit the stator iron loss. The stator iron loss variable includes the laminations, which are used as the objective function of the optimization. To apply particle swarm optimization technique, another objective function has to be defined to evaluate how good each motor design is specially related to the weight. The objective functions are related to weight minimization. The mathematical expression of the weight of material, of the six-phase induction motor is similar to that of a three-phase induction motor in their form except their weight may differ because of stator winding is different. The weight of iron used for stator diameter is determined as follows.

$$W_{isd} = p_{fe}L(\frac{\pi}{4}(D_o^2 - (D_o - 2d_{sc})^2)) \tag{3.198}$$

where
W_{isd}=weight of iron of stator diameter,
$p_{fe} =$ the resistivity of Iron,
$L=$ the length of stator,
$Do =$diameter of stator,
$dsc =$ diameter of stator core,
The weight of iron used for stator bore diameter is determined as follows.

$$W_{isbd} = p_{fe}L(\frac{\pi}{4}(D^2 - (D - 2d_{sc})^2)) \tag{3.199}$$

where
W_{isbd}=weight of iron of stator bore diameter and
$D =$ the bore diameter of stator,
The weight of iron used for stator teeth is determined as follows.

$$W_{ist} = p_{fe}L(S_s w_{st} d_{ss}) \tag{3.200}$$

where
W_{ist}=weight of iron of stator teeth,
S_s = number of stator slot,
W_{st} = width of stator teeth and
d_{ss} = diameter of rotor slot
The weight of iron used for rotor teeth is determined as follows.

$$W_{irt} = p_{fe}L(S_r w_{rt} d_{rs}) \tag{3.201}$$

where
W_{irt}=weight of iron of rotor teeth,
S_r=number of rotor slot,
w_{rt}=width of rotor teeth and
d_{rs}=diameter of rotor slot
The total weight of iron used W_{it} is determined as follows.

$$W_{it} = W_{isd} + W_{isbd} + W_{ist} + W_{irt} \tag{3.202}$$

$$W_{it} = p_{fe}L(\frac{\pi}{4}(D_o^2-(D_o-2d_{sc})^2))+p_{fe}L(\frac{\pi}{4}(D^2-(D-2d_{sc})^2))+p_{fe}L(S_s w_{st} d_{ss})+p_{fe}L(S_r w_{rt} d_{rs}) \tag{3.203}$$

$$W_{it} = p_{fe}L((\frac{\pi}{4}(D_o^2-(D_o-2d_{sc})^2)+\frac{\pi}{4}(D^2-(D-2d_{sc})^2)+(S_s w_{st} d_{ss})+(S_s w_{rt} d_{rs})) \tag{3.204}$$

The weight of copper includes stator-winding weight, rotor bars weight and two end rings weight made up of copper materials. The weight of copper used for stator winding is determined as follows.

$$W_{swc} = p_{cu}N_{ph}l_{mt}a_{cu} \tag{3.205}$$

where
W_{swc}=weight of stator winding copper,
p_{cu} = the resistivity of copper,
N_{ph}=number of turns per slot per phase,
l_{mt} =mean turn length and
a_{cu}= the area of stator winding of stator
The weight of copper used for rotor bars is determined as follows.

$$W_{rbc} = p_{cu}(S_r A_{bar}(L + l_{bar})) \tag{3.206}$$

where
W_{rbc}=weight of rotor bar copper,
S_r =number of rotor slot,
A_{bar}=cross-sectional area of rotor bar and
l_{bar}=length of rotor bar
The weight of copper used for two end rings are determined as follows.

$$W_{erc} = p_{cu}(2A_e\pi * D_e) \tag{3.207}$$

where

W_{erc}=weight of end rotor copper,
A_e = area of end ring of rotor and
D_e =diameter of end ring of rotor
The total weight of copper materials W_{ct} used is determined as follows.

$$W_{ct} = W_{swc} + W_{rbc} + W_{erc} \tag{3.208}$$

$$W_{ct} = p_{cu}N_{ph}l_{mt}a_{cu} + p_{cu}(S_r A_{bar}(L + l_{bar})) + p_{cu}(2A_e\pi * D_e) \tag{3.209}$$

Therefore, the total weight of iron and copper material W_t, for six-phase induction motor is determined as follows.

$$W_t = W_{it} + W_{ct} \tag{3.210}$$

$$W_t = p_{fe}L(\frac{\pi}{4}(D_o^2 - (D_o - 2d_{sc})^2) + p_{fe}L(\frac{\pi}{4}(D^2 - (D - 2d_{sc})^2) + p_{fe}L(S_s w_{st}d_{ss})$$
$$+p_{fe}L(S_r w_{rt}d_{rs}) + p_{cu}N_{ph}l_{mt}a_{cu} + p_{cu}(S_r A_{bar}(L + l_{bar})) + p_{cu}(2A_e\pi * D_e) \tag{3.211}$$

3.10   Cost Optimization for Six Phase Induction Motor

The third objective function is cost optimization (minimizing the cost). The cost variable includes lamination cost, copper cost, rotor end-ring cost and core-punching cost. The weight of iron can be found already as follows.

$$W_{it} = p_{fe}L(\frac{\pi}{4}(D_o^2 - (D_o - 2d_{sc})^2) + p_{fe}L(\frac{\pi}{4}(D^2 - (D - 2d_{sc})^2) + p_{fe}L(S_s w_{st}d_{ss}) + p_{fe}L(S_r w_{rt}d_{rs}) \tag{3.212}$$

And the weight of copper is already determines as follows.

$$W_{ct} = p_{cu}N_{ph}l_{mt}a_{cu} + p_{cu}(S_r A_{bar}(L + l_{bar})) + p_{cu}(2A_e\pi * D_e) \tag{3.213}$$

The punching cost is estimated as 20% of the total cost of the material.

$$Punching_{cost} = 0.2 * (Cost of iron + Cost of copper) \tag{3.214}$$

Therefore, the total cost is determined as follows.

$$C_t = W_{it}Iron_{cost} + W_{ct}Copper_{cost} + Punching_{cost} \tag{3.215}$$

where
C_t=total cost of material,
$Copper_{cost}$= cost of unit weight of copper per kilogram and
$Iron_{cost}$=cost of unit weight of iron per kilogram

CHAPTER FOUR

4 SIMULINK RESULT AND DISCUSSION

4.1 MATLAB/Simulink Implementation

In MATLAB/Simulink, the voltage, torque equations, and transformation matrices are used to construct the Six Phase Induction Motor model. The motor receives power from a six-phase sinusoidal voltage supply. The six-phase to two-phase conversion block converts six-phase stator voltages to voltages on the d- and q-axis.
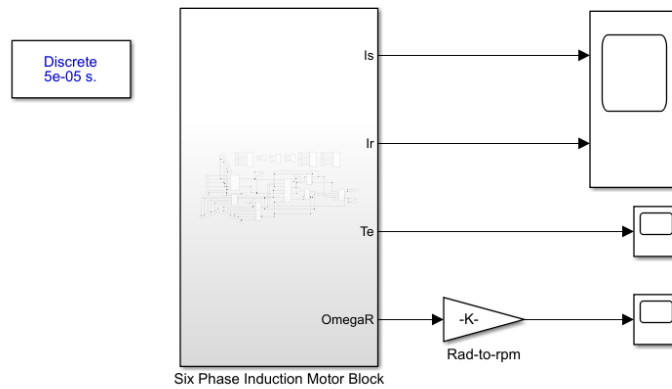
Figure 4.1: Simulink Model of Six Phase Induction Motor
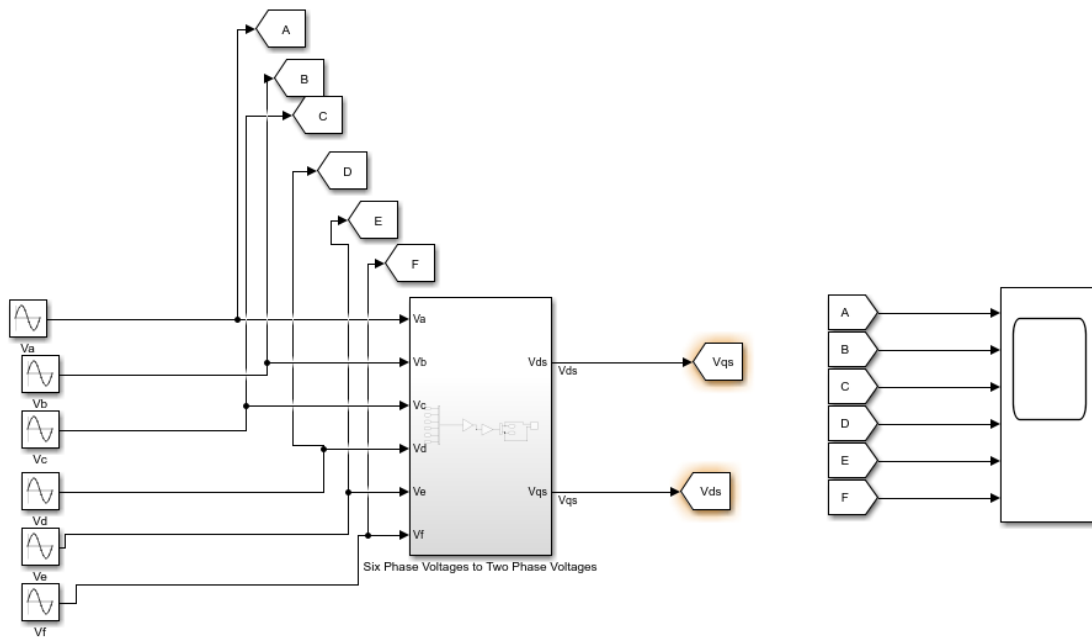
Figure 4.2: Six Phase Supply to Vdq Voltages Conversion block
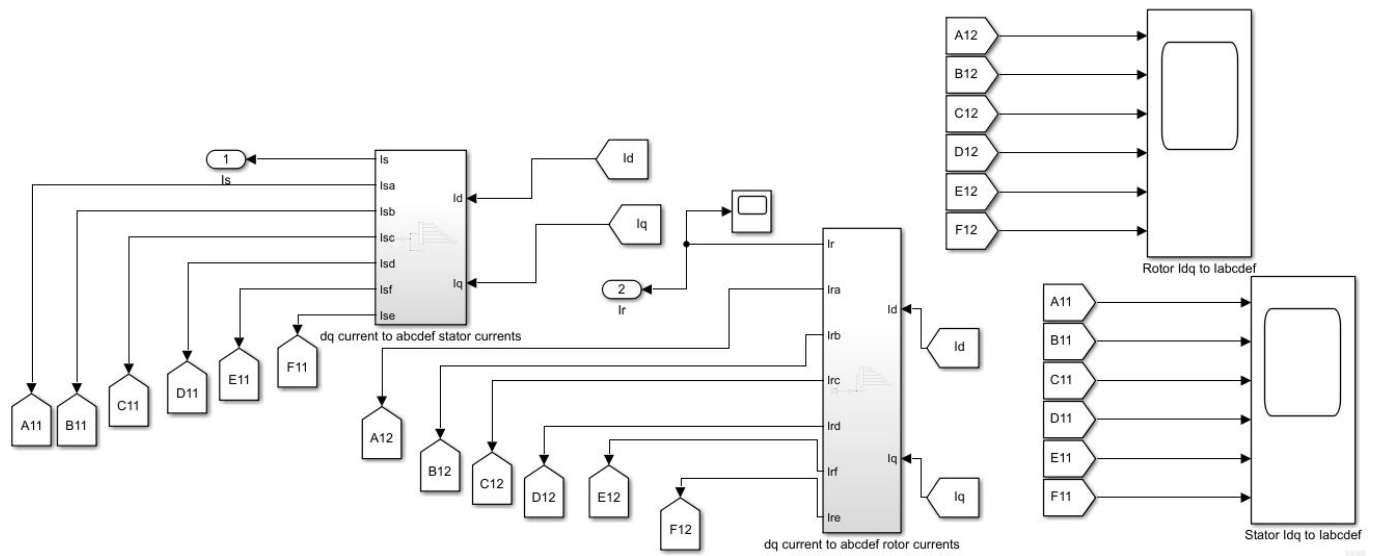
Figure 4.3: Idq currents to Iabcdef Currents Conversion block
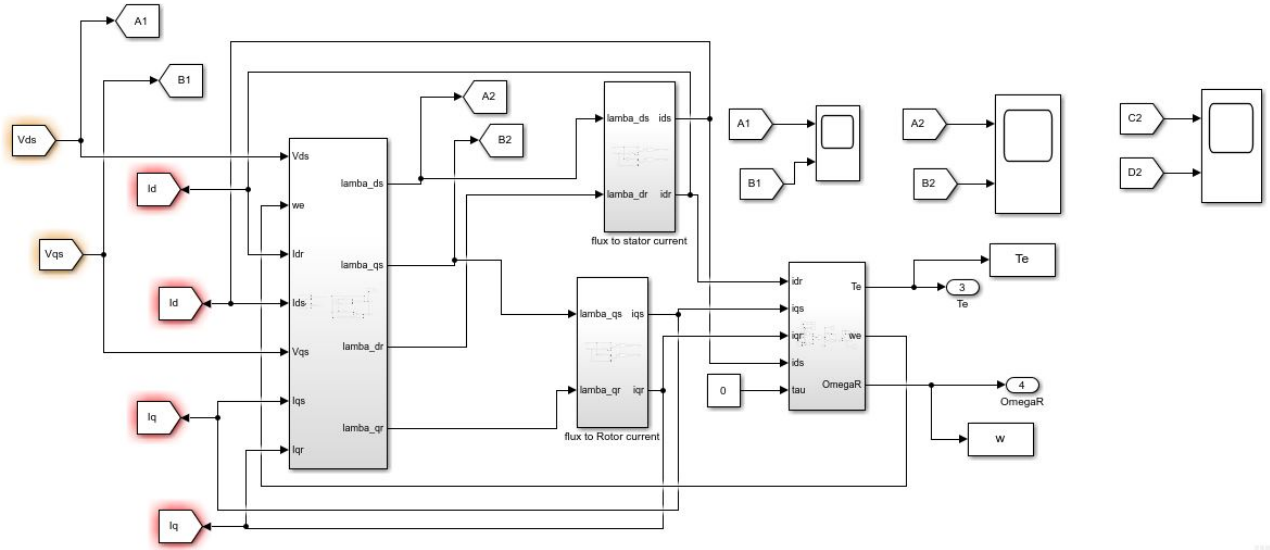
Figure 4.4: Torque and Speed Block

The designd six phase squirrel cage induction motor is simulated in this paper, and the simulation was carried out using the MATLAB/SIMULINK and ANSYS Motor CAD. The software takes the stator and rotor parameters calculated in previous chapter as input. The torque, speed, currents, flux linkages, and performance curve of the motor are simulation outputs or simulation results. The goal of this simulation is to assess the performance of the modeled motor and compare the simulation results to that of ANSYS Motor CAD.

4.2 Overview on ANSYS Motor CAD

Ansys Motor-CAD is a specialised electric machine design tool that allows for quick multi-physics simulations throughout the whole torque-speed working range. In order to build designs that are compact, quick, and efficient, evaluate motor topologies and ideas over the whole operating range. EMag, Therm, Lab, and Mech are four integrated modules of Motor-CAD software that conduct multi-physics calculations rapidly and repeatedly, helping you to get from idea to final design faster. With shorter development cycles, motor designers must make design decisions quickly and confidently, knowing that difficulties will not arise later. Because of faster calculations and better data entry techniques, Motor-CAD users may explore more motor topologies and thoroughly analyze the influence of advanced loss effects in the early phases of a design. The layout technique is simplified through motor-CAD software's intuitive, template-based totally setup and embedded multi physics expertise, which reduces reliance on multiple teams for precise electromagnetic, thermal, or mechanical experience, permitting motor designers to hold more manipulate over their designs.

4.2.1 EMag: Electromagnetic Performance Predictions

A 2D finite element (FE) environment and analytical approaches are integrated for fast electromagnetic performance estimates. You can easily optimize your designs using our large collection of parameterized templates and geometry.

70

4.2.2 Therm: Predictions of thermal performance and improved cooling system design

This is the industry-standard equipment for thermal analysis of electric machinery, having been in use for over 20 years. Calculate the temperature of motor components in steady-state and transient operating conditions in seconds, and accurately mimic thermal behavior.

4.2.3 Lab: Efficiency mapping and performance throughout a duty cycle

Allows for rapid and precise analysis of any electric machine design across its complete operating range. You may do efficiency mapping and driving cycle analysis in minutes.

4.2.4 Mech: Analysis of mechanical systems

Using a 2D FEA-based solution in Motor-CAD, analyzes stress and displacement in rotors during operation.

Now launch the software and enter the information of the motor to be designed. Manual modeling is used to determine the value of those data. The software created a model of the stator core, stator slot, stator winding, rotor core, rotor slot, and the model when the rotor is inserted in the stator using the input parameters. In the following diagrams, those models are described one by one. Figure ?? shows a representation of the stator core and rotor core. The stator core is the outer stationary portion of an induction motor. M19 29 Gauge steel material was used to model this stator core, which has minimal core loss, excellent permeability at low and moderate inductions, and outstanding stamping properties. The rotor core was built of the same steel as the stator core. It has thirty-eight slots that are ready for rotor bar casting. When the rotor core is put into the stator core with a sufficient air gap between them, as shown below.

The model of one of the stator slots is illustrated in Figure ??, along with its dimensions and shape. One of the most important elements affecting motor performance is the slot design and dimension. As a result, the optimal value of motor performance is obtained by carefully selecting the slot's shape and dimensions. The model of one of the rotor slots figure is illustrated in the Appendix, along with its dimensions and shape. This rotor slot shape is known as tapered, and it is a popular choice for optimizing design and simplifying manufacture.

When the stator core mode, stator slot model, stator winding, rotor core, rotor slot, and shaft are joined together, it contains the entire model.

Material consumptions

Figure ?? shows material consumption for software simulation of a developed six phase induction motor.

Equivalent Circuit

The equivalent circuit of the six phase induction motor obtained from the ANSYS MotorCAD is given in the Appendix.

Motor CAD Design

First, a machine model was created. This machine's data was known from previous chapter, and the model's outputs could be compared to validate it. The machine in question was a 30hp ABB MBT 180L type.

Geometry Configuration

The values used for stator and rotor dimensions are given in the Appendix.

Winding Pattern

Each conductor in this motor is made up of two strands. The winding of the machine is separated into two parallel paths. As can be seen in figure below. The windings are connected in a star pattern.

Flux Density

The magnitude of flux density in the stator and rotor of six phase induction motor at rated speed is shown in Appendix. The flux density of the stator yoke is about 1.533T, which is within the acceptable range.

Motor-CAD Lab: Efficiency Maps

The efficiency map is automatically displayed when simulation is finished and different values can be plotted by changing parameters to be plotted. The graphs below are automatically generated when calculation electromagnetic performance is finished.

4.3   MATLAB/Simulink Results and Discussion

Six-phase induction motor design and modeling can be discussed in the form of mathematical calculations on design and modeling when we combine both of them they can fit the operational characteristic of induction machine property or not by investigating SIMULINK results. When we model relying on the value we obtain from designing machine parameter is operated or not, we can compare depending on the findings starting with the input voltage per phase and the commanded value determined from the planned parameter based on the machine capacity, the following discussion can be followed.
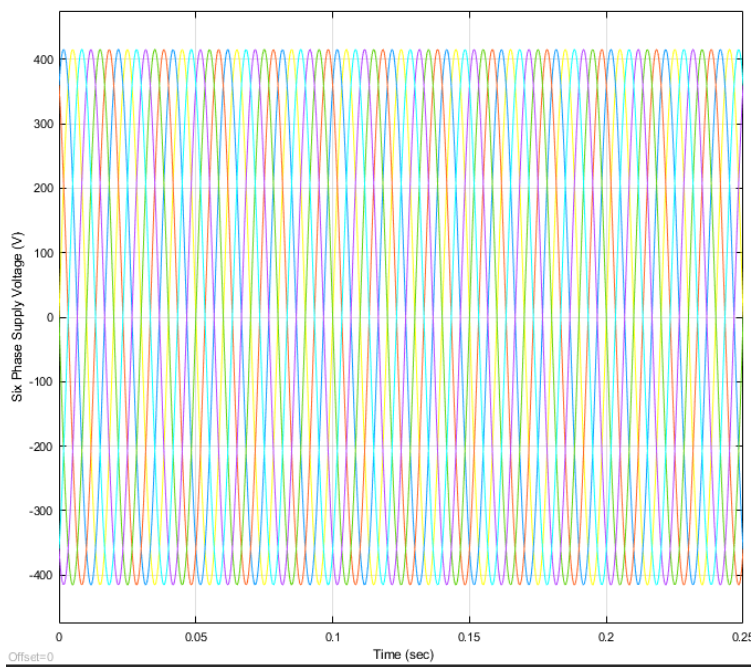
Figure 4.5: Six phase supply voltages
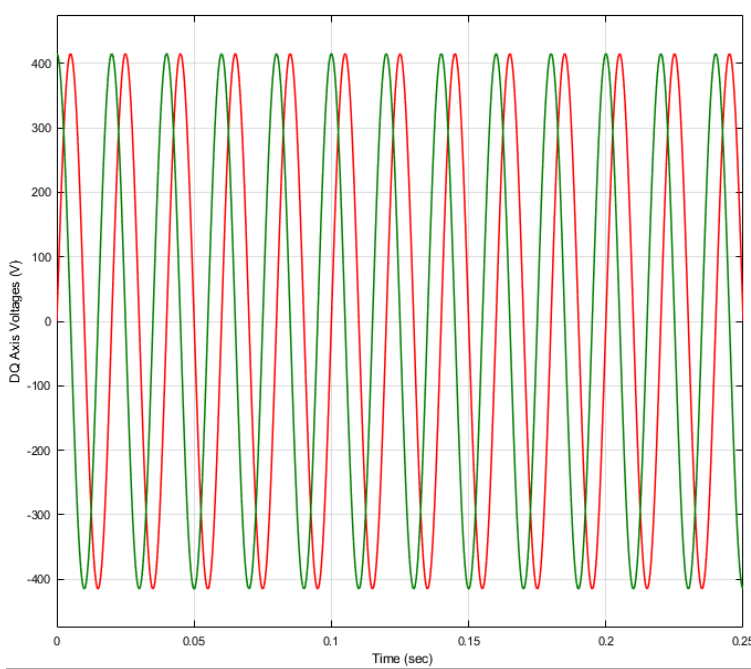
Figure 4.6: Q and D Axis Voltage

Running the Manual Design, GA and PSO Test m-file yields the results in the table **??**. From those particle swarm optimization results in a better collection of variables (X1 to X9) as indicated in the table **??**, resulting in loss and weight reduction. By manual design the losses are It can be seen that by using PSO six-phase squirrel-cage induction motor's
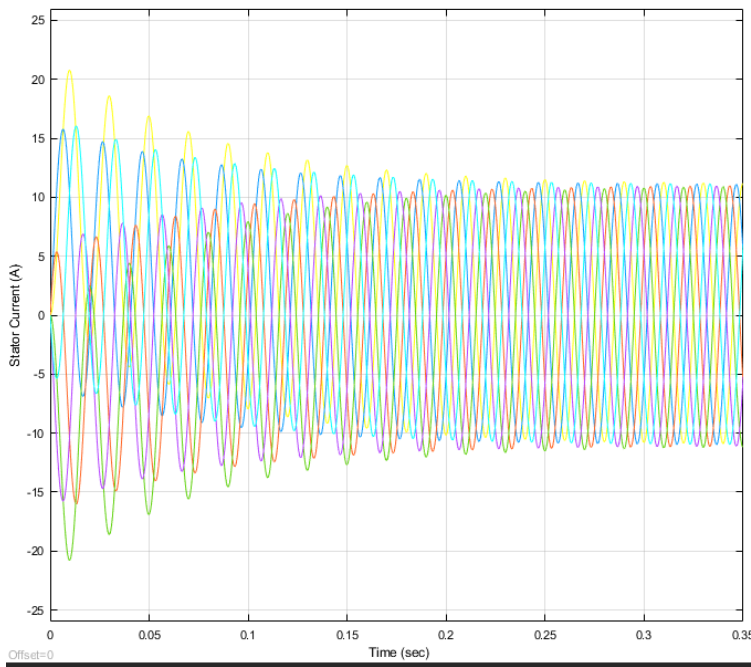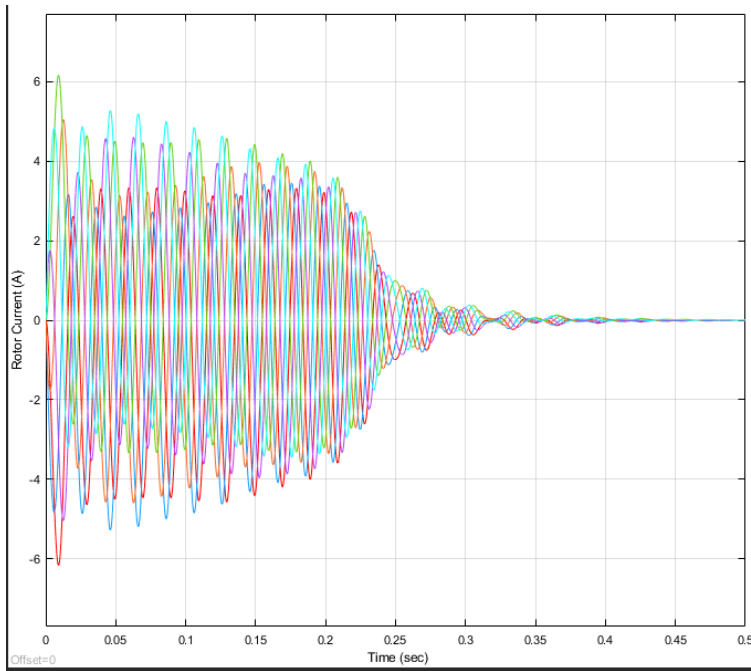
Figure 4.7: Stator Currents

Figure 4.8: Rotor Currents

performance is improved and the losses (copper and iron) are reduced to 935.9W, when compared to manual design and GA of 2033.7W and 1608W respectively. The weight of the motor is lowered by roughly to 161kg while attaining performance increases, which is an important achievement. It has been discovered that PSO based optimal design has a higher
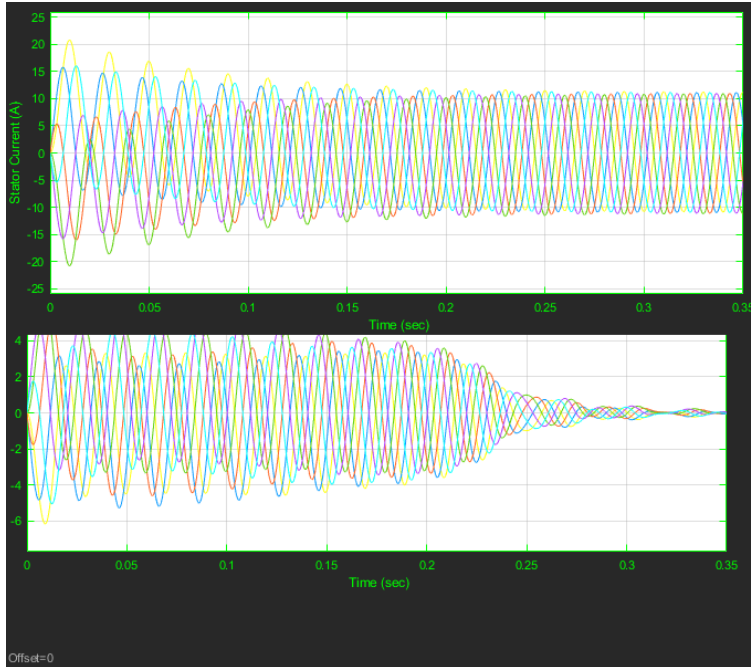
Figure 4.9: Stator and Rotor Currents
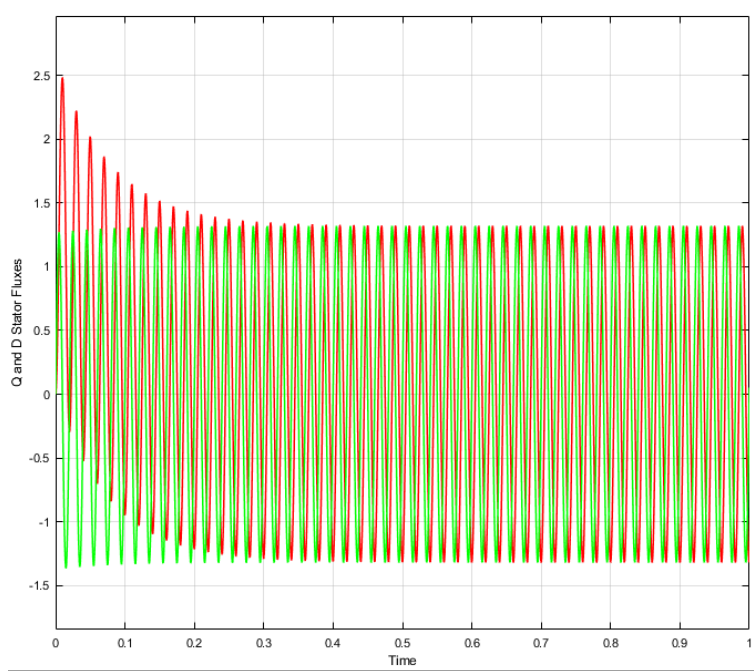
Figure 4.10: Q and D Axis Fluxes

efficiency than conventional and GA based approaches. As a result, PSO delivers greater optimization in terms of performance. Particle swarm optimization has a total loss of 935.826 W and total weight of 161kg which is lower than the manual deign and GA, indicating that it is more energy efficient. The obtained values of the various parameters demonstrate that,
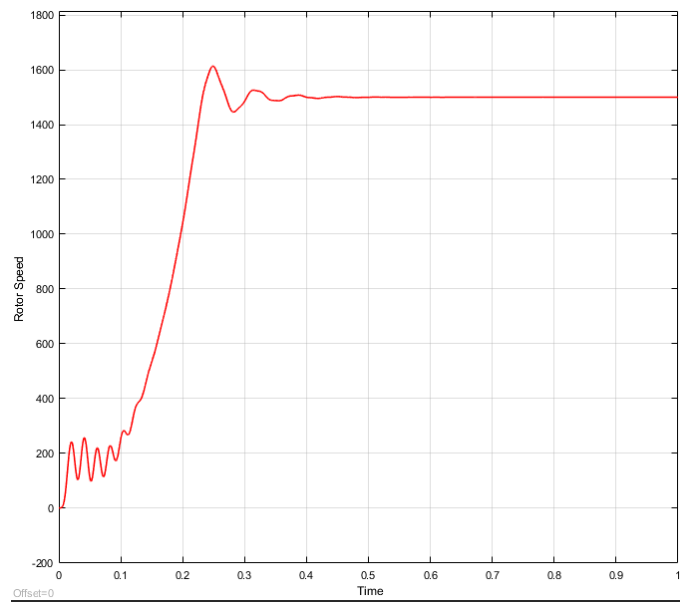
Figure 4.11: Speed vs Time
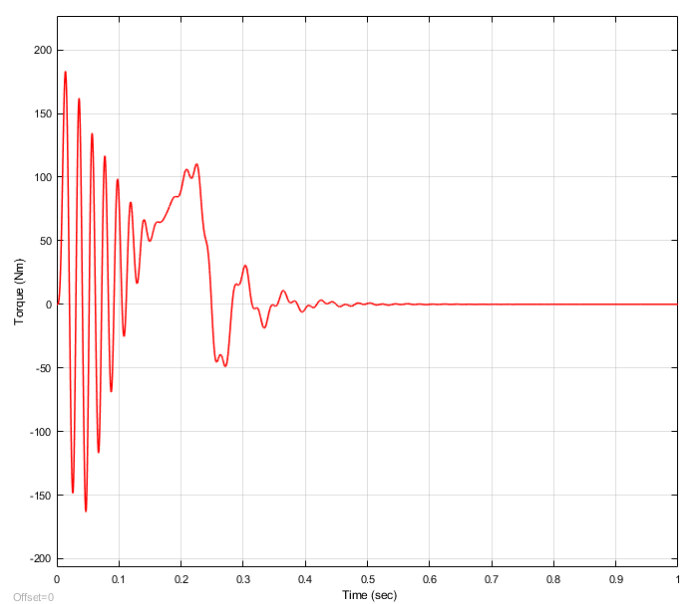
Figure 4.12: Torque vs Time

when compared to manual approaches, particle swarm optimization reduces the size of the six-phase induction motor significantly. As a result, the material cost is also decreased as weight is optimized. From these design calculation, it can be shown that the particle swarm optimization based optimized design produces a more efficient and smaller motor with the same ratings as the manual and GA approach .

The optimized result from the PSO is as shown in the table **??**.

Table 4.1: Comparision of Design Optimization Techniques

No	Parameters	Manual Design	GA	PSO
1	Stator Bore Diameter	195mm	189.97mm	180.93mm
2	Stator Outer Diameter	298mm	278.98mm	269.94mm
3	Stator Core Length	230mm	240mm	240mm
4	Airgap Length	0.6235mm	0.603mm	0.5931mm
5	Rotor Outer Diameter	194mm	188.76mm	179.76mm
6	Rotor Inner Diameter	100mm	97.67mm	87.688mm
7	Total Power Loss	2.0337Kw	1.608Kw	0.9359Kw
8	Rated Slip	0.02	0.0154	0.012
9	Input Power	24.434Kw	24.008Kw	23.336Kw
10	Rated Efficiency	0.9168	0.933	0.9599
11	Rated Power Factor	0.8345	0.8499	0.8767
12	Rated Torque	145.5Nm	154.66Nm	162Nm
13	Peripheral Velocity	15.395m/s	14.92m/s	14.21m/s
14	Stator Slot Pitch	12.76mm	12.43mm	11.84mm
15	Mean Turn Length	1050mm	815mm	808mm
16	Stator Core Diameter	29.5mm	28mm	28mm
17	Net Core Length	207mm	192.4mm	192.4mm
18	Stator Slot Diameter	22mm	17mm	17mm
19	Rotor Slot Pitch	9mm	8.075mm	7.25mm
20	Weight of motor	200kg	188.6857kg	161.7243kg

Table 4.2: PSO Optimized Variables

Variables	Values
X1	269.94mm
X2	28mm
X3	17mm
X4	6mm
X5	180.93mm
X6	28mm
X7	19mm
X8	4.3mm
X9	240mm

V/F Control Method

Induction motors use an electromechanical energy conversion system that is simple but

effective. The rotor is inaccessible in squirrel-cage motors, which make up the vast bulk of induction devices. There are no moving contacts in ac synchronous motors and generators, such as the commutator and brushes in dc machines or slip rings and brushes in dc machines. This configuration considerably improves induction motor durability and removes the risk of sparking, allowing squirrel-cage machines to be utilized safely in difficult conditions, including explosive environments. The lack of wiring in the rotor, whose winding comprises of uninsulated metal bars forming the squirrel cage that gives the motor its name, adds to the motor's toughness. A rotor with this much strength can run at high speeds and endure mechanical and electrical overloads. The low electric time constant in adjustable-speed drives accelerates the dynamic response to control commands. Induction motors typically have a large torque reserve and a low speed dependence on load torque. The speed control of an induction motor can be done in a variety of ways. Pole Changing, Variable Supply Frequency Control, Variable Supply Voltage Control, Variable Rotor Resistance Control, V/f Control, Slip Recovery, and Vector Control are the ones to look out for. Because of its simplicity, V/f Control is the most popular of the systems discussed above and has found broad use in both industrial and home applications. However, as compared to vector control, it has a lower dynamic performance. As a result, V/f Control is not employed in areas where precision is essential. Some of the benefits of V/f Controls are wide speed range, performs well in both running and transitory situations, has a low initial current demand and larger stable functioning region. At base speed the voltage and frequencies attain their rated values. The rate of change in supply frequency can be used to adjust the acceleration. It is inexpensive and simple to apply. The speed of an induction motor is controlled by the adjustable magnitude and frequency of stator voltages and frequency in the V/Hz control so that the air gap flux is always maintained at the desired value at steady-state. Because it just considers the steady state dynamic, this technique is sometimes referred to as scalar control. In v by f control technique speed of induction motor is controlled by adjusting magnitude of stator voltage and frequency. For any change in frequency V/F ratio must be maintained constant so as to maintain flux constant. In this case torque becomes independent on the supply frequency. As speed increases stator voltage must be increased proportionally so as to maintain constant V/F ratio. Open loop speed control can be used when accuracy in speed response is not concern. We provide reference speed that speed is converted in to corresponding frequency. This frequency is again converted in to angle theta. The relation of induced voltage, stator flux and supply frequency is given by,
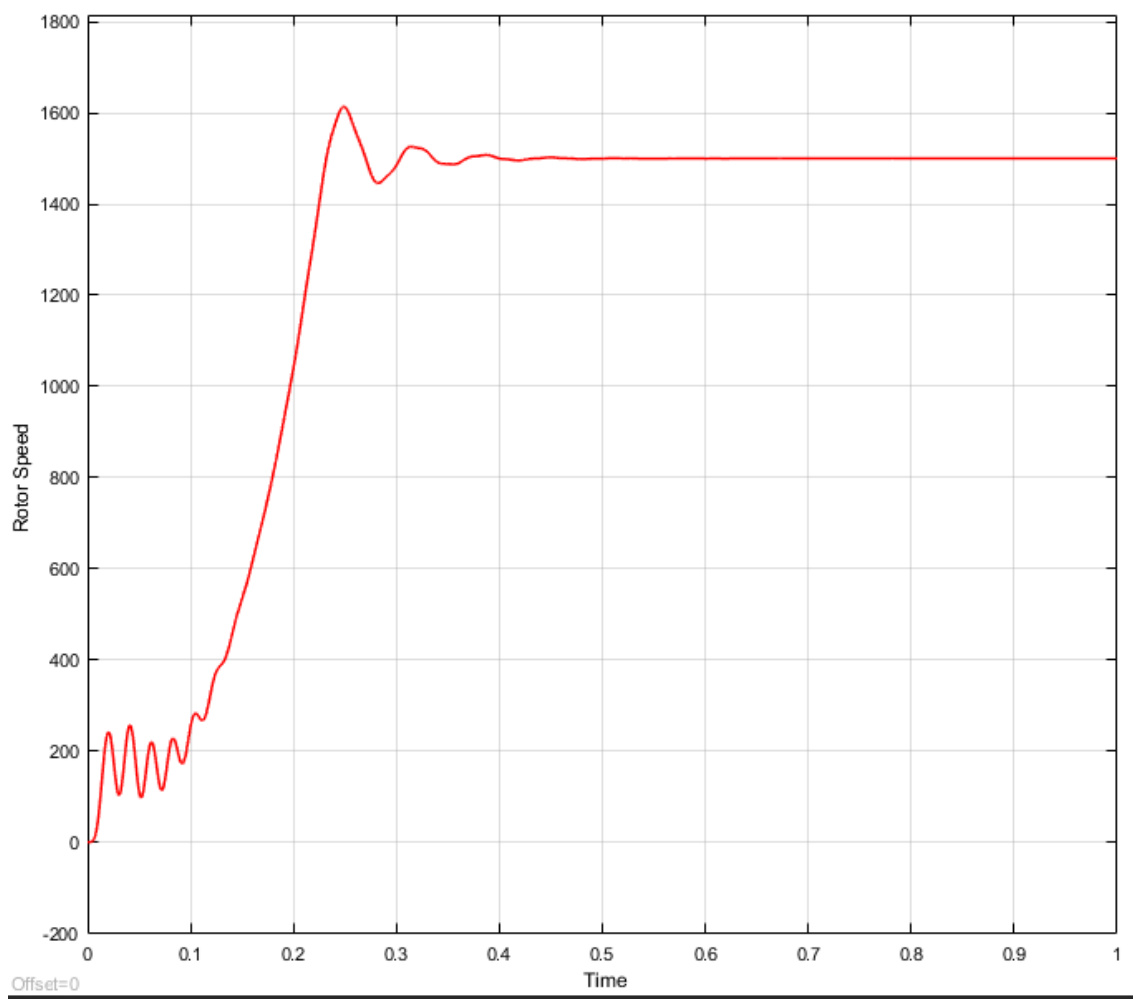
$$E = \frac{d\Psi}{dt} \tag{4.1}$$

Figure 4.13: Speed vs Time

$$E = K_w * f_s * \phi_m \tag{4.2}$$

$$\phi_m = \frac{E}{f_s} \tag{4.3}$$

where E is induced stator voltage

Ψ is stator flux linkages

ϕ_m is stator flux

Stability of six phase induction motor analytical results

Small signal stability analysis is best performed by determining the system eigenvalue using the characteristic formula.

$$det(A - \Psi I) = 0$$

where A, I, and Ψ the roots of the characteristic formula are the system matrix, identity matrix, and roots, respectively. Only if all of the real or real components of the eigenvalues are negative is a system considered to be stable. For six-phase induction motor, the above
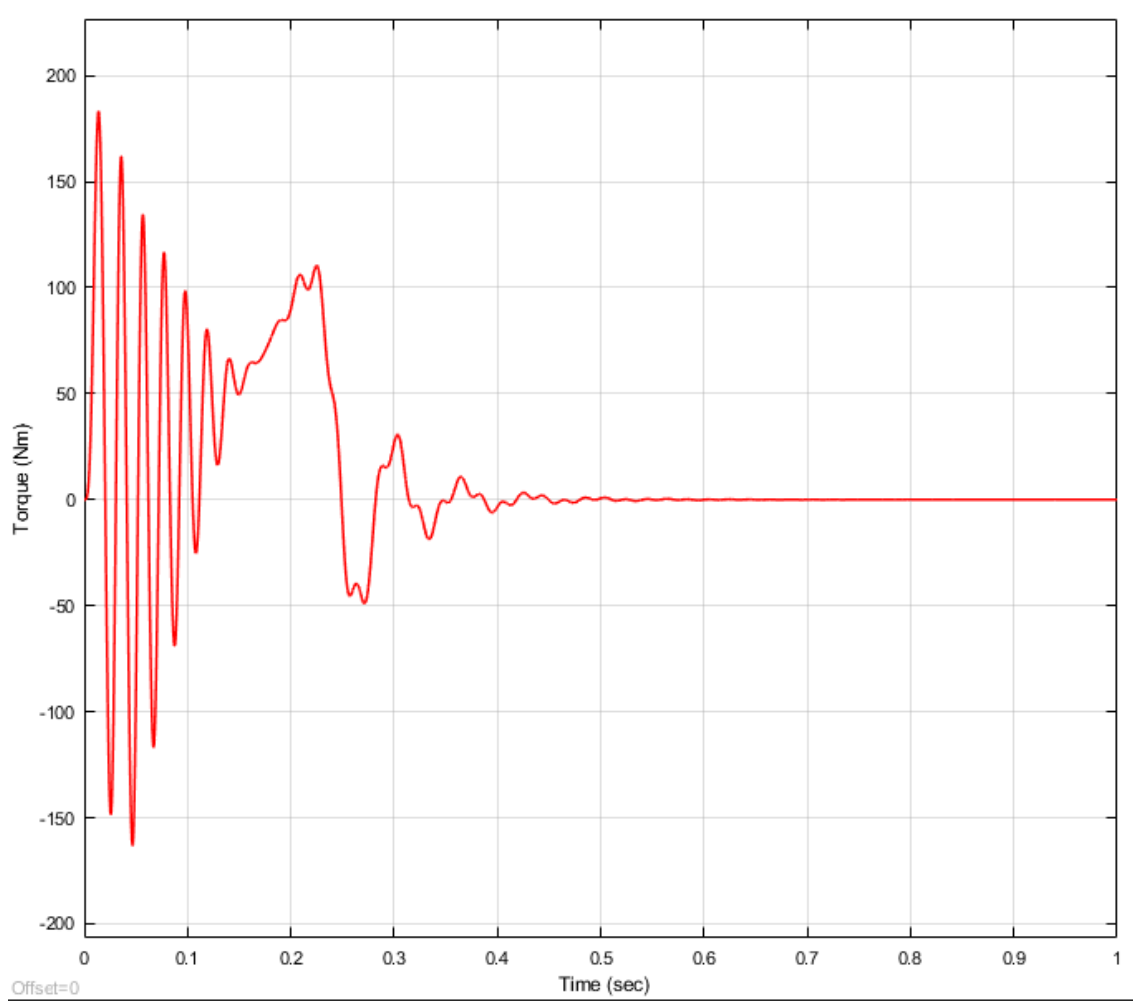
Figure 4.14: Torque vs Time

stated formula produce seven state variables, which include both real and complex values. Six-phase induction motor, have three complex complex conjugate pairs and one real eigenvalues are obtained. A 4-pole, 415 V, 50 Hz Six phase induction motor is simulated, with the following characteristics stated in per unit: $R_{s1} = 0.0847, R_{s2} = 0.0847, X_1 = 0.0543, X_2 = 0.0543, X'_{lm} = 0.003, R'_r = 0.0376, X_1 = 0.0543, X'_{lr} = 0.003, X_m = 1.521, H = 0.6$.
Using the matlab the following eigenvalues are obtained. So according to the stability criteria of eigenvalues, real components of the eigenvalues are negative. This shows that the system is stable.

$-1.1176 + 0.0000i$
$- 0.1218 + 1.8114i$
$- 0.1218 - 1.8114i$
$- 0.4314 + 0.6471i$
$- 0.4314 - 0.6471i$
$- 0.0779 + 1.1749i$
$- 0.0779 - 1.1749i$

80

4.4   Controller Design

The selection of the common reference frame's speed is the foundation of scalar control. In a v/f control scheme, the reference frame's speed is set to be equal to the induction motor's rated speed. Due to a lack of data on multi-phase machines, per-phase characteristics and ratings for multi-phase induction machines are believed to be the same as for three-phase induction machines. All simulations are based on a four-pole, 50-Hz six-phase induction machine.

4.4.1   Design of PID controller

A continuous PID and a discrete PID are the two types of integral PID speed controllers. The speed controllers employed in this simulation are both continuous type and discrete type. The continuous speed controller's design is presented first. In general, series controllers are favored over feedback controllers because higher order systems require a large number of state variables to detect during feedback, which necessitates a large number of transducers. As a result, series controllers are widely used. The lower order model is connected to the controller, and the closed loop response is observed. The controller's parameters are fine-tuned to provide a response that meets the desired standards. For stabilization procedures, the tuned parameters are introduced into the higher order system. The transfer function of PID controller is written for a continuous system as

$$G_c(s) = K_p + \frac{K_i}{s} + K_d s \tag{4.4}$$

The design involves the determination of the values of the constants Kp, Ki and Kd, meeting the required performance specifications. The general block diagram of the PID controller is shown in Figure ?? below.   Because the original system transfer function is a higher order
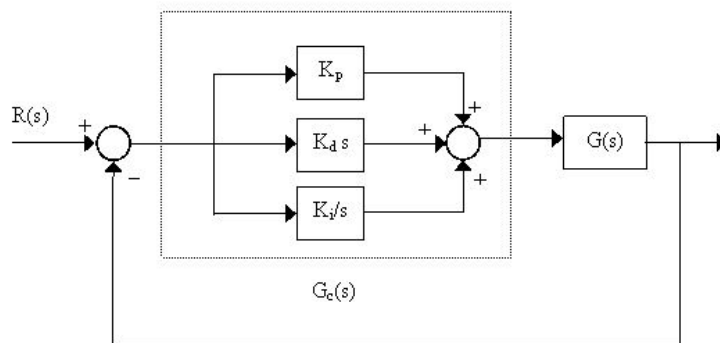

Figure 4.15: Control System with PID Controller [?]

system, we must reduce it to a lower order model that retains the important properties of the original system and approximates its response as nearly as feasible for the same sort of inputs.

The following is the process for determining the reduced order model transfer function of a higher order system. The nth order reduced model with unknown parameters created by linearizing the Simulink G(s) is equal to the kth order reduced model with unknown parameters represented by the second order equation M(s) provided below.

Consider an nth order stable linear time invariant system described by the transfer function.

$$G(s) = \frac{N(s)}{D(s)} = \frac{a_0 + a_1 s + a_2 s^2 + ... + a_i s^i}{b_0 + b_1 s + b_2 s^2 + ... + b_i s^i} \quad (4.5)$$

where a_i and $b_i \geq 0$ The corresponding stable k^{th}(k¡ n) order reduced model is of the form

$$M(s) = \frac{N_r(s)}{D_r(s)} = \frac{d_0 + d_1 s + d_2 s^2 + ... + d_i s^i}{e_0 + e_1 s + e_2 s^2 + ... + e_i s^i} \quad (4.6)$$

where d_i and $e_i \geq 0$

Hence,G (s) = M (s)

$$\frac{a_0 + a_1 s + a_2 s^2 + ... + a_i s^i}{b_0 + b_1 s + b_2 s^2 + ... + b_i s^i} = \frac{d_0 + d_1 s + d_2 s^2 + ... + d_i s^i}{e_0 + e_1 s + e_2 s^2 + ... + e_i s^i} \quad (4.7)$$

On cross-multiplying and rearranging the equation ??,

$$a_0 e_0 + (a_0 e_1 + a_1 e_0)s + (a_0 e_2 + a_1 e_1 + a_2 e_0)s^2 + ... + a_{n-1} e_k s^{n-1+k} = b_0 d_0 + (b_0 d1 + b_1 d_0)s + (b_0 d_2 + b_1 d_1 + b_2 d_0)s^2 + ...$$

Equating the coefficients of the corresponding terms in the equation, the following relations are obtained:

$$a_0 e_0 = b_0 d_0 \quad (4.8)$$

$$a_0 e_1 + a_1 e_0 = b_0 d1 + b_1 d_0 \quad (4.9)$$

$$a_0 e_2 + a_1 e_1 + a_2 e_0 = b_0 d_2 + b_1 d_1 + b_2 d_0 \quad (4.10)$$

$$...$$

$$a_0 e_{k-1} + a_1 e_{k-2} + a_2 e_{k-3} + ... = b_0 d_{k-1} + b_1 d_{k-2} + b_2 d_{k-3} + ... \quad (4.11)$$

$$a_0 e_k + a_1 e_{k-1} + a_2 e_{k-2} + ... = b_1 d_{k-1} + b_2 d_{k-2} + b_3 d_{k-3} + ... \quad (4.12)$$

$$a_1 e_k + a_2 e_{k-1} + a_3 e_{k-2} + ... = b_2 d_{k-1} + b_3 d_{k-2} + b_4 d_{k-3} + ... \quad (4.13)$$

$$...$$

$$a_{n-1} e_k = b_n d_{k-1} \quad (4.14)$$

The unknown parameters are determined by taking any positive values for d_0 or e_0, for simplification, choosing $d_0 =1$ or $e_0 =1$, and using the above relations, the other unknown parameters are evaluated. The reduced order models are tested for stability using Routh array.

The original higher order derived system is fourth order system transfer function given as follows.

$$G(s) = \frac{2.789s^3 + 253.4s^2 + 7026s + 5.404e04}{s^4 + 103.5s^3 + 3672s^2 + 5.133e04s + 2.458e05} \quad (4.15)$$

and

Consider a second order reduced model transfer function represented by the following representations.

$$G(s) = \frac{d_1 s + d_0}{e_2 s^2 + e_1 s + e_0} \tag{4.16}$$

where d_0, d_1, e_0, e_1 and e_2 are unknown parameters. Now, equating G(s) and M(s) together and cross-multiplying we have the following.

$$(2.789s^3+253.4s^2+7026s+54040)(d_0+d_1 s) = (s^4+103.5s^3+3672s^2+51330s+245800)(e_0+e_1 s+e_2 s^2) \tag{4.17}$$

$2.789e_0 s^3+253.4e_0 s^2+7026e_0 s+54040e_0+2.789e_1 s^4+253.4e_1 s^3+7026e_1 s^2+54040e_1 s+2.789e_2 s^5+253.4e_2 s^4+$

Equating the coefficients of the corresponding terms in the above equation, the following relations are obtained.

$$54040e_0 = 245800d_0 \tag{4.18}$$

$$7026e_0 + 54040e_1 = 51330d_0 + 245800d_1 \tag{4.19}$$

$$253.4e_0 + 7026e_1 + 54040e_2 = 3672d_0 + 51330d_1 \tag{4.20}$$

$$2.789e_0 + 253.4e_1 + 7026e_2 = 103.5d_0 + 3672d_1 \tag{4.21}$$

$$2.789e_1 + 253.4e_2 = d_0 + 103.5d_1 \tag{4.22}$$

$$2.789e_2 = d_1 \tag{4.23}$$

Now, for simplification, choosing d_0 =1, and solving the above equation ?? , we have the following.

$54040e_0 = 245800$

And solving for e_0 we have

e_0=4.55

A standard second order transfer function have unity coefficient, therefore e_2 value is 1.

e_2 =1

From equation ?? , substituting the value of e_2 we got the value of d_1 .

d_1=2.789

By substituting values of e_0, e_2 , d_0 and d_1 into equation ?? and solving, we obtained values of e_1. e_1 =13.044

Now reduced order transfer function is written as follows.

$$G(s) = \frac{d_1 s + d_0}{e_2 s^2 + e_1 s + e_0} \tag{4.24}$$

Substituting the values of the parameters, we have

$$G(s) = \frac{2.789s + 1}{s^2 + 13.044s + 4.55} \tag{4.25}$$

The closed loop transfer function of a unity feedback system with G(s) as the open loop transfer function is given in equation ?? as:

$$TF(s) = \frac{G(s)}{1 + G(s)} \tag{4.26}$$

If the system output response does not satisfy the specifications, the PID controller is added to the forward path and the closed loop transfer function of the system is given in equation **??** as:

$$TF_c(s) = \frac{G_c(s)G(s)}{1 + G_c(s)G(s)} \tag{4.27}$$

where $G_c(s)$ is the transfer function of the PID controller. Applying pole-zero cancellation method to the reduced model, the initial values of K_p, K_i and K_d are obtained as **??**: Using the simulation procedure, initial parameters are tuned to get unit response of the

Table 4.3: Initial parameters of K_p, K_i and K_d

Variables	Values
K_p	13.044
K_i	4.55
K_d	1

compensated system to meet the required specifications. The tuned values obtained are as follows: The designed PID controller Gc(s) is attached with the original higher order

Table 4.4: Tuned parameters of PID controller

Variables	Values
K_p	6.8134
K_i	101.18
K_d	0.0364

system. The closed response is found to meet the required specifications. Figure **??** and **??** shows the step response of the original system and step response of original system with PID controller respectively. Figure **??** and **??** respectively show the step response of the reduced order system and reduced order system with PID controller.

4.4.2 Adaptive Fuzzy PID controller

The Adaptive PID auto-tuner is a hybrid controller that combines PID and PID auto-tuner controllers. This combined controller has the ability to adapt to any situation, such as the rising quantity of input decision changes. Both controllers are connected in series in the Adaptive PID auto-tuner block. The motor transfer function is depicted inside the Adaptive PID auto-tuner controller block, which is coupled in series with the Adaptive PID auto-tuner controller. There are two inputs and one output on Fuzzy Logic Control. These
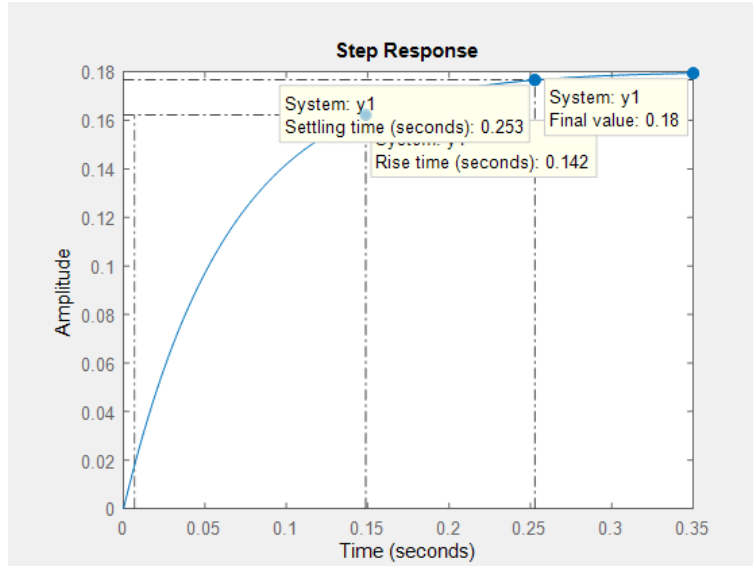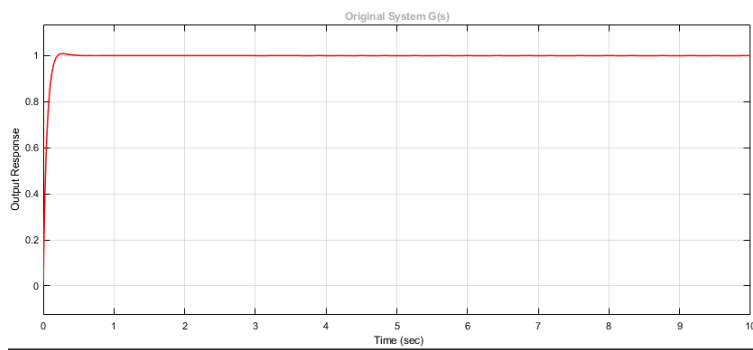
Figure 4.16: Step Response of Original System

Figure 4.17: Step Response of Original System with PID Controller

are, respectively, error (e), error change (de), and control signal. Linguistic variables that implies inputs and output have been classified as: NB, NM, NS, Z, PS, PM and PB.

Adaptive Fuzzy PID controller is based on two input and three output. Fuzzy PID controller have three outputs, which are Kp, Ki and Kd.

Error speed (e) and Change in error speed (ce) are fuzzy control input and fuzzy outputs are ΔKp, ΔKi and ΔKd.

$\Delta Kp = Kp.\Delta Kp*$
$\Delta Ki = Ki.\Delta Kp*$
$\Delta Kd = Kd.\Delta Kp*$

The Control Rules of Fuzzy Controller

The three PID arithmetic parameters will affect the system's stability, response speed, overshoot, and stable precision.

- When E is large, we should use the larger Kp and the smaller Kd to ensure that the
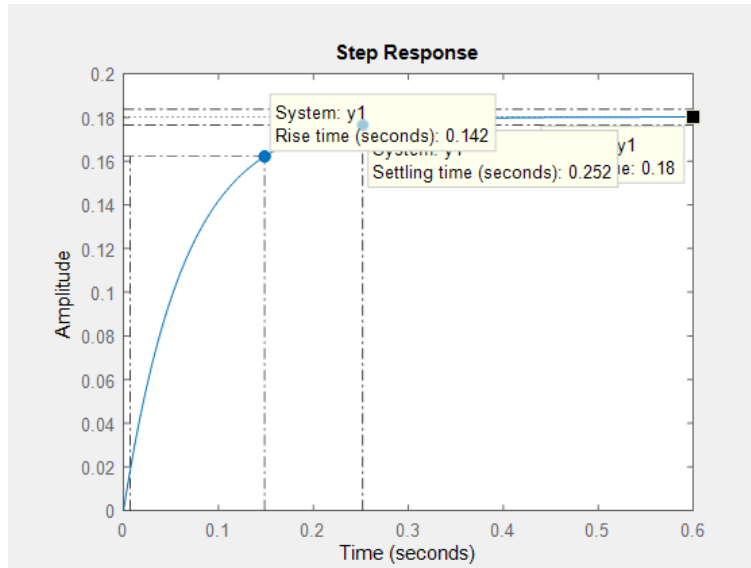
Figure 4.18: Step Response of Reduced Order System
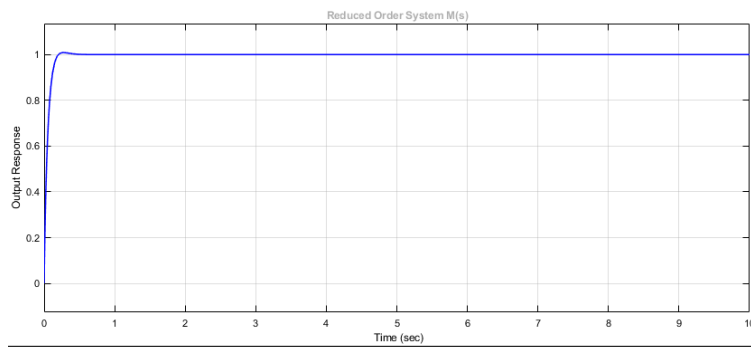
Figure 4.19: Step Response of Reduced Order System with PID Controller

system performs well in tracking. We should also take a proactive approach to avoid the system experiencing a larger overshoot. Usually, Ki = 0 is used;

- When E and Ec are both acceptable, we should reduce Kp to ensure that the system has a reduced overrun. We should use the appropriate Ki in this case, as Kd has a significant impact on the system.

- When E is very tiny, we should use the larger Kp and Ki to ensure that the system performs consistently. To avoid the system oscillation appearing in the set value, we should also choose an appropriate Kd that is based on Ec. If Ec is little, choose a larger Kd; if Ec is large, choose a smaller Kd.

Membership Function of Linguistic Variable

Negative Big (NB), Negative Medium (NM), Negative Small (NS), Zero (Z), Positive Small (PS), Positive Medium (PM), Positive Big (PB) were the linguistic labels used to characterize

86

Table 4.5: Kp Fuzzy Control Rules

E/Ec	NB	NM	NS	Z	PS	PM	PB
NB	PB	PB	PM	PM	PS	Z	Z
NM	PB	PB	PM	PS	PS	Z	NS
NS	PM	PM	PM	PS	Z	NS	NS
Z	PM	PM	PS	Z	NS	NM	NM
PS	PS	PS	Z	NS	NS	NM	NM
PM	PS	Z	NS	NM	NM	NM	NB
PB	Z	Z	NM	NM	NM	NB	NB

Table 4.6: Ki Fuzzy Control Rules

E/Ec	NB	NM	NS	Z	PS	PM	PB
NB	NB	NB	NM	NM	NS	Z	Z
NM	NB	NB	NM	NS	NS	Z	Z
NS	NB	NM	NS	NS	Z	PS	PS
Z	NM	NM	NS	Z	PS	PM	PM
PS	NM	NS	Z	PS	PS	PM	PB
PM	Z	Z	PS	PS	PM	PB	PB
PB	Z	NM	NS	PS	PM	PB	PB

Table 4.7: Kd Fuzzy Control Rules

E/Ec	NB	NM	NS	Z	PS	PM	PB
NB	NB	NB	NM	NM	NS	Z	Z
NM	NB	NB	NM	NS	NS	Z	Z
NS	NB	NM	NS	NS	Z	PS	PS
Z	NM	NM	NS	Z	PS	PM	PM
PS	NM	NS	Z	PS	PS	PM	PB
PM	Z	Z	PS	PS	PM	PB	PB
PB	Z	Z	PS	PM	PM	PB	PB

the Fuzzy sets (PB). The fuzzy rules are extracted from fundamental information and human experience about the process. Inputs are normalized in the range [-3, 3], and outputs are Kp interval [-0.3, 0.3], Kp interval [-0.06, 0.06], and Kd interval [-0.3, 0.3]. These rules describe the control strategy by defining input and output relationships. There are seven fuzzy sets for each control input, for a total of 49 fuzzy rules.
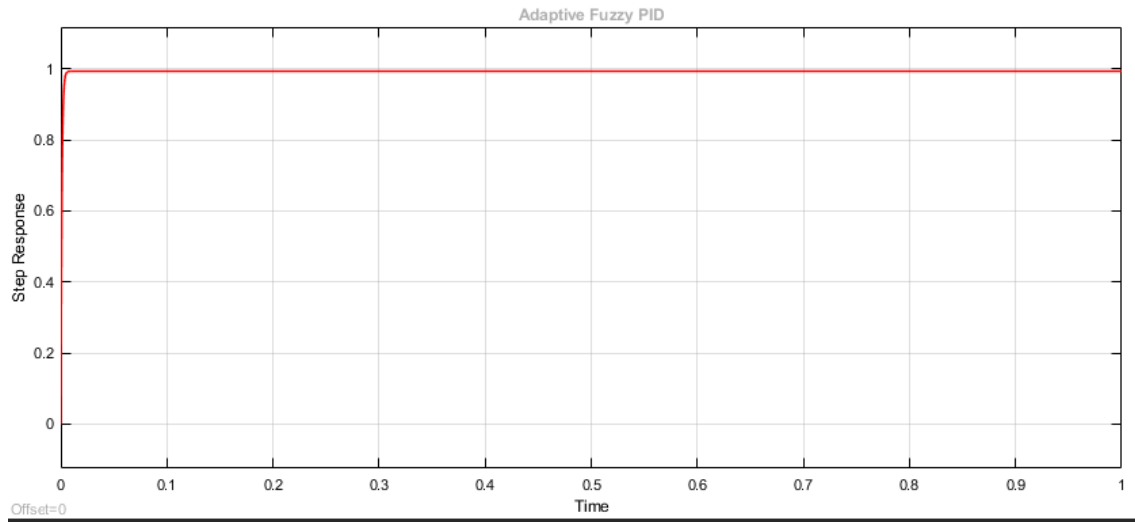
Figure 4.20: Step response of Adaptive Fuzzy PID Controller
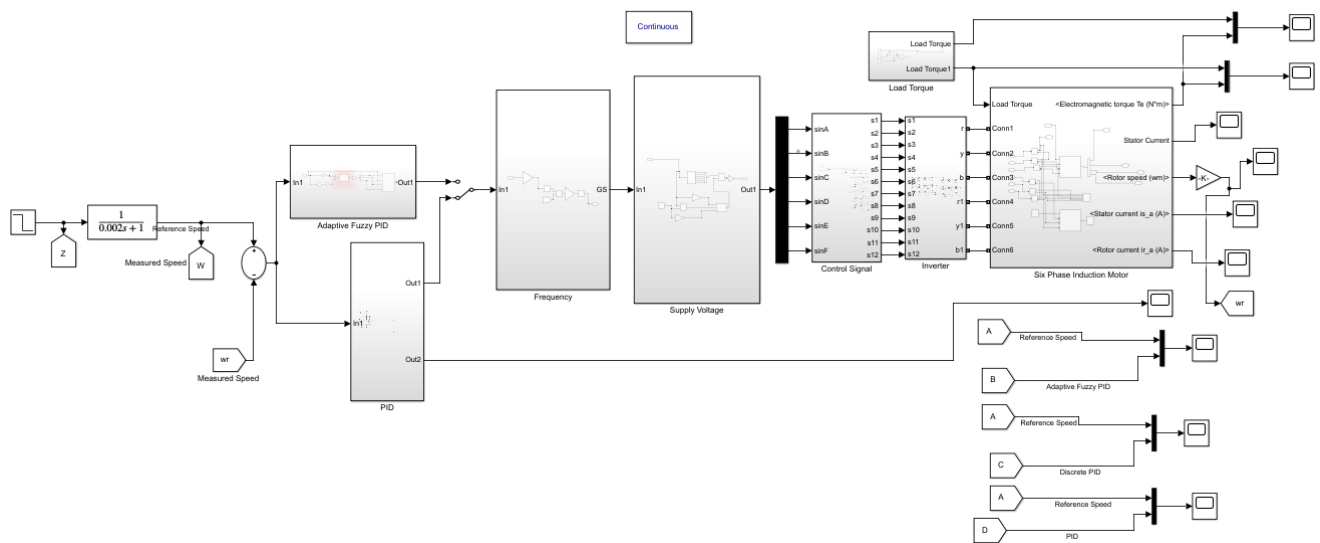
Figure 4.21: Speed Control of Six Phase Induction Motor Circuit

The simulation tests are used to examine the performance of the controller in question while varying the parameters. Different reference torques are taken into account in the simulation results due to variable loading conditions. The steps of increasing load torque begin at t=0 and progress to 0, 5, 10, 20, and 0, 0.3, 0.5,0.8,0.1 seconds, respectively with matching variations in stator and rotor current, torque, and speed. It is assumed that the speed was increased and decreased, starting at 50 rad/s and ending at 1500 rad/s, for this purpose.

88
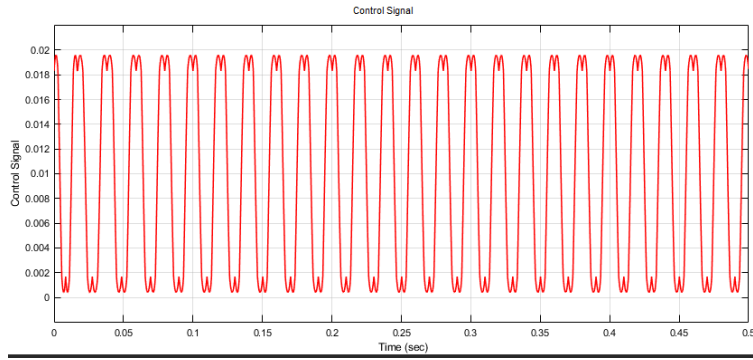
Figure 4.22: Generated Control signal of Space Vector PWM
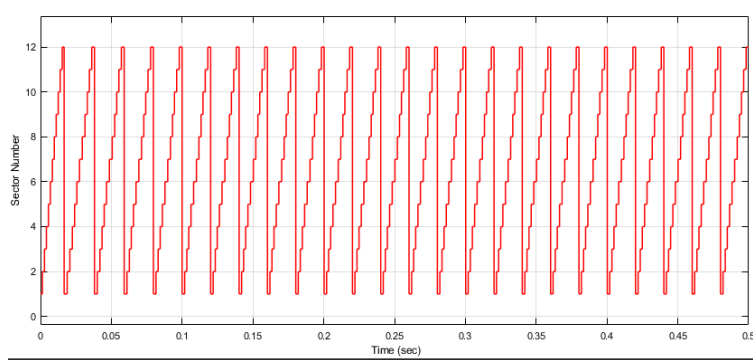
Figure 4.23: Number of Sectors of Twelve switches
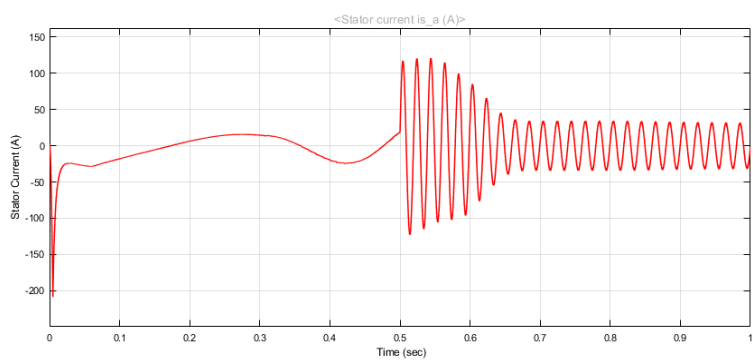
Figure 4.24: Stator Current Response to Step Change in Speed Reference and Load Torque
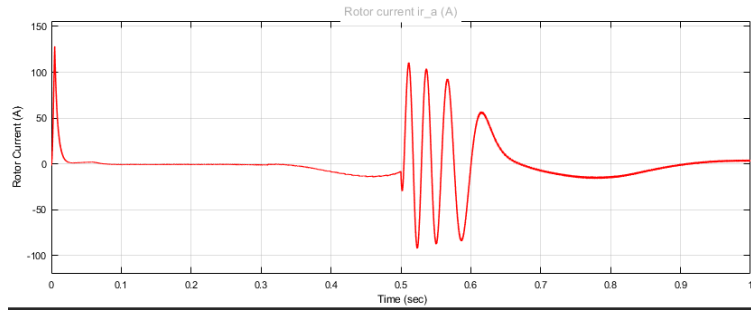
Figure 4.25: Rotor Current Response to Step Change in Speed Reference and Load Torque
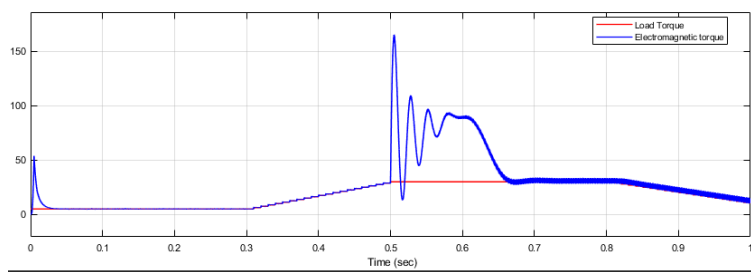
Figure 4.26: Electromagnetic Torque Response to Step Change in Speed and Load Torque

Figure **??** shows that the transient of load torque is maximum at the starting and last for 0.05 seconds. At the first step the load torque is constant which is 5Nm for 0.3 seconds, then increased to 20Nm and constant for the next 0.3 seconds and falls to 10Nm for the last seconds and there is step change by reference speed from 1500 rad/sec for 0.3 seconds and 650 rad/sec for the next 0.2 seconds. In this case varying the load torque varies the stator and rotor current and Electromagnetic torque while it is no impact on the measured speed. The electromagnetic torque is increased as load torque increased and decreased as load torque decreased.
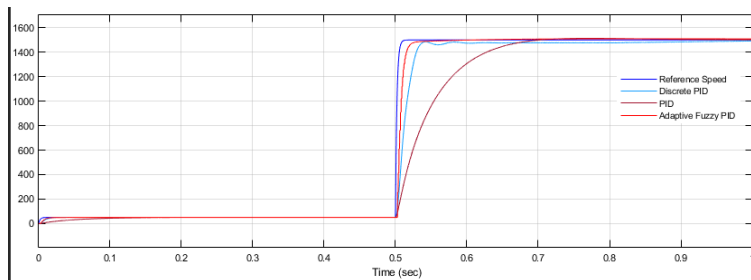
Figure 4.27: Measured Speed Response to Step Change in Speed Reference

Figure **??** shows that measured speed response of the system for PID, Discrete PID and Adaptive fuzzy PID. It is observed that Adaptive fuzzy PID controller have good transient and steady state response than othe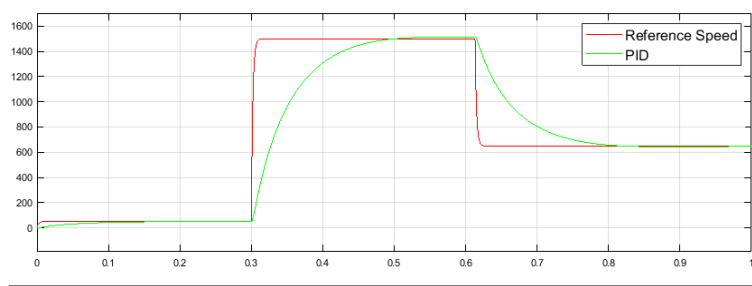r controller. Figure **??** shows that the measured and reference speed when PID controller is used, the reference speed is 50 rad/sec for 0.3 seconds and 1500 rad/sec for the next 0.3 seconds. Then after 0.6 seconds the reference speed then falls down to 550 rad/sec and the measured speed is varying with speed reference condition, which is decreased.

Figure 4.28: PID Speed Controller

Figure **??** shows that the measured and reference speed when Discrete PID controller is used, the reference speed is 50 rad/sec for 0.3 seconds and 1500 rad/sec for the next 0.3 seconds. Then after 0.6 seconds the reference speed then falls down to 550 rad/sec and the measured speed is varying with speed reference condition, which is decreased and and have more performance than PID controller by following the Reference speed.
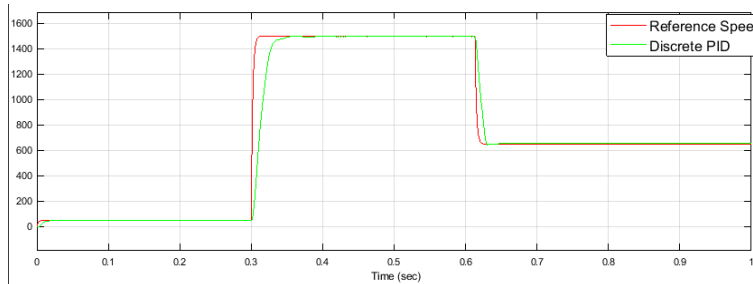

Figure 4.29: Discrete PID Speed Controller

Figure **??** shows that the measured and reference speed when Adaptive Fuzzy PID controller is used, the reference speed is 50 rad/sec for 0.3 seconds and 1500 rad/sec for the next 0.3 seconds. Then after 0.6 seconds the reference speed then falls down to 650 rad/sec and the measured speed is varying with speed reference condition, which is decreased and and have more performance than PID and Discrete PID controller by following the Reference speed.
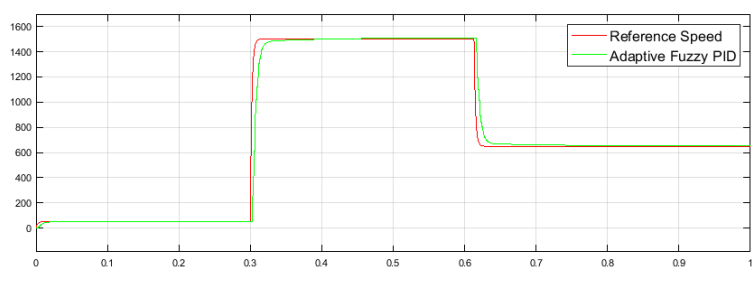

Figure 4.30: Adaptive Fuzzy PID Speed Controller

Reduction in Speed

Figure **??** shows that the transient of load torque is maximum at the starting and last for 0.05 seconds. At the first step the load torque is constant which is 5Nm for 0.3 seconds, then increased to 20Nm and constant for the next 0.2 seconds and falls to 10Nm for the last seconds and there is step change by reference speed from 900 rad/sec for 0.3 seconds and 300 rad/sec for the next 0.7 seconds. In this case varying the load torque varies the stator and rotor current and Electromagnetic torque while it is no impact on the measured speed. The electromagnetic torque is increased as load torque increased and decreased as load torque decreased.
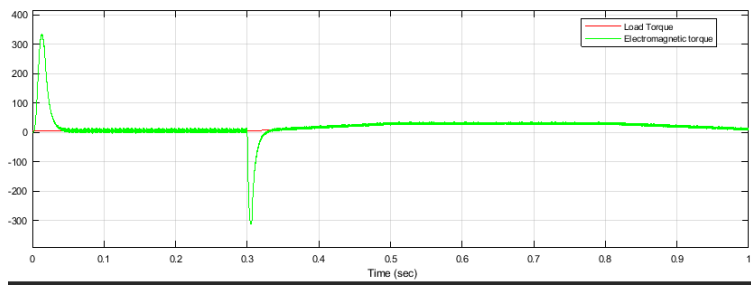
Figure 4.31: Electromagnetic Torque Response to Step Change in Speed Reference and Load Torque
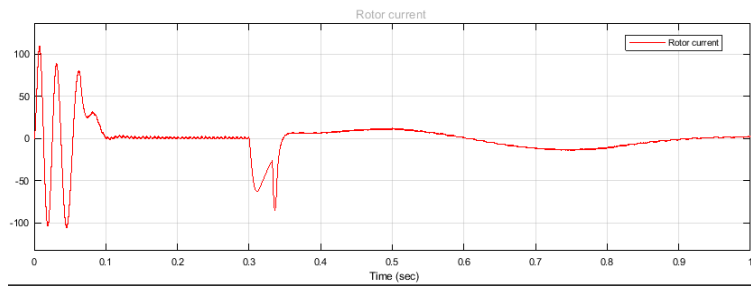

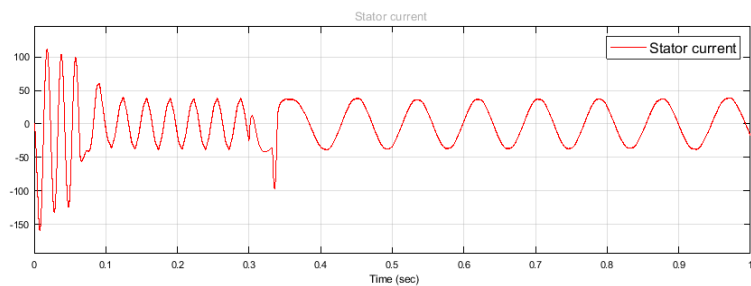Figure 4.32: Rotor Current Response to Varying Load Torque

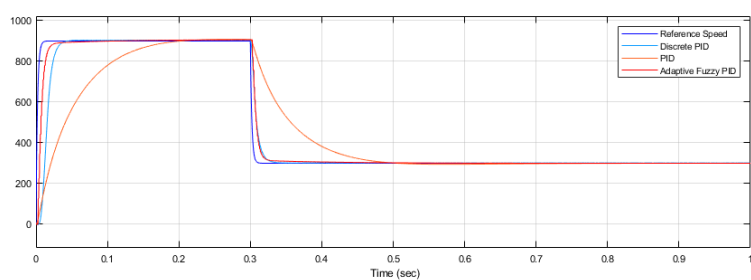Figure 4.33: Stator Current Response to Varying Load Torque

Figure 4.34: Measured Speed Response to Step Change in Speed Reference

Figure **??** shows that measured speed response of the system for PID, Discrete PID and Adaptive fuzzy PID. It is observed that Adaptive fuzzy PID controller have good transient and steady state response than other controller when the speed is high at starting and

93

decreasing after some time.

Disturbance of Sudden Load Torque

The devices were in a constant state of operation. Then the load torque increased from 5Nm to 20Nm in 0.3 seconds. As illustrated in the figure **??**, the produced torque increases but has no effect on the speed characteristic. Then load torque was then reduced from 20 to 10 Nm, as shown in figure **??**. As seen in this figure, the produced torque reduces but has no effect on the speed characteristic. The developed torque dropped, and the rotor speed was unaffected. For a drive with a load torque of 5Nm, the drive system's beginning performance was evaluated. Figure **??** shows the motor speed during the starting transient condition, illustrating that the motor reaches the set speed in around 0.015 seconds for Adaptive fuzzy PID and 0.2 seconds for PID without oscillation. As the motor speed approaches the reference speed, the motor phase currents decrease.

As the load increases, the stator current and motor torque all increase. For a load variation from zero loads to varied load torque condition, Adaptive Fuzzy PID, Discrete PID, and PID controllers notice the transient oscillations of the torques. When Adaptive fuzzy PID is applied, electromagnet torque, rotor speed, and stator phase currents reveal that the system has strong transient and steady state responsiveness under various load conditions. At the transient response, which oscillates for 0.15 seconds, the initial torque is considerable. Motor torque and stator current rise as load increases, but rotor speed remains unchanged. It can be seen that the speed closely follows the reference value and is unaffected by load variations. When the Adaptive fuzzy PID is employed, the torque has a superior performance. The figure **??** depicts the results of a series of testing of step changes in speed reference. Time from 0 to 0.5sec, speed = 50 rad/s, and time from 0.5sec to 1sec, speed= 1500 rad/s are used to vary the reference speeds of the motors. The controllers' performance is measured in terms of speed response in this simulation. It can be seen that with Adaptive fuzzy PID, the magnitude of transient speed oscillations is reduced. The results reveal that the Adaptive fuzzy PID controller outperforms the PID and Discrete PID controllers in terms of performance. Finally, the simulation results of employing Adaptive fuzzy PID, PID, and Discrete PID controllers for load torques and speed fluctuations were examined. These results confirm that the Adaptive fuzzy PID controller demonstrate better performance under changing operating environments and present satisfactory performance.

Proposed Slide Mode Controller

A SMC uses a nonlinear control scheme that have a power to control the systems to slide along a defined surface to robustly stabilize, it alters the system dynamics to adapt to these behaviors. In these scheme, the value of the electromagnetic torque and actual speed generated by the induction motor were designed to be compared to the desired value to generate an error signal, and the error was controlled by the SMC. In sliding mode control, the system is well controlled in this manner that the tracking error and its value of exchange constantly flows in the direction of a sliding surface. The speed control goal is to force the rotor speed ω_r to track the desired rotor speed reference ω_{ref}. For the speed control system,

the mechanical equation of an induction motor drive can be represented as:

$$\omega'_r = \frac{1}{J}(-B\omega_r - T_L + T_e) \tag{4.28}$$

The sliding surface is defined as in the state space representation by following equation: $S(e, e', t)=0$

where S is sliding surface

The switching surface is chosen as $S = e + \eta e'=0$

$e = \omega_{ref} - \omega_r$

η is the positive constant which depend on bandwidth of the models. Parameters of Slide mode controllers are: SMC1 is K=1200,Lamda=2 and $\delta = 0.1$

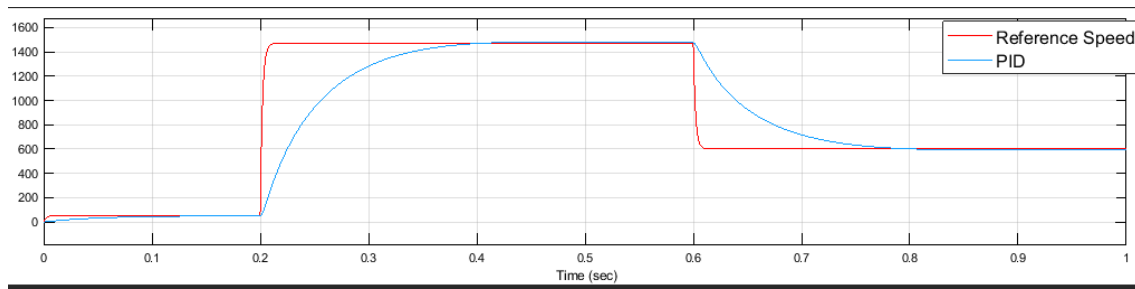SMC2 is K=1800,Lamda=2 and $\delta = 0.15$

Figure 4.35: Measured and Reference Speed With PID Controller

Figure ?? shows that the measured and reference speed when PID controller is used, the reference speed is 50 rad/sec for 0.2 seconds and 1470 rad/sec for the next 0.4 seconds respectively. Then after 0.6 seconds the reference speed then falls down to 600 rad/sec and the measured speed is varying with speed reference condition, which is decreased following the Reference speed.
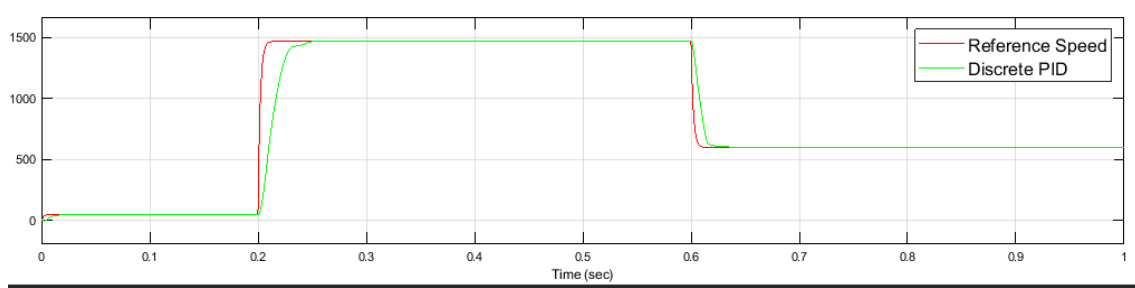

Figure 4.36: Measured and Reference Speed With Discrete PID Controller

Figure ?? shows that the measured and reference speed when Discrete PID controller is used, the reference speed is 50 rad/sec for 0.2 seconds and 1470 rad/sec for the next 0.4 seconds. Then after 0.6 seconds the reference speed then falls down to 600 rad/sec and the measured speed is varying with speed reference condition, which is decreased and and have more performance than PID controller by following the Reference speed.
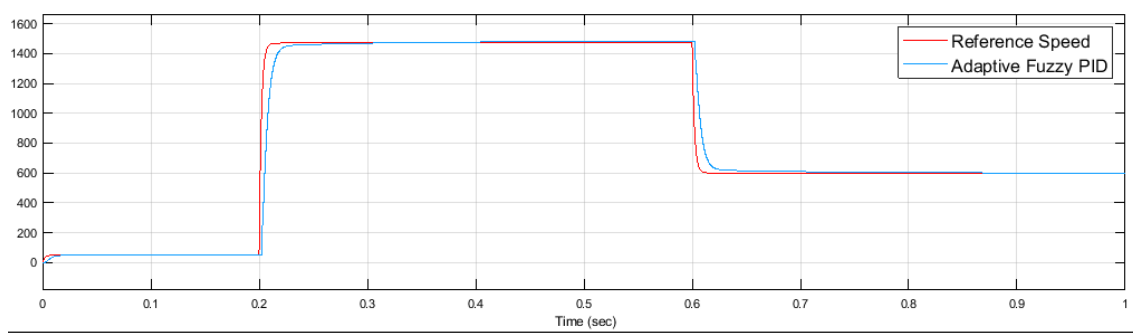
95

Figure 4.37: Measured and Reference Speed With Adaptive Fuzzy PID Controller

Figure **??** shows that the measured and reference speed when Adaptive Fuzzy PID controller is used, the reference speed is 50 rad/sec for 0.2 seconds and 1470 rad/sec for the next 0.4 seconds. Then after 0.6 seconds the reference speed then falls down to 600 rad/sec and the measured speed is varying with speed reference condition, which is decreased and and have more performance than PID and Discrete PID controller by following the Reference speed.
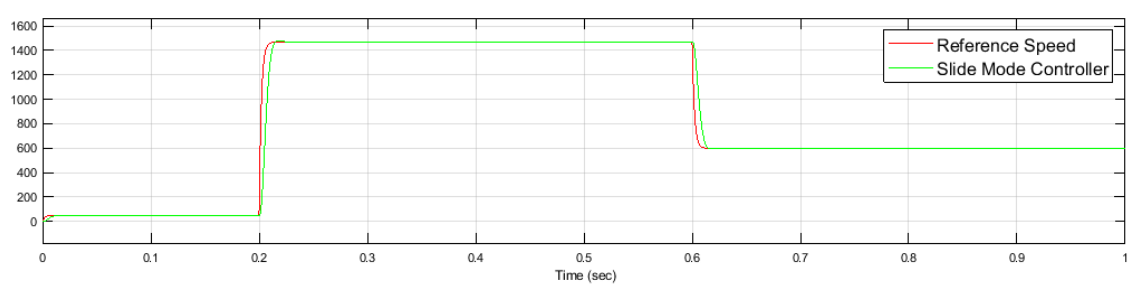

Figure 4.38: Measured and Reference Speed With Slide Mode Controller

Figure **??** shows that the measured and reference speed when Slide Mode Controller is used, the reference speed is 50 rad/sec for 0.3 seconds and 1500 rad/sec for the next 0.3 seconds. Then after 0.6 seconds the reference speed then falls down to 650 rad/sec and the measured speed is varying with speed reference condition, which is decreased and and have more performance than PID, Discrete PID and Adaptive Fuzzy PID controller by following the Reference speed.
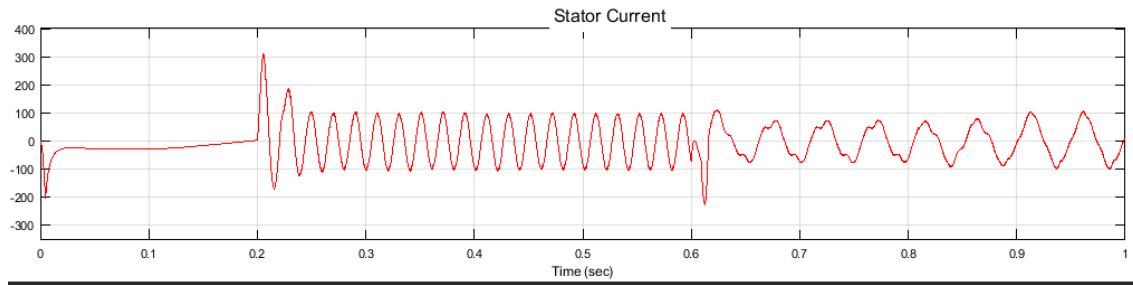
Figure 4.39: Stator Current Response to Varying Speed

Figure **??** shows that the Stator Current Response to Varying Speed, the reference speed is 50 rad/sec for 0.3 seconds and 1470 rad/sec for the next 0.3 seconds. Then after 0.6 seconds the reference speed then falls down to 600 rad/sec and the measured speed is varying with speed reference condition, which is decreased. At the starting since the load is so small stator current is also small and when the speed is increased the stator current oscillates and increased. At the time of speed reduction the stator current also reduced following the speed.
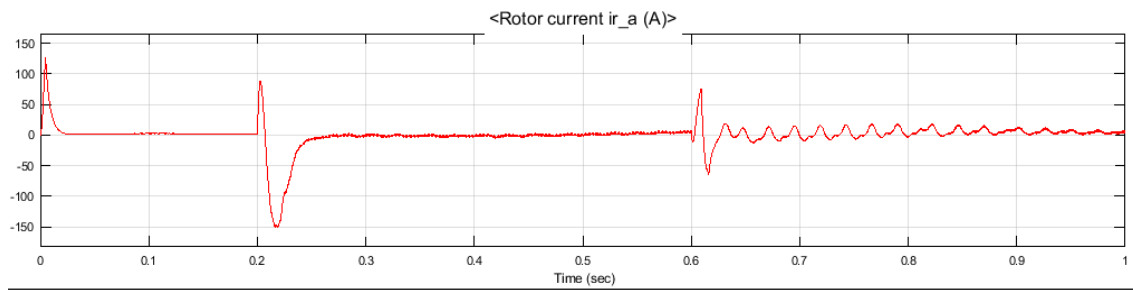

Figure 4.40: Rotor Current Response to Varying Speed

Figure **??** shows that the Rotor Current Response to Varying Speed, the reference speed is 50 rad/sec for 0.3 seconds and 1470 rad/sec for the next 0.3 seconds. Then after 0.6 seconds the reference speed then falls down to 600 rad/sec and the measured speed is varying with speed reference condition, which is decreased. At the starting since the load is so small rotor current high due to low resistance and comes to stationary and when the speed is increased the rotor current oscillates slightly toward the stationary. At the time of speed reduction the rotor current also reduced and slightly oscillates following the speed.
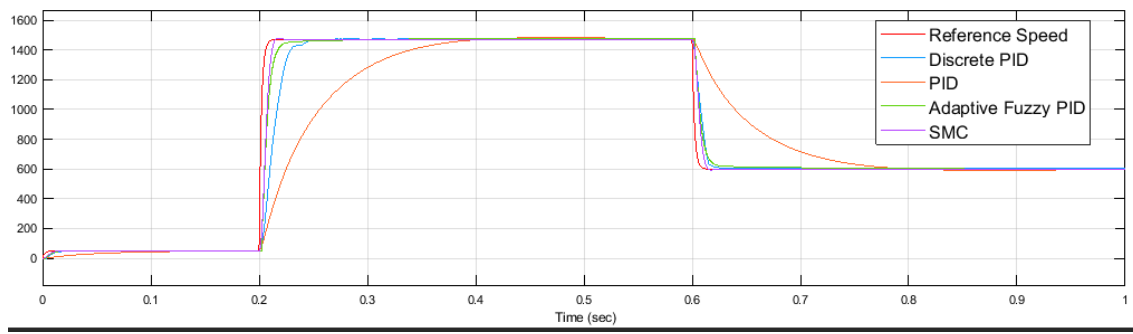
Figure 4.41: Measured Speed to Step Change with Different Controllers

Figure **??** shows that the measured and reference speed when PID, Discrete PID,Adaptive Fuzzy PID and Slide Mode controller is used, the reference speed is 50 rad/sec for 0.2 seconds and 1470 rad/sec for the next 0.4 seconds respectively. Then after 0.6 seconds the reference speed then falls down to 600 rad/sec and the measured speed is varying with speed reference condition, which is decreased.

Table 4.8: Comparison of Controllers

Time Domain	Tuned PID	Tuned Discrete PID	Adaptive Fuzzy PID	SMC1	SMC2
Rise Time(s)	0.1058	0.1050	0.0046	0.0080	0.0086
Peak Time(s)	0.2715	0.2715	0.2600	0.0177	0.0875
Settling Time(s)	0.1668	0.1668	0.0840	0.0132	0.0152
Steady State Error	0.0028	0	0	0	0
Overshoot	0.9148	0.9120	0.1460	0.7173	0.0047

From the table **??** and from **??**, it can be seen that the Slide Mode Controller and Adaptive Fuzzy PID Controller has the better response when compared to the PID and Discrete PID controllers of that SMC has best. The target of this thesis is that to reduce settling time, steady state error, minimizing overshoot and improving the efficiency and power factor while keeping the weight and power loss to the minimum point. The settling time is fast and small overshoot is present in case of SMC, hence the Slide Mode Controller gives a better speed control of six phase induction motor.

CHAPTER FIVE

5 CONCLUSION AND RECOMMENDATIONS

5.1 CONCLUSION

The main aim of this research paper is optimal designing of six phase squirrel cage induction motor to increase reliability, efficiency and reduce the volume and cost. For this purpose, the six-phase squirrel cage induction motor has been optimized by Particle Swarm Optimization algorithm to compare and contrast with manual design and GA and which results in maximum efficiency and minimum size. This design procedure considers efficiency as the objective function and shows how much this motor is efficient and considering weight as objective function, shows the optimized motors weight.Some parameters are treated as empirical variables in the traditional six-phase squirrel-cage submersible induction motor design technique. The parameters values were obtained by using manual design, GA and PSO with the objective function of motor Efficiency, Power factor, Power Losses, Weight Losses and Cost Minimization in this study as optimization variables. The results demonstrate that when compared to the usual technique, the motor efficiency, power factor, power losses, weight losses and cost minimization attained by PSO optimization strategy is significantly higher than manual design and GA. Furthermore, the PSO designed six-phase squirrel-cage submersible induction motor outperforms than manually and GA designed six-phase squirrel-cage submersible induction motor in terms of performance. The Finite Element Analysis (FEA) was used to validate the outcomes of the suggested optimization strategies. The motor properties calculated by design techniques have an acceptable accuracy, according to FE analysis. The motor efficiency of the motors designed using PSO is higher than the motor efficiency of the conventional approach, according to FE analysis. It also demonstrates the advantages of the PSO designed six-phase squirrel-cage submersible induction motor over the manually and GA designed six-phase squirrel-cage submersible induction motor. This research makes a significant contribution to a fascinating issue in the field of electric motor design and other technical applications. Furthermore, the algorithms were tested on two kinds of copper and iron for losses and weights. In the study, the particle swarm algorithm outperformed the manual design and GA. The acquired findings demonstrate that the methodology employed is a viable solution to the specified optimization issue. It can be seen that by using PSO six-phase squirrel-cage induction motor's performance is improved and the losses are reduced. As a result, efficiency has increased. The weight of the motor is also lowered while attaining performance increases, which is an important achievement. In terms of the cost of different components and their dependencies on area, manufacturer, and time, the optimal cost-based design obtained. The proposed slide mode controller is used for the speed control of six phase induction motor and results in the good performance when compared with the other controllers within the paper.

5.2 RECOMMENDATIONS

Induction motors have a wide range of uses in industry, ranging from modest household appliances to larger industrial. Induction motors are used in almost every applications. However, this really helpful and interesting motor in case of submarines propulsion results in the problem cost, power losses and weight increment as number of phases increased. As a result, a standard optimized motor design is necessary to apply six-phase squirrel cage induction motor to submarines and improve the above stated problems. A manual and optimized PSO design of six-phase squirrel cage induction motor was used in this research paper, followed by ANSYS MotorCAD software simulation. This article focuses on the shape and size of the stator and rotor slot, which have a direct influence on the performance of an six-phase squirrel cage induction motor, in order to achieve an optimum design. In the future, a prototype of this hardware design will be implemented. As a recommendation particularly those who specialize in the design of electric machines, should collaborate to design an efficient and optimized cost motor for critical applications like submarines.

References

[1] Akpama and E. J., *Six Phase Induction Motor Modelling For Submarine Application*,IOSR Journal of Electrical and Electronics Engineering (IOSR-JEEE), Volume 13, Issue 1 Jan-Feb, 2018, pp. 61-66 DOI: 10.9790/1676-1301046166

[2] E. Ali and B.C. Ghosh, *Comparison of Performances of Six Phase Induction Motor Consisting of Dual Three Phase Windings fed from Sinusoidal Voltage and Current Sources under Normal and Abnormal Operating Conditions* , International Journal of Innovations in Engineering and Technology (IJIET), Volume 14 Issue 4 November 2019 ISSN: 2319-1058 http://dx.doi.org/10.21172/ijiet.144.05

[3] Samuel E. Iduh, Silas E. Omugbe, *THE DESIGN AND PRACTICAL IMPLEMENTATION OF A SIX-PHASE INDUCTION MOTOR*, Journal of Advances in Science and Engineering, volume 3 Issue 1, pp.1-77, 2020 DOI: $https : //doi.org/10.37121/jase.v3i1.95$

[4] Pratyush Prasanna Das and S. N. Mahato, *Design Optimization of a Six-Phase Induction Motor by Flower pollination and Modified Artificial Bee colony Algorithms* , IEEE, 2016 pp. 3315-3317

[5] Youssef Dhieb, *et al, PID Controller Tuning using Ant Colony Optimization for Induction Motor*,Journal of Electrical Systems Systems, Volume 15(1), Oct, 2018, pp. 133-141

[6] Akpama and E. J., *Modelling Of Six-Phase Induction Machine Including Saturation Effect*,Journal of Multidisciplinary Engineering Science and Technology (JMEST), Volume 6 Issue 7, July, 2019 ISSN: 2458-9403

[7] M SOWMIYA1, and S HOSIMIN THILAGAR, *Design and performance analysis of a dual stator multiphase induction motor using finite element method*,Indian Academy of Sciences, Volume 46, Issue 67, pp. 1-11, March 8, 2021, $https : //doi.org/10.1007/s12046 − 021 − 01603 − 6S$

[8] Roma RINKEVIČIENĖ, Benas KUNDROTAS and Sonata TOLVAIŠIENĖ, *Model of Six-Phase Induction Motor*, Solid State Phenomena Vol 220-221, pp. 510-514, may 26, 2015. DOI:10.4028/www.scientific.net/SSP.220-221.510

[9] Akpama Eko James, Linus Anih and Ogbonnaya Okoro, *Transient Analysis and Modelling of Sixphase Asynchronous Machine*, American Journal of Electrical Power and Energy Systems volume 4 Issue 6, pp.77-83, 2015 Published online October 31, 2015($http : //www.sciencepublishinggroup.com/j/epes$) doi: 10.11648/j.epes.20150406.11 ISSN: 2326-912X (Print); ISSN: 2326-9200 (Online)

[10] A.T. Abdullah and Dr. A. Mejbel Ali, *Thermal analysis of a three-phase induction motor based on motor-CAD, flux2D, and matlab*, Indonesian Journal of Electrical Engineering and Computer Science,Volume 15, No. 1, July 2019, pp. 46-53 ISSN: 2502-4752, DOI: 10.11591/ijeecs.v15.i1.pp46-53

[11] M. Fawzi *et al, Finite Element Analysis of Multi-Phase Squirrel Cage Induction Motor to Develop the Optimum Torque*, IEEE Conference on Power Electronics and Renewable Energy (CPERE) , 2019 , pp. 504 –510

[12] M.R.Djalal and Faisal, *DESIGN OF OPTIMAL PID CONTROLLER FOR THREE PHASE INDUCTION MOTOR BASED ON ANT COLONY OPTI-MIZATION*,SINERGI , Volume 24, No. 2, June 2020: pp. 125-132 $http : //doi.org/10.22441/sinergi.2002.2.006$

[13] A.S. ABDEL-KHALIK *et al, Postfault Control of Scalar (V/f) Controlled Asymmetrical Six-Phase Induction Machines*,IEEE, Volume 6, October 5, 2019, pp. 59211-59220 ISSN: 2502-4752, DOI: 10.1109/ACCESS.2018.2874133

[14] S.S.Sivaraju and N. Devarajan, *GA BASED OPTIMAL DESIGN OF THREE PHASE SQUIRREL CAGE INDUCTION MOTOR FOR ENHANCING PERFOR-MANCE*,International Journal of Advanced Engineering Technology, Volume 2, Issue 4 October 5, 2016, pp. 202-206 E-ISSN 0976-3945

[15] H. Reza Mohammadi and A. Akhavan, *Parameter Estimation of Three-Phase In-duction Motor Using Hybrid of Genetic Algorithm and Particle Swarm Optimiza-tion*,Hindawi Publishing Corporation Journal of Engineering, 1 December, 2019, pp. 1-6 $http : //dx.doi.org/10.1155/2014/148204$

[16] M. Ben Slimene, *PERFORMANCE ANALYSIS OF SIX-PHASE INDUCTION MACHINE MULTILEVEL INVERTER WITH ARBITRARY DISPLACEMENT* , Electrical Engineering & Electromechanics , 2020 pp. 12-16 DOI: 10.20998/2074-272X.2020.4.02

[17] G. Rezazadeh *et al, Analysis of Six-Phase Induction Motor with Distributed and Con-centrated Windings by Using the Winding Function Method*, IEEE, pp. 2423-2429, 2018. ISSN 978-1-5386-2477-7

[18] Chih-Hong Lin, *Altered Grey Wolf Optimization and Taguchi Method with FEA for Six-Phase Copper Squirrel Cage Rotor Induction Motor Design*,Energies,Volume 13, Issue 4 May 5, 2020, pp. 1-17 doi:10.3390/en13092282

[19] Anupama Johnson *et al, Comparison of Six Phase and Three Phase Induction Motors for Electric Vehicle Propulsion as an Improvement Toward Sustainable Transportation*, Springer, Volume 13, Issue 1 Jan-Feb, 2019, pp. 239-247 $doi.org/10.1007/978 - 981 - 13 - 1202 - 1 - 21$

[20] B. Alizadeh1 and S. Asghar Gholamian, *Application of Ant Colony Optimization Al-gorirhm for Optimal Design of Squirrel Cage Induction Motor*,International Journal of Mechatronics, Electrical and Computer Technology, Volume 4, Issue 13 October, 2014, pp. 1674-1690, ISSN: 2305-0543

[21] Paulo S. Dainez and Edson Bim, *A New Multiphase Rotor Model for the Squirrel Cage Rotor of a Six-phase Induction Machine* , ResearchGate , October , 2018 DOI: 10.1109/IECON.2018.8592703

[22] Nicolas Rivière, Marco Villani and Mircea Popescu, *Optimisation of a High Speed Copper Rotor Induction Motor for a Traction Application* , IEEE , 2019 pp. 2720-2725

[23] Mustafa Turan, *et al, Squirrel Cage Induction Motor Design and the Effect of Specific Magnetic and Electrical Loading Coefficient*, International Journal of Applied Mathematics Electronics and Computers, Volume 7 Issue 1 December 23, 2018, pp.1-8 ISSN:2147-82282

[24] A.S. ABDEL-KHALIK, M.S. ABDEL-MAJEED and SHEHAB AHMED, *Effect of Winding Configuration on Six-Phase Induction Machine Parameters and Performance* , IEEE POWER & ENERGY SOCIETY SECTION, Volume 8, December 10, 2020, pp. 223009 – 223020 DOI 10.1109/ACCESS.2020.3044025

[25] Mohamed I. Abdelwanis and Ragab A. El-Sehiemy, *A Fuzzy-Based Controller of a Modified Six-Phase Induction Motor Driving a Pumping System* , Springer , Vol. 8, No. 4, may 11, 2018, pp. 580 – 587 https://doi.org/10.1007/s40998-018-0066-4

[26] Pravin Kumbhar *et al, Open Loop V/F Control of Six Phase Induction Motor* , International Research Journal of Engineering and Technology (IRJET) , Volume 8 Issue 3 Mar, 2021 , pp. 750 –755 e-ISSN: 2395-0056

[27] Bhupesh Kumar Pal *et al, Control of Grid Side Converter for Grid Connected Six Phase Induction Generator* , International Research Journal of Engineering and Technology (IRJET) , Volume 1 Issue 2 April 12, 2019

[28] P.Manikandan (2015) *DESIGN OF ELECTRICAL MACHINES* [PowerPoint slides]. Available: $EE2355 DESIGN OF ELECTRICAL MACHINES A... - Course...http : //www.coursehero.com/file/EE2355 - DEM pdf$

[29] E. C. Abunike1, O. I. Okoro and G. D.Umoh *STEADY AND DYNAMIC STATES ANALYSIS OF INDUCTION MOTOR: FEA APPROACH* , Nigerian Journal of Technology (NIJOTECH), Volume 36, No. 4, October 2017, pp. 1202 – 1207 ISSN: 2467-8821

[30] E. M. Shaban *et al. A novel discrete PID controller applied to higher order/time delayed nonlinear systems with practical implementation* , International Journal of Dynamics and Control(Springer), 23 August 2018

[31] P.P. Das and S. N. Mahato *Artificial Bee Colony Based Design Optimization of a Six-Phase Induction Motor* , 2nd International Conference on Control, Instrumentation, Energy and Communication (CIEC), 23 August 2016, pp. 526 – 530

[32] Man Mohan *et al. A COMPARATIVE STUDY ON PERFORMANCE OF 3KW INDUCTION MOTOR WITH DIFFERENT SHAPES OF STATOR SLOTS* , International Journal of Engineering Science and Technology (IJEST), Volume 4 Number 06 23 June 2018, pp. 2446 – 2452

APPENDIX

A. MATLAB codes

A MATLAB code for manual design

$fprintf('InputtheSpecificationsoftheSixPhaseInductionMotor');$

    P=input('input power in KW=);

    V=input ('input voltage in volts=);

    f=input('input frequency on hz=);

    p=input('input no of poles=);

    $Bav = input('inputbavinWb/m^2 =);$

    ac=input('ac in a/m=);

    pf=input('power factor=);

    eff=input('eff of m/c=);

    Y=input('design consideration of Length to pole pitch ratio=')

    Js=input('current density=')

    sf=input('space factor sf=')

    h=input(' height of the core in m=)

    Bcs=input('flux density stator core Bcs=')

    Hs0=input(' lip in meters =)

    Hs1=input(' wedge in meters =)

    Hs2=input('Space occupied by insulated conductor =')

    m=6;

    K=1;

    stackingfactor=0.9;

    Ss=48;

    Sr=38;

    Kw=0.955;

    Ns=120*f/p

    ns=(2*f)/p

Q=P/(eff*pf)

$Co = 11 * Kw * Bav * ac * 10^{-3}$

    $D = abs((Q * p/(Co * ns * pi * Y))^{1/3})$

L=Y*pi*D/(p)

Pp=(pi*D)/p

v=(pi*D*ns)

Li=L*stackingfactor

fx=Bav*(pi*D*L)/p

fxp=Bav*(pi*D*L)/p

Tph=V/(4.44*f*fx*Kw)

Zph=2*Tph

$Is = Q/(6 * V * pf) * 10^3$

IsL=sqrt(3)*Is;

lg=0.2+2*sqrt(D*L)
As=Is/Js
Zt=2*m*Tph
Zss=2*m*Tph/(Ss)
Yss=pi*D/(Ss)
S=Zss*As
Cs=Ss/p Ass=S/(sf)
Ac=2*m*Tph*Is/(pi*D)
fsc=fx/2
Acs=fsc/Bcs
dcs=Acs/Li
dss=Hs0+Hs1+Hs2
Lmt=2*L+2.3*Pp+0.24
Rs =0.021*Tph*Lmt/As
$Pcl = m * Is^2 * Rs$ Mintapp=fx/1.7
wst= Mintapp/((Ss/p)*Li)
Bst=fx/((Ss/p)*wst*Li)
Ys=(pi*D)/Sr
At=wst*Li
Ws=Ys-wst
ntp=Ss/p
Ast=wst*Li*ntp
Bt=fx/At
Bmax=1.5*Bt
Do=D+2*dcs+2*dss
dcs= 1/2*(Do-D-2*dss)
Acs=Li*dcs
fsc=1/2*fx
Bc=fsc/Acs
Jb=input('rotor bar current density ab=')
Ib=((2*m*Is*Tph)/Sr)*pf
Ab=Ib/Jb
Afs=input('allowance for skewing Afs=')
Lb = L + Afs

    Rb=0.021*Lb*Sr/(Ab)
Dr=D-2*lg
Yrs=pi*Dr/Sr
$Pclr = Ib^2 * Rb$
Ibav=0.45045*Sr*Ib/p
Ie=Sr*Ib/(p*pi)
Je=input('end current dencity ae=')
Ae=Ie/Je
Dme=input('Mean diameter of end ring Dme=')
Lme=pi*Dme

Re=0.021*Lme/Ae
$Pler = 2 * Ie^2 * Re$
Ir=0.85*Is
Ptotal=Pler+Pclr
$Rr = Ptotal/(m * (Ir)^2)$
Ysr=pi*D/Sr
hso=1;
hso1=1;
hs1=2;
hs2=18;
dsr=hso+hso1+hs1+hs2
Bcr=input('flux density 0f Bcr=')
dcr=fx/(2*Bcr*Li)
Di=Dr+2*dsr+2*dcr
kcs=0.5;
kcd=0.5;
Bso=1.5;
Bro=1.5;
$Kgss = Yss/(Yss - kcs * (Bso * 10^{-3}))$
$Kgsr = Ysr/(Ysr - kcd * (Bro * 10^{-3}))$
Kg=Kgss*Kgsr
lge=lg*Kg

   Bg =1.36*Bav
$perm = 4 * pi * 10^{-7};$
Mmfg=Bg*lge/(2*perm)
Atst=input('mmf per metre for stator teeth Atst=')
Mmfst = Atst*dss
$Lsc = pi * (D + 2 * dss * 10^{-3} + 2 * dcs * 10^{-3})/(3 * p)$
Atsc=input('mmf per metre for stator core Atsc=')
Mmfsc=Atsc*Lsc
Atrt=input('mmf per metre for rotorr teeth Atrt=')
Mmfrt=Atrt*dsr
$Lrc = pi * (D - 2 * dsr * 10^{-3} - dcs * 10^{-3})/3 * p$
Atrc=input('mmf per metre for rotor core Atrc=')
Mmfrc=Atrc*Lrc
Tmmf=Mmfg+Mmfst+Mmfsc+Mmfrc+Mmfrt
Im=pi*p*Tmmf/(12*Kw*Tph)
Pfw=0.02*P;
Psl=0.005*P;
$Pnll = Psl * 10^3 + Pfw * 10^3$
Ic=Pnll/(6*V)
$Io = sqrt(Im^2 + Ic^2)$
Ploadloss=Pcl+Ptotal
Pt=Pnll+Ploadloss

$$s = Ptotal/(Ptotal + P * 10^3)$$
Nm=Ns*(1-s)
fr=s*f
wm=Nm*2*pi/60
$$Tsh = P * 10^3/wm$$
$$Pin = P * 10^3 + Pt$$
$$Rpf = Pin * 10^{-3}/Q$$
$$Reff = P/(P + Pt * 10^{-3})$$

PSO Algorithm MATLAB Code

Main Program

```
tic
clc
clear all
close all
rng default
LB = [0.21 0.028 0.017 0.0645 0.18 0.076 0.088 0.0035 0.18];
UB = [0.27 0.032 0.022 0.0665 0.21 0.0885 0.092 0.005 0.24];
m=9;
n=100;
wmax=0.9;
wmin=0.4;
c1=2;
c2=2;
maxite=1000;
maxrun=10;
for run=1:maxrun
run
for i=1:n
for j=1:m
x0(i,j)=round(LB(j)+rand()*(UB(j)-LB(j)));
end
end
x=x0;
v=0.1*x0;
for i=1:n
f0(i,1)=ofuntry(x0(i,:));
end
[fmin0,index0] = min(f0);
pbest=x0;
gbest=x0(index0,:);
ite=1;
```

```
tolerance=1;
while ite <= maxite & tolerance >= 10^-12
w=wmax-(wmax-wmin)*ite/maxite;
for i=1:n
for j=1:m
v(i,j)=w*v(i,j)+c1*rand()*(pbest(i,j)-x(i,j))+c2*rand()*(gbest(1,j)-x(i,j));
end
end
for i=1:n
for j=1:m
x(i,j)=x(i,j)+v(i,j);
end
end
for i=1:n
for j=1:m
if x(i,j)<LB(j)
x(i,j)=LB(j);
elseif x(i,j)>UB(j)
x(i,j)=UB(j);
end
end
end
for i=1:n
f(i,1)=ofun(x(i,:));
end
for i=1:n
if f(i,1)<f0(i,1)
pbest(i,:)=x(i,:);
f0(i,1)=f(i,1);
end
end
[fmin,index] = min(f0);
ffmin(ite,run)=fmin;
ffite(run)=ite;
if fmin<fmin0
gbest=pbest(index,:);
fmin0=fmin;
end
if ite>100;
tolerance=abs(ffmin(ite-100,run)-fmin0);
end
if ite==1
disp(sprintf('Iteration Best particle Objective fun'));
end
disp(sprintf('%8g %8g %8.4f',ite,index,fmin0));
```

ite=ite+1;
end
gbest;
$fvalue = 7800*gbest(9)*(pi/4)*(gbest(1)^2 - (gbest(1) - 2*gbest(2))^2) + 7800*gbest(9)*48*gbest(3)*gbest(4) + 7800*gbest(9)*(pi/4)*(gbest(5)^2 - (gbest(5) - 2*gbest(6))^2) + 7800*gbest(9)*46*gbest(7)*gbest(8) + 8940*8*7 + 8940*2*pi*6*9 + 8940*122*1.05*8;$
fff(run)=fvalue;
rgbest(run,:)=gbest;
disp(sprintf('————————————————————'));
end
$disp(sprintf('));$
disp(sprintf('**'));
disp(sprintf('Final Results————————————————'));
$[bestfun, bestrun] = min(fff)$
$best_variables = rgbest(bestrun, :)$
disp(sprintf('**'));
toc
plot(ffmin(1:ffite(bestrun),bestrun),'-k');
xlabel('Iteration');
ylabel('Fitness function value');
title('PSO convergence characteristic')

Function of the main program

function f=ofuntry(x)
$of = 7800*x(9)*(pi/4)*(x(1)^2 - (x(1) - 2*x(2))^2) + 7800*x(9)*48*x(3)*x(4) + 7800*x(9)*(pi/4)*(x(5)^2 - (x(5) - 2*x(6))^2) + 7800*x(9)*46*x(7)*x(8) + 8940*8*7 + 8940*2*pi*6*9 + 8940*122*1.05*8;$
c0=[];
c0(1)=x(1)-2*x(2)-2*x(3)-x(5);
for i=1:length(c0)
$if c0(i) \geq 0$
c(i)=1;
else
$c(i) = 0;$
end
end
penalty=1000;
f=of+penalty*sum(c);

Power Losses Optimization MATLAB Code

1. main program

clear
n = 9;
lb = [0.21 0.028 0.017 0.0645 0.18 0.076 0.088 0.0035 0.18];
ub = [0.27 0.032 0.022 0.0665 0.21 0.0885 0.092 0.005 0.24];
Aeq = [1 -2 -2 0 -1 0 0 0 0; 0 0 0 0 0 0 0 0 0;0 0 0 0 0 0 0 0 0;0 0 0 0 0 0 0 0 0;0 0 0 0 0 0 0 0 0;0 0 0 0 0 0 0 0 0;0 0 0 0 0 0 0 0 0;0 0 0 0 0 0 0 0 0;0 0 0 0 0 0 0 0 0];
Beq = [0;0;0;0;0;0;0;0;0];
options = gaoptimset('PlotFcns',...
@gaplotbestf,@gaplotbestindiv,@gaplotexpectation,@gaplotstopping);
$[x, lossfunction, exitflag, output] = ga(@loss_obj, n, [], [], Aeq, Beq, lb, ub, @loss_nonlinearconconstraint);$
X = [num2str(x(1)),' ', num2str(x(2)), ' ', num2str(x(3)),' ', num2str(x(4)),' ', num2str(x(5)),' ', num2str(x(6)),' ', num2str(x(7)),' ', num2str(x(8)),' ', num2str(x(9)),' ', num2str(weight)];
disp(X)

2.Objective Function of power loss optimization

$functionlossfunction = loss_{obj}(x)$
m = 6;
kw = 1;
Ss = 48;
$S_r = 38$;
V = 380;
p = 4;
pf=0.85;
eff=0.85;
Rvt=0.021;
Bav = 0.45;
f = 50;
J=4;
Vph = 380;
Pin = 22400;
Q=Pin/(eff*pf)
Iph = Pin/(6*Vph*0.85);
As = Iph/J;
$Nph = (Vph * p)/(4.44 * f * pi * x(5) * x(9) * Bav * kw)$;
$I_b = (0.85 * m * Nph * Iph)/S_r$;
$A_b = I_b/J$;
$Ie = (S_r * I_b)/(pi * p)$;
$Ae = Ie/J$;
$De = (x(5) + x(1))/2$;
$Lmt = (2 * x(1) + (2.3 * pi * x(5)))/p + 0.24)$;

$L_b = (x(9) + (2 * 1.5)/100 + 1/100);$
$Pst = 6 * Rvt * Lmt * Nph * Iph * J;$
$Pb = Rvt * L_b * J * S_r * I_b;$
$Pe = Rvt * 2 * pi * J * Ie * De;$
$Pfe = Rvt * (x(4) * x(3) * 0.8 * 0.03427 * 50 * (0.7)^2 + pi * x(2) * x(9) * (x(5) + 2 * x(3) + x(2)) * 0.00000544 * (50)^2 * (0.7)^2);$
$loss = (Pst + Pb + Pe + Pfe);$
$Eff = Pin/(loss + Pin)$
$Po = Pin + loss$
$pfrated = Po/Q$
end

3. nonlinear costraint function

$function[C, Ceq] = loss_nonlinearconconstraint(x)$
C = (0.0002 + (0.0002*sqrt(x(5)*x(9))) - 0.008);
Ceq = [];
end

B. ANSYS Motor CAD Components
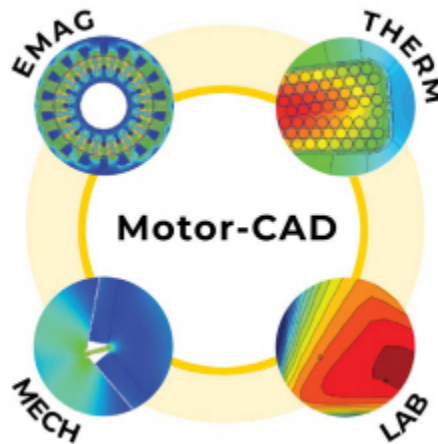
Figure 5.1: Components of ANSYS Motor CAD

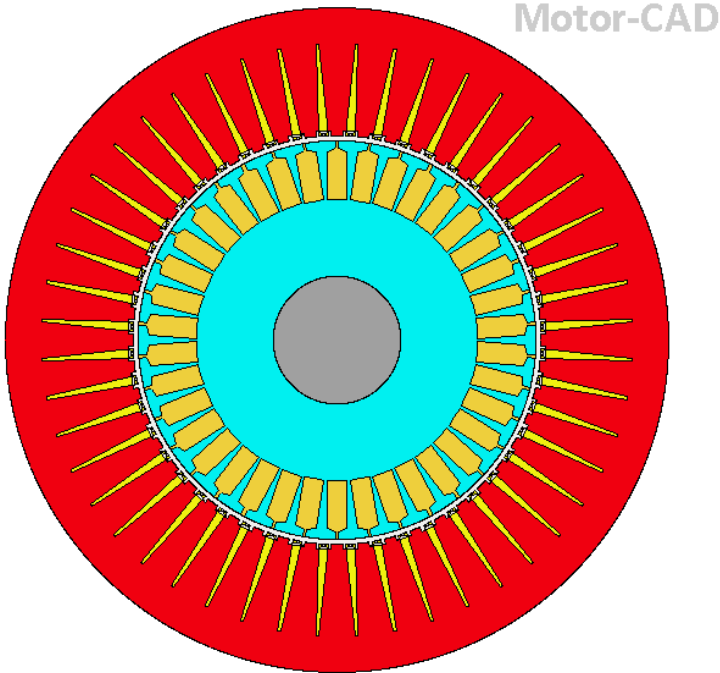## C. Stator core and Rotor Cross Section

Figure 5.2: A Cross Section of Stator core and Rotor core

D. Material consumption

ANSYS Motor-CAD v14.1.2 (Motor CAD going on1.mot)*

File   Edit   Model   Motor Type   Options   Defaults   Editors   View   Results   Tools   Licence   Print   Help

Geometry | Winding | Input Data | Calculation | Temperatures | Output Data | Sensitivity | Scripting

Cooling | Losses | Materials | Interfaces | Radiation | Natural Convection | End Space | Settings | Material databa

Component	Material from Database	Thermal Conductivity	Specific Heat	Density	Weight Internal	Weight Multiplier	Weight Addition	Weight Total
Units		W/m/°C	J/kg/°C	kg/m³	kg		kg	kg
Housing [Active]	Copper (Annealed)	401	385	8933	8.255	2	0	16.51
Housing [Front]	Copper (Annealed)	401	385	8933	3.096	1	0	3.096
Housing [Rear]	Copper (Annealed)	401	385	8933	3.096	1	0	3.096
Housing [Total]					14.45			22.7
Endcap [Front]	Brass (70% Cu, 30% Zn)	111	385	8522	3.489	2	0	6.979
Endcap [Rear]	Brass (70% Cu, 30% Zn)	111	385	8522	3.314	1	0	3.314
Stator Lam (Back Iron)	POLYCOR 0.3% Si	54	460	7650	21.33	2	0	42.65
Inter Lam (Back Iron)		0.02723	1007	1.127	9.717E-05	1	0	9.717E-05
Stator Lam (Tooth)	Copper (Annealed)	401	385	8933	12.16	1	0	12.16
Inter Lam (Tooth)	Copper (Annealed)	401	385	8933	0.3761	1	0	0.3761
Stator Lamination [Total]					33.86			55.19
Armature Winding [Active]	Copper (Annealed)	401	385	8933	1.039	1	0	1.039
Armature EWdg [Front]	Copper (Annealed)	401	385	8933	1.097	1	0	1.097
Armature EWdg [Rear]	Copper (Annealed)	401	385	8933	1.097	1	0	1.097
Armature Winding [Total]					3.234			3.234
Wire Ins. [Active]	Copper (Annealed)	401	385	8933	0.2993	1	0	0.2993
Wire Ins. [Front End-Wdg]	Copper (Annealed)	401	385	8933	0.316	1	0	0.316
Wire Ins. [Rear End-Wdg]	Copper (Annealed)	401	385	8933	0.316	1	0	0.316
Wire Ins. [Total]					0.9313			0.9313
Impreg. [Active]	M19 29 Gauge Steel	28	460	7800	0.8582	1	0	0.8582
Impreg. [Front End-Wdg.]	M19 29 Gauge Steel	28	460	7800	1.867	1	0	1.867
Impreg. [Rear End-Wdg.]	M19 29 Gauge Steel	28	460	7800	2.067	1	0	2.067
Impreg. [Total]					4.793			4.793
Coil Divider	Copper (Annealed)	401	385	8933	0.2894	1	0	0.2894

Component	Material from Database	Thermal Conductivity	Specific Heat	Density	Weight Internal	Weight Multiplier	Weight Addition	Weight Total
Slot Wedge	Copper (Annealed)	401	385	8933	0.03966	1	0	0.03966
Slot Liner	M19 29 Gauge Steel	28	460	7800	0.4959	1	0	0.4959
Rotor Lam (Back Iron)	Copper (Annealed)	401	385	8933	19.02	2	0	38.05
Rotor Inter Lam (Back Iron)	M19 29 Gauge Steel	28	460	7800	0.5138	1	0	0.5138
Rotor Lam (Tooth)	Copper (Annealed)	401	385	8933	3.925	1	0	3.925
Rotor Inter Lam (Tooth)	M19 29 Gauge Steel	28	460	7800	0.106	1	0	0.106
Rotor Lamination [Total]					23.57			42.59
Rotor Cage Top Bar	Copper (Annealed)	401	385	8933	7.047	1	0	7.047
Rotor Cage Top Bar Opening	Copper (Annealed)	401	385	8933	0.04077	1	0	0.04077
Rotor Cage (Front End)	Copper (Annealed)	401	385	8933	3.809	1	0	3.809
Rotor Cage (Rear End)	Copper (Annealed)	401	385	8933	3.809	2	0	7.618
Rotor Cage					14.71			18.51
Shaft [Active]	M19 29 Gauge Steel	28	460	7800	0.5359	1	0	0.5359
Shaft [Front]	M19 29 Gauge Steel	28	460	7800	0.3455	1	0	0.3455
Shaft [Rear]	M19 29 Gauge Steel	28	460	7800	0.2573	1	0	0.2573
Shaft [Total]					1.139			1.139
Bearing [Front]	M19 29 Gauge Steel	28	460	7800	0.1195	1	0	0.1195
Bearing [Rear]	M19 29 Gauge Steel	28	460	7800	0.1195	1	0	0.1195
Flange Mounted Plate	M19 29 Gauge Steel	28	460	7800	20.68	1	0	20.68
Motor Weight [Total]					104.5			160.5

Figure 5.3: Material consumptions of designed motor

E. Equivalent Circuit Six Phase induction Motor
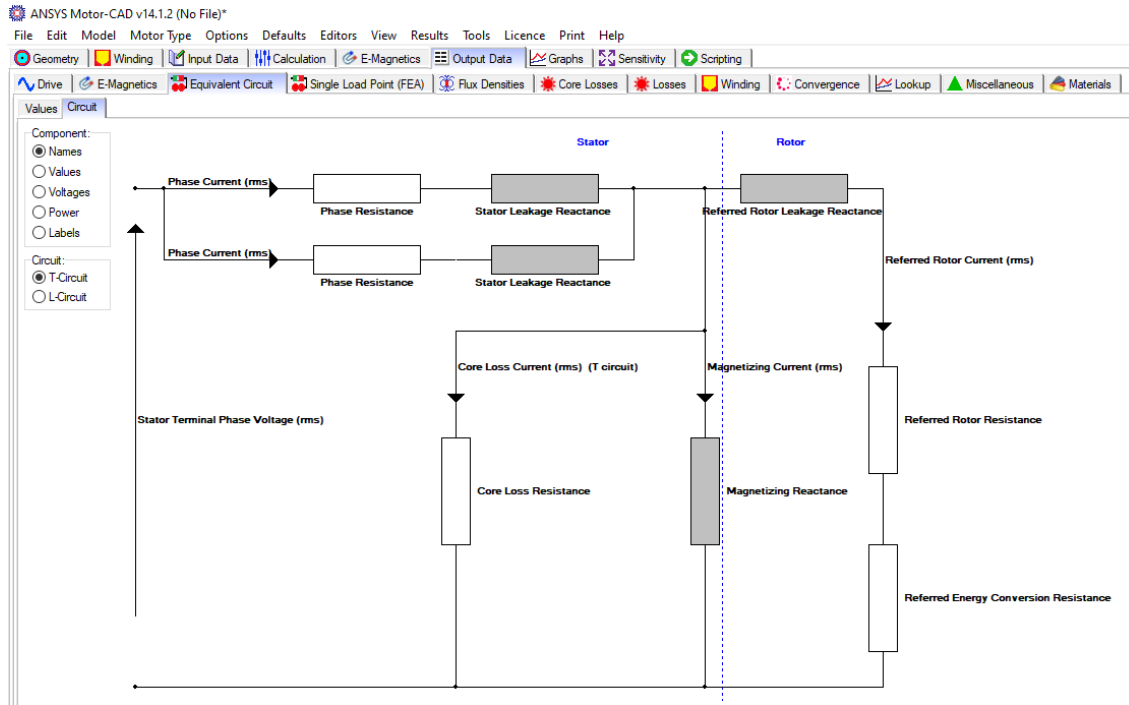

Figure 5.4: Equivalent Circuit Obtained from ANSYS MotorCAD

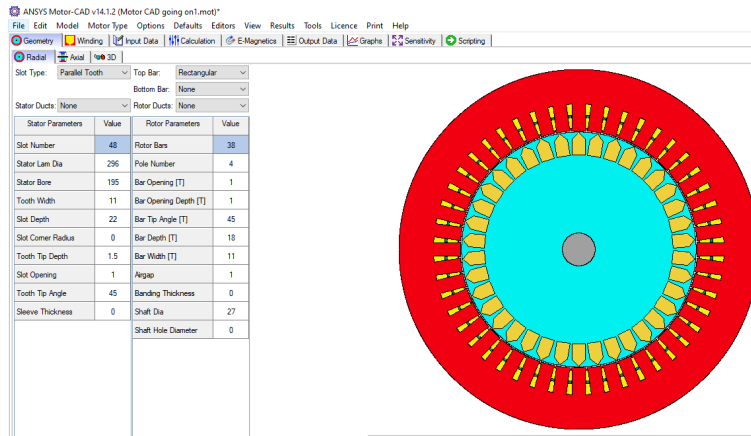## F. Designed Motor geometry in MotorCAD

Figure 5.5: Motor geometry in MotorCAD with its stator and rotor parameter values

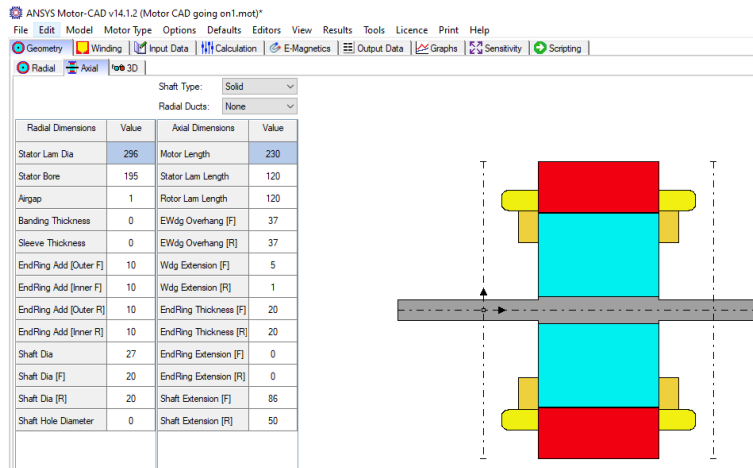## G. Axial Geometry of the Motor with its Radial and Axial General Data

Figure 5.6: Axial Geometry of the Motor with its Radial and Axial General Data
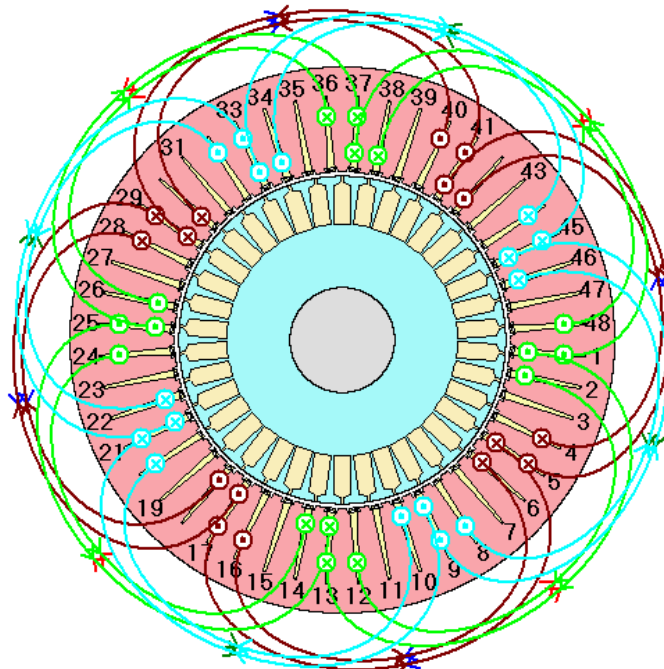
H. Radial and Linear Pattern of winding

Figure 5.7: Radial Pattern of the Six Phase Induction Motor Winding
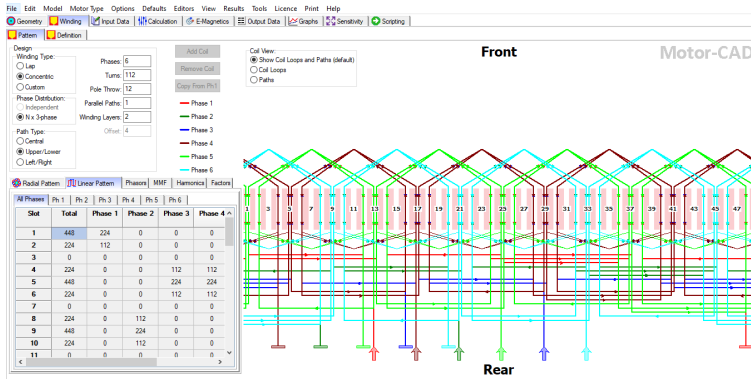
Figure 5.8: Linear Pattern of the Six Phase Induction Motor Winding

I. Flux Density
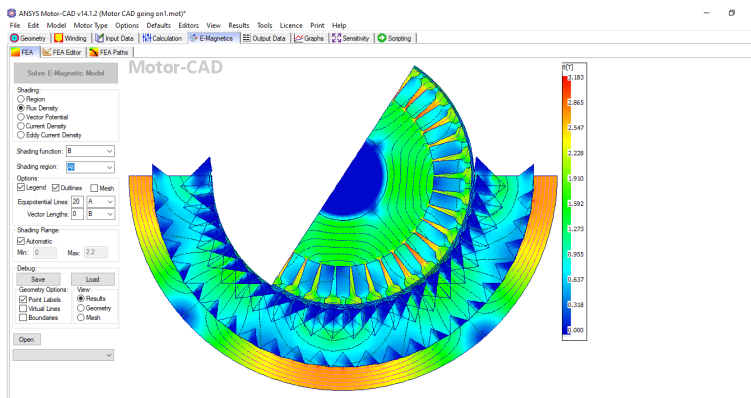
Figure 5.9: Plot of Flux Density

J. Motor-CAD Lab: Efficiency Maps
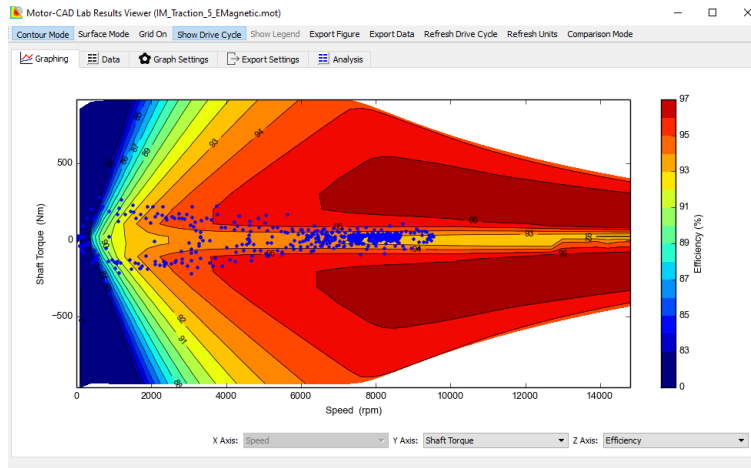
Figure 5.10: Optimized Efficiency Map with Drive Cycle

K. Power Loss per Weight
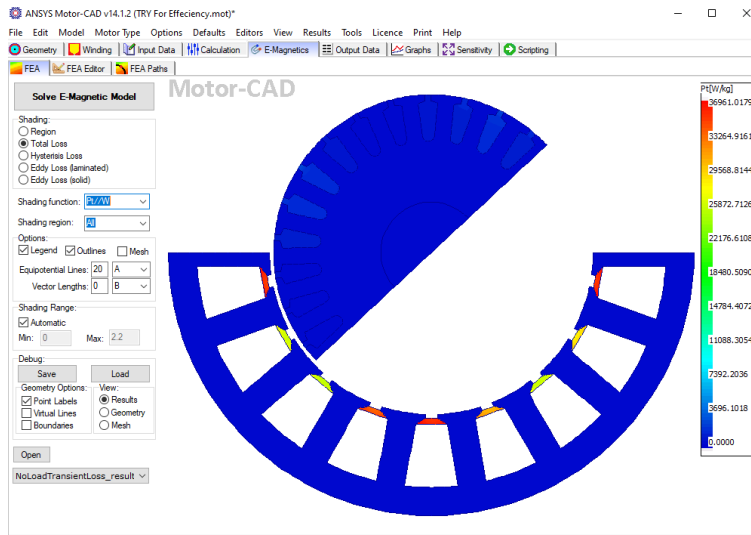
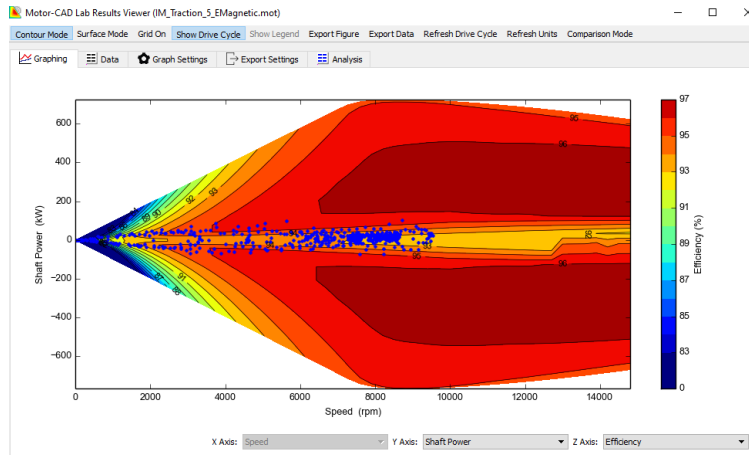Figure 5.11: Loss per Weight of Designed Motor

L. Shaft Power

Figure 5.12: Shaft Power Designed Motor
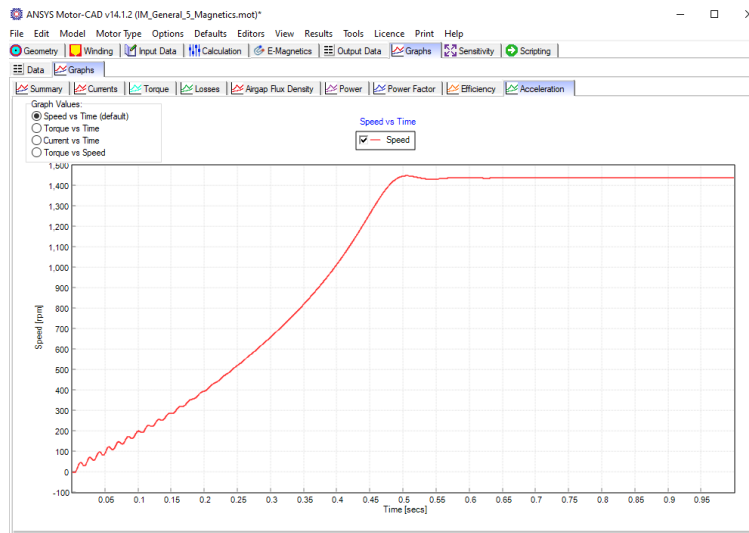
L. Rotor Speed

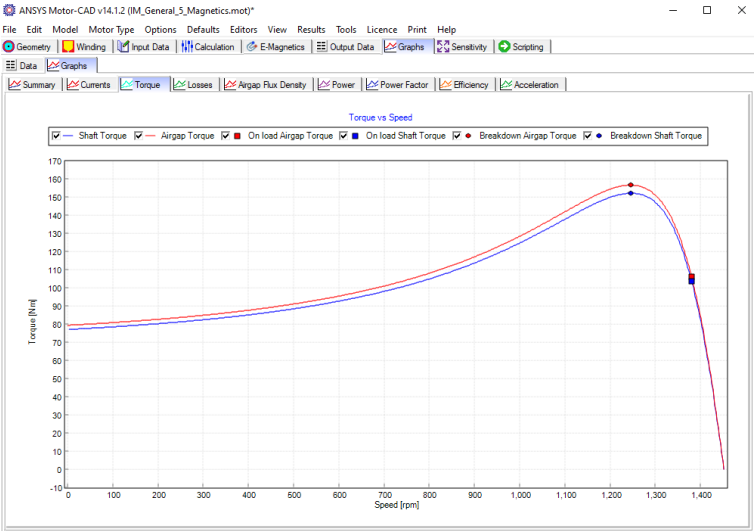

Figure 5.13: Speed of Designed Motor

M. Designed MotorCAD Torque Versus Speed

Figure 5.14: MotorCAD Torque Versus Speed